Electronic Thesis and Dissertation Repository

10-2-2017 4:45 PM

Influence of Scapular Notching on Contact Mechanics and Simulator Wear of Reverse Total Shoulder Arthroplasty Implants

Michael William Griffiths, *The University of Western Ontario*

Supervisor: Dr. James Johnson, *The University of Western Ontario*
Co-Supervisor: Dr. John Medley, *The University of Western Ontario*
Joint Supervisor: Dr. George Athwal, *The University of Western Ontario*
A thesis submitted in partial fulfillment of the requirements for the Master of Engineering Science degree in Biomedical Engineering
© Michael William Griffiths 2017

Follow this and additional works at: https://ir.lib.uwo.ca/etd

Part of the Biomechanical Engineering Commons, and the Biomechanics and Biotransport Commons

Recommended Citation

Abstract

Scapular notching is a common complication of reverse total shoulder arthroplasty (RTSA) wherein the predominant focus of current literature has been on changes in osseous anatomy. However, the implications on RTSA performance from the damaged humeral cup is largely unknown. Therefore the present work describes the effects of the initiation and propagation of the humeral cup defect resulting from scapular notching through the use of finite element modeling and wear simulation, in order to assess changes in RTSA contact mechanics and tribological properties. A significant decrease in articular contact area and increase in maximum contact stress values was found for the tested abduction range of motion for damaged humeral cups. Wear testing of high-mobility RTSA implants indicated a relatively low wear rate, which decreased with the propagation of the scapular notching defect. However, the simulated defect from notching also resulted in a more visibly concentrated secondary wear region within the inferior aspect. Through inferior tilting of the glenosphere, articular contact mechanics were improved, with a significant increase in contact observed, without affecting maximum contact stress values, indicating that this intraoperative parameter may be beneficial beyond the reduced risk for developing scapular notching. Overall, it was indicated that scapular notching damage of the humeral cup may well be detrimental to the assessed articular implant performance parameters, possibly attributing to a decreased lifespan of the implant.

Keywords

Reverse total shoulder arthroplasty, scapular notching, contact mechanics, tribology, wear simulation, glenosphere tilt.

Co-Authorship Statement

Chapter 1: MW Griffiths – sole author

Chapter 2: MW Griffiths – study design, developed models, data collection, statistical analysis, wrote manuscript

GDG Langohr – study design, model development

GS Athwal – study design

JB Medley – study design

JA Johnson – study design, reviewed manuscript

Chapter 3: MW Griffiths – study design, data collection, statistical analysis, wrote manuscript

GDG Langohr – development of wear simulation strategy, study design, companion model development, technical oversight

GS Athwal – study design

JA Johnson – study design, companion model development, reviewed manuscript

JB Medley – development of wear simulation strategy, study design, reviewed manuscript

Chapter 4: MW Griffiths – study design, developed models, data collection, statistical analysis, wrote manuscript

GDG Langohr – study design, model development

GS Athwal – study design

JA Johnson – study design, reviewed manuscript

Chapter 5: MW Griffiths – sole author

Appendix A: MW Griffiths – sole author

Appendix B: MW Griffiths – sole author

Appendix C: MW Griffiths –scanning methodologies and processing development, data collection, processing, and analysis

CE Padmore – scanning methodologies and processing development

GDG Langohr – scanning methodologies

JA Johnson – reviewed document

Acknowledgments

First and foremost, I would like to acknowledge my advisory committee; Dr. George Athwal, Dr. Jim Johnson, Dr. Dan Langohr, and Dr. John Medley. It is through your guidance and support that this work in this thesis was even possible. At one point or another, you have all impacted me in some way to expand my horizons and grow as an individual. I would also like to acknowledge the Carson imaging lab for facilitating the scanning of the humeral cups as part of the wear study.

To all of the other HULC students, thank you so much for your contribution, both within and outside of academics. All of you have contributed to make this experience as fulfilling and enjoyable as it was.

Finally, to my family, thank you for your never-ending love and support. It is through your encouragement that all of this was possible. From the bottom of my heart, thank you so much for everything you have done, it truly means more to me than you will ever know.

Table of Contents

List of Tables

List of Figures

List of Appendices

Chapter 1

Introduction

OVERVIEW: The primary focus of this chapter is to provide the relevant background information from the prospective of the objectives for subsequent investigations. This includes an initial illustration of the native shoulder joint, specifically the glenohumeral joint, highlighting structures of interest in reverse total shoulder arthroplasty (RTSA). Further insight from literature on RTSA and its common complications of scapular notching and articular wear will be explored. Finally, the motivation for the present investigation, as well as its specific objective questions and hypotheses, are outlined.

1.1   The Shoulder Anatomy and Articulations

The shoulder, shown in Figure 1-1, is comprised of three bones, the clavicle, scapula, and humerus, forming four articulations, being the glenohumeral, sternoclavicular, acromioclavicular, and scapulothoracic joints, collectively generating the largest range of motion of any joint (Culham & Peat, 1993). While all are important in their own respect to the overall function of the shoulder, the glenohumeral joint, and its related osseous anatomy and musculature, will be the primary focus of the present work.
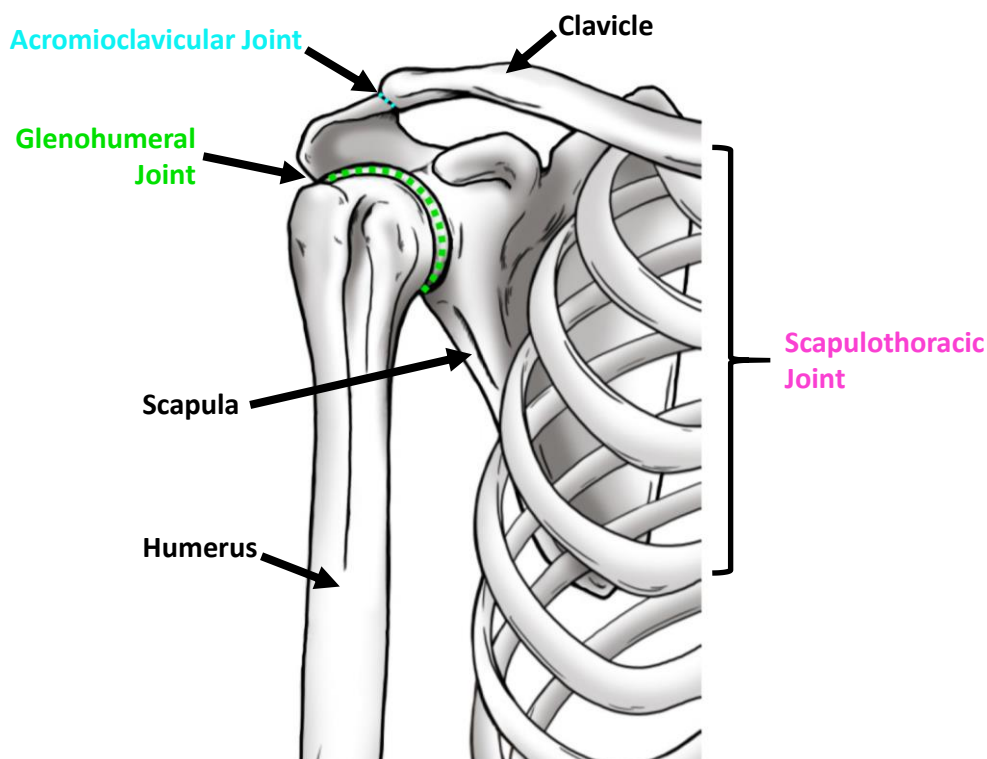
Figure 1-1: The osseous structures of the shoulder with the joints highlighted

Note the sternoclavicular joint is not depicted.

The clavicle extends from the sternum laterally to the acromion of the scapula, attaching the scapula to the torso. It articulates at both facets and aids in preventing displacement of the scapula (Marieb, 2012) while assisting in guiding scapulothoractic rotation. It also contains insertion sites for musculature, including segments of the deltoid (Halder, Itoi, & An, 2000).

The scapula, as seen in Figure 1-2, forms the point of attachment for the upper limb. As previously alluded to, this bone rotates about the scapulothoraccic joint in conjunction with the humerus during abduction, with a 2:1 ratio of humeral elevation to scapular rotation (Inman, Saunders, & Abbott, 1996). Additionally the glenoid, a shallow, concave surface, is located laterally on the scapula, and forms the glenohumeral joint with the proximal aspect of the humerus. The scapula is also the point of origin for several muscles. Specifically, the rotator cuff group, comprised of the suprasinatus, infraspinatus, teres minor, and subscapularus, envelops the glenoid on all but the inferior aspect (Halder et al., 2000). As a result, they aid in protecting the glenohumeral joint capsule with its inner surface covered in synovium (Halder et al., 2000). This musculature also serves to stabilize the gelnohumeral joint, resisting translation (Halder et al., 2000), while also contributing in the motion of the shoulder, with the supraspinatus in particular contributing to abduction (Halder et al., 2000; McMahon et al., 1995; Sharkey, Marder, & Hanson, 1994; Yanagawa et al., 2008).
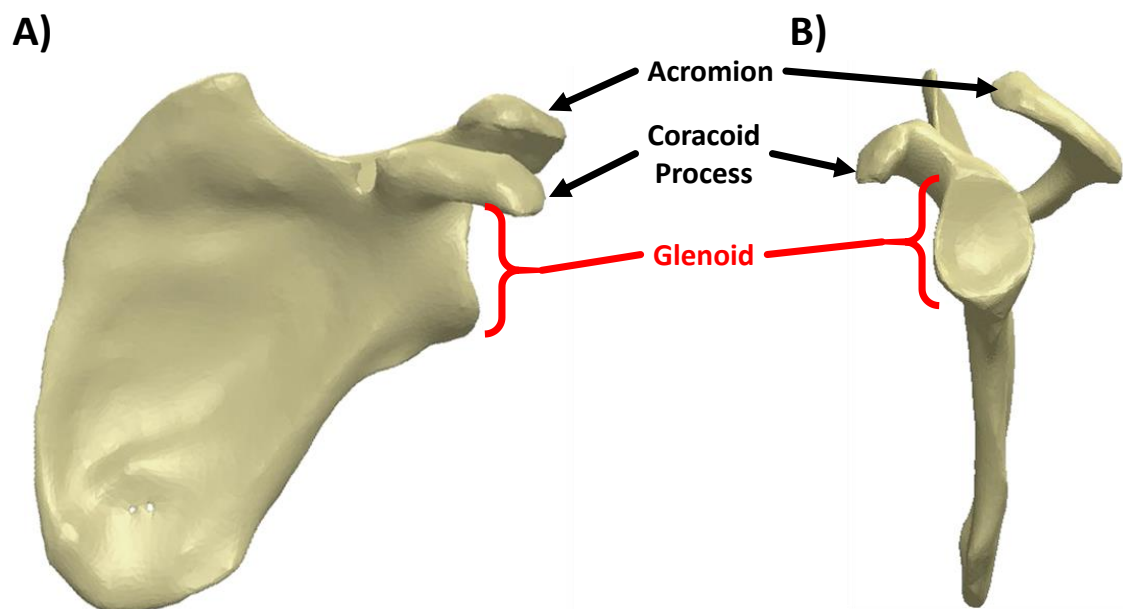
Figure 1-2: (A) Anterior and (B) medial view of a left scapula

4

The humerus, as depicted in Figure 1-3, is the proximal bone of the arm. The humeral head offset from the shaft of the humerus at the humeral neck located proximally, is the largely spherical facet which articulates with the glenoid of the scapula, forming the glenohumeral joint. This joint exhibits three degrees of freedom, and is able to elicit a wide range of motion through flexion/extension, abduction/adduction, and rotation, which along with elbow motion is capable of accommodating any hand position within the visual space (Culham & Peat, 1993). It is this proximal end of the humerus which also contains insertion points for muscles of the rotator cuff. Additionally at the approximate mid-length of the humerus the deltoid inserts at the deltoid tuberosity on the lateral side. It is this muscle which is the primary contributor to the abduction of the upper limb (Halder et al., 2000; McMahon et al., 1995; Yanagawa et al., 2008).
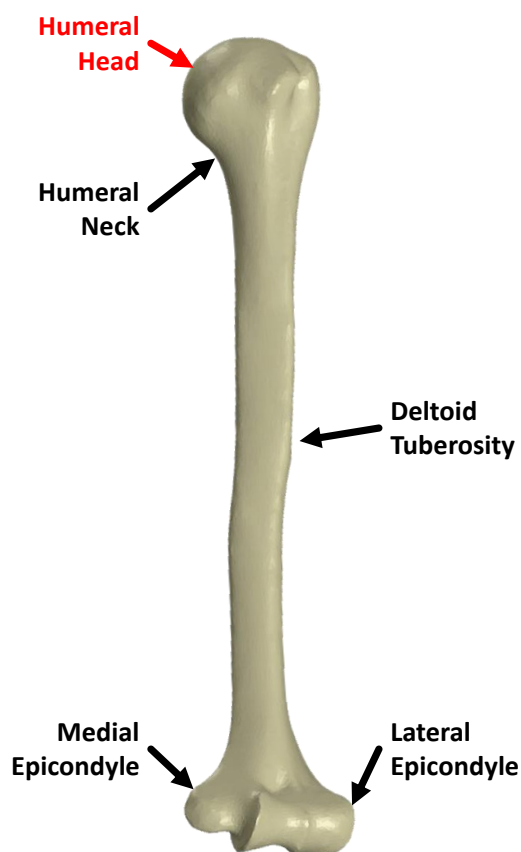
Figure 1-3: Anterior view of a left humerus

1.2 Reverse Total Shoulder Arthroplasty

Reverse total shoulder arthroplasty (RTSA) prostheses consist of a spherical glenosphere and concave humeral component (Figure 1-4). As the name would imply, RTSA systems reverse the native geometry of the glenohumeral joint, replacing the convex humeral head with a concave polyethylene humeral cup and the concave glenoid with a convex metallic glenosphere. As a result of this configuration, the shoulder's center of rotation is constrained medially, relative to the native shoulder joint, at the center of the glenosphere's medial aspect in addition to increasing the moment arms of the deltoid muscles (Ackland, Roshan-Zamir, Richardson, & Pandy, 2010), as depicted in Figure 1-5. This results in a mechanical advantage which aids in eliciting active abduction (Ackland et al., 2010), which has been illustrated through the restoration of function, specifically through significant increases in active abduction range of motion, for patients receiving RTSA (Castagna et al., 2013; Ek, Neukom, Catanzaro, & Gerber, 2013; Flury, Frey, Goldhahn, Schwyzer, & Simmen, 2011; Muh et al., 2013; Mulieri, Dunning, Klein, Pupello, & Frankle, 2010; Nolan, Ankerson, & Wiater, 2011).
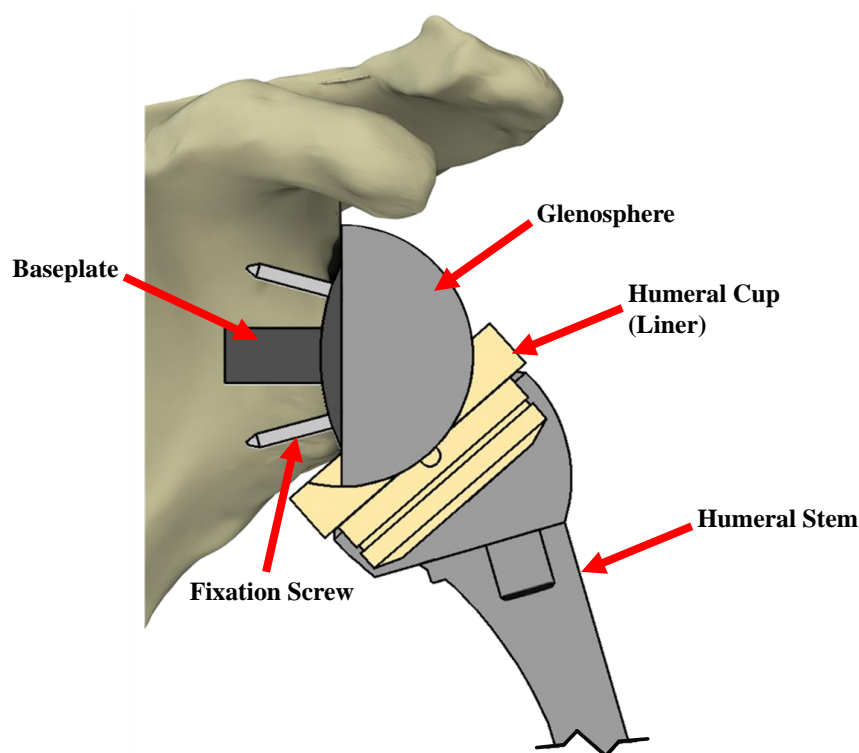
Figure 1-4: Reverse total shoulder arthroplasty implant system
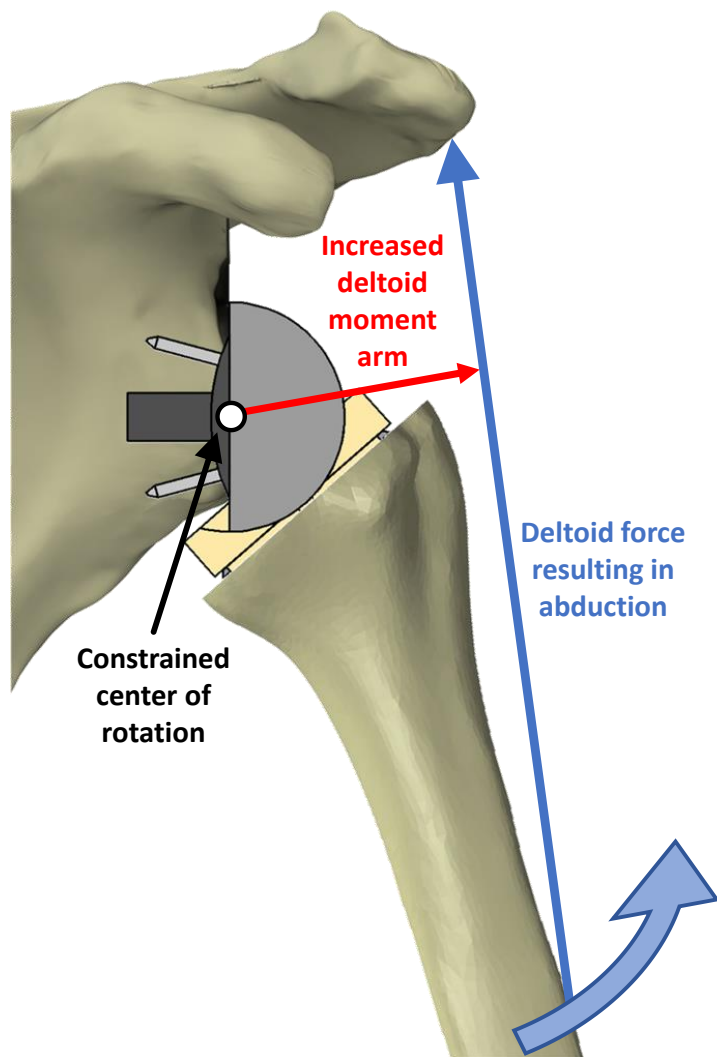
Figure 1-5: The effects of RTSA on joint center of rotation and deltoid line of action

There are several pathologies which could require the implementation of a RTSA system. One of the main functional indicators is the onset of pseudoparalysis of the shoulder, which is the inability to actively abduct above 90°, where passive elevation is unaffected (Ek et al., 2013; Werner, Boehm, & Gohlke, 2013). This functional deficit, while often painful, can also greatly affect daily living. Furthermore, RTSA has been demonstrated to be effective in the treatment of several other shoulder conditions. These include those with rotator cuff insufficiency, rotator cuff tears with or without the presentation of osteoarthritis, chronic dislocations, and proximal humeral fractures (Boileau, Watkinson, Hatzidakis, & Hovorka, 2006; Castagna et al., 2013; Ek et al., 2013; Flury et al., 2011; Muh et al., 2013; Mulieri et al., 2010; Nolan et al., 2011; Weber-Spickschen, Alfke, &

Agneskirchner, 2015; Werner et al., 2013; Young, Everts, Ball, Astley, & Poon, 2009). Additionally, it has been utilized in the application of revising failed shoulder arthroplasty or hemiarthroplasty (Boileau et al., 2006; Castagna et al., 2013; Flury et al., 2011; Muh et al., 2013; Mulieri et al., 2010; Weber-Spickschen et al., 2015; Werner et al., 2013; Young et al., 2009).

1.3 Reverse Total Shoulder Arthroplasty Performance and Complications

While RTSA is an effective treatment of several conditions, this prosthesis system is not without its issues. There are several different complications related to the implant which occur rather frequently, but are accepted when weighed against the improvement in shoulder function and quality of life (Farshad & Gerber, 2010). However, focus will be given to scapular notching and the material wear of the humeral cup articular surface, as they relate to the present work. Moreover, the development and severity of these complications have been demonstrated to be further influenced by the selected parameters for the prosthesis, which will be further examined as well.

1.3.1 Humeral Cup Wear

It has been commonly reported in surgical retrieval studies that the tribological interaction of the metallic glenosphere and polyethylene humeral cup can result in damage to the articular surface of the humeral cup. This encompasses multiple mechanisms, including abrasion (Day et al., 2012; Nam et al., 2010; Wiater et al., 2015), pitting (Nam et al., 2010), as well as delamination (Day et al., 2012). Specifically, Nam et al (2010) reported that articular surface damage was most frequently located within the inferior quadrant. The significance of this is highlighted through two finite element studies (Langohr, Willing, Medley, Athwal, & Johnson, 2016; Terrier, Merlini, Farron, & Pioletti, 2009) which indicated that both contact area and the location of maximum contact stress is situated inferomedially. Additionally, the generation of polyethylene debris can ultimately lead to an increased rate of polyethylene wear induced osteolysis, further contributing to the scapular notching process (Vaupel, Baker, Kurdziel, & Wiater, 2012).

1.3.1.1   In-Silico Wear Evaluation

A finite element model to evaluate and compare the polyethylene wear of anatomic and reverse shoulder prostheses was developed by Terrier et al (2009) utilizing a musculoskeletal model including 6 muscles from electromyography data. However, the rotator cuff muscles were excluded from this RTSA model. This testing was conducted for 8 angles of abduction relevant to activities of daily living. It was reported that the contact pressure for the anatomic prosthesis model was approximately 20 times greater than the reverse (Terrier et al., 2009). Conversely, the annual volumetric wear rate for the anatomic prosthesis was only 8.4 mm^3 compared to 44.6 mm^3 for the reverse, which was suggested to contribute to the loosening of these implant system components due to the increased concentrations of polyethylene debris produced inducing osteolysis (Terrier et al., 2009).

1.3.1.2   In-Vitro Wear Studies

Simulation-based studies have been conducted to assess the effect on polyethylene wear from the alteration of articular components. A summary of the previous studies' methodologies are provided in Table 1-1.

Table 1-1: Summary of previous RTSA wear studies' methodologies and their results

Author	Test Variable	Simulator Range of Motion	Simulator Loading (N)	Lubricant	Wear Rate (mm^3/Mc) (Mc = 1×10^6 cycles)	Notes
Carpenter et al., 2015	Retentive humeral cup	46° ABD-ADD†	20-618 (90% BW)	Bovine calf serum (21 g protein/L) 0.2% sodium azide 7.0×10^{-3} g/mL EDTA Deionized water	88.1 ± 19.1 (nonretentive) 96.8 ± 21.9 (retentive)	
		46° FLEX-EXT†	20-927 N (135% BW)			
Dieckmann et al., 2013	Reversed material RTSA system	70° ABD-ADD 20° FLEX-EXT	100-500	Bovine calf serum (30 g protein/L)	29.9* (reversed material, PE glenosphere) 9.93* (PE humeral cup)	
Haider, Sperling, & Throckmorton, 2013	XPE and HXPE humeral cup	41° ABD-ADD 57° INT-EXT	50-1700	Not specified	19.1 ± 0.910* (XPE) 3.66 ± 0.235* (HXPE)	
Kohut et al., 2012	Reversed material RTSA system	11° ABD-ADD 43° FLEX-EXT 13° INT-EXT ROT	250-1000	Bovine calf serum (30 g protein/L)	19.85* (reversed material, PE glenosphere) 14.12* (PE humeral cup)	
Langohr, 2015		45° ABD-ADD 45° FLEX-EXT	813-914	Bovine calf serum (30 g protein/L) PBS 1.5 g/L hyaluronate	201.1 ± 86.5	
Langohr, Athwal, et al., 2016	Notched humeral cup	45° ABD-ADD 45° FLEX-EXT	813-914	Alpha calf serum (30 g protein/L) PBS 1.5 g/L hyaluronate	42.0 (intact) 38.8 (notched)	Artificially notched humeral cup
Peers et al., 2015	XPE humeral cup	46° ABD-ADD†	20-617.8 (90% BW)	Bovine calf serum (21 g protein/L) 0.2% sodium azide 7.0×10^{-3} g/mL EDTA Deionized water	83.6 ± 20.6 (PE) 36.5 ± 10.0 (XPE)	Custom machined humeral cups
		46° FLEX-EXT†	20-926.7 (135% BW)			
Smith et al., 2015	Activity of daily living	13° ABD-ADD 28° FLEX-EXT 25° INT-EXT ROT	180-250	Newborn calf serum (26 g protein/L)	14.3 ± 2	Simulator parameters for "mug to mouth" activity of daily living
Vaupel et al., 2012	Glenospheres with added fixation holes	46° ABD-ADD†	20-617.8 (90% BW)	Bovine calf serum (21 g protein/L) 0.2% sodium azide 7.0×10^{-3} g/mL EDTA Deionized water	125 ± 32 (intact) 126 ± 29 (with holes)	Included some custom machined humeral cups
		46° FLEX-EXT†	20-926.7 (135% BW)			

* wear rate calculated using density of PE = 0.935 mg/mm^3 (Langohr, Athwal, et al., 2016)   † Alternated between ABD-ADD & FLEX-EXT motions every 0.25 Mc

There have been two studies which involve the investigation of alterations to the articular surfaces of the implant components. Vaupel et al (2012) did not report a significant difference in wear for glenospheres with added holes, to be used for fixation, relative to those without. Langohr et al (2016) conducted a study where a humeral cup was artificially notched to replicate damage indicated from scapular notching. The humeral cup with simulated scapular notching damage was observed to have an 8% decrease in wear rate relative to the intact component. However, it should be noted that this study was confined to a single specimen.

The effect of humeral cup depth on wear rates was examined by Carpenter et al (2015), where retentive cups were found to significantly increase the polyethylene wear rate. It should be noted that the retentive cups also exhibited greater surface deviation, relative to the non-retentive specimens, with the most prominent wear occurring inferomedial region in both test groups. A similar wear region was also reported in the surface deviation maps from the two studies conducted by Langohr (Langohr, 2015; Langohr, Athwal, et al., 2016).

Furthermore, the implications of activities of daily living have also been evaluated through the modality of wear testing. In a wear simulation test by Smith et al (2015), a "mug to mouth" motion was simulated, resulting in an average wear rate of 14.3 mm^3/MC. It was also reported that while the surface roughness of the glenospheres were relatively unchanged as a result of testing, the surface roughness values of the humeral cups were reduced, from the polishing of the abrasive wear.

Two wear simulation studies were also conducted on the aforementioned reverse articular RTSA systems (Dieckmann et al., 2013; Kohut et al., 2012). These systems employ an alternate strategy in an attempt at decreasing polyethylene debris interacting with the scapula and the resulting biological notching through reversing the articular materials (Kohut et al., 2012). In this case the RTSA components consisted of a polyethylene glenosphere interacting with a metallic humeral cup. While this strategy aims to avoid biologic degradation of the scapula from the polyethylene debris, it is possible that damage from contact could still persist due to the higher moduli, metallic humeral liner if scapular impingement is present. Moreover, there is still the issue of polyethylene wear, with both

studies observing an increase in wear rate, relative to a conventional RTSA system. Specifically, Kohut et al (2012) and Dieckmann et al (2013) reported an 40% and 302% increase respectively.

Additionally, two wear simulation studies on crosslinked polyethylene have been conducted, both of which indicated reduced wear rates with the use of crosslinking (Haider et al., 2013; Peers et al., 2015). The crosslinking of polyethylene has been investigated for orthopedic applications since the early 1970's and involves the irradiating of polyethylene, through sources such as γ-radiation or electron beam radiation, to disrupt the bonds within a polymer chain, and the subsequent formation of bonds between chains, in addition to the formation of free radicals (Oonishi et al., 2006). Therefore additional processing is required in order to ensure the material's stability. The study conducted by Peers et al (2015) indicated that crosslinked polyethylene humeral cups significantly reduced wear by 56% relative to the non-crosslinked components. Moreover, Haider et al (2013) performed wear testing on two groups of crosslinked polyethylene humeral cups, one being highly crosslinked and vitamin E doped and the other being only moderately crosslinked. It was reported that the increased crosslinking, induced through the doubling of the radiation dosage, reduced humeral cup wear by 81%. The improved wear characteristics of this material has been echoed in many other applications, including pin-on-plate wear testing (Bistolfi, Turell, Lee, & Bellare, 2009; Brandt et al., 2014; Kilgour & Elfick, 2009), hip arthroplasty, in both wear simulation (Affatato et al., 2005; Oonishi et al., 2006) and clinical evaluation (Capello, D'Antonio, Ramakrishnan, & Naughton, 2011; McCalden et al., 2009; Oonishi et al., 2006), as well as total shoulder arthroplasty (Wirth et al., 2009). However, these improvements do occur at the expense of other physical properties of the material. Specifically, this includes the degradation of fracture propagation resistance (Pruitt, 2005) and ability to plastically deform subsequently contributing to the failure of implants in some cases (Pruitt et al., 2013).

As it can be discerned from the aforementioned information presented in Table 1-1, while studies have covered a variety of factors, there has not been consistency with respect to methodologies and test parameters, as there is currently no established test standard for RTSA wear simulation. Therefore it is difficult to directly compare results between

studies, with wear rates ranging from 9.93 mm^3/MC (Dieckmann et al., 2013) to 201.1 mm^3/MC (Langohr, 2015) for conventional polyethylene, standard depth humeral cups. Beyond the obvious differences in loading and motion simulated, many other experimental variables have been demonstrated to affect wear simulation results. Even performing an experiment with the same equipment at two different locations (Schwenke, Kaddick, Schneider, & Wimmer, 2005) or changing the test station of specimens within a simulator (Brandt, Charron, Zhao, Macdonald, & Medley, 2011) can result in observable differences in wear rates.

Additionally lubricant selection and composition can affect wear rates reported. Lubricant protein concentration (Schwenke et al., 2005; Wang, Essner, & Schmidig, 2003), relative albumin/globulin concentrations (Wang et al., 2003), and protein degradation rates (Brandt, Charron, Zhao, Macdonald, & Medley, 2012; Reinders, Sonntag, & Kretzer, 2015) have all been demonstrated to effect wear rates. The addition of hyaluronic acid, to replicate this component of synovial fluid, has demonstrated conflicting results, with some indicating an increased wear rate (DesJardins et al., 2006), whereas others did not observe an effect (Wang et al., 2003). Even the volume of lubricant in a test station has been shown to significantly affect wear rates, where a decrease in lubricant volume from 250 ml to 45 ml reduced the observed wear rate by 970% (Reinders et al., 2015).

Work by both DesJardins et al (2006) and Brandt et al (2010) examined lubricant composition relative to synovial fluid of osteoarthritic, total knee replacement patients, in order to better replicate the environment of an implant. DesJardins et al (2006) indicated bovine serum, diluted by 50% with water, and the addition of hyaluronic acid demonstrated similar biochemical and viscosity properties as the collected synovial fluid. Furthermore, Brandt et al (2010) indicated that a lubricant solution of alpha calf serum diluted with phosphate-buffered saline solution and added hyaluronic acid best replicated the osmolarity, thermal stability, and relative protein concentrations of osteoarthritic synovial fluid. It should be noted that the average protein concentration of the collected synovial fluid was 34 g/L whereas the recommended lubricant protein concentration as per ISO 14243 states 17 g/L (Brandt et al., 2010). Additionally, alpha calf serum was found to have reduced microbial growth performance relative to other serum sources (Brandt et al., 2012).

Conversely, alternatives to bovine sourced lubricants has been explored by Scholes & Joyce (2013), however no suitable replacement was reported, mainly due to differences in protein degradation performance.

1.3.2   Scapular Notching

The inferior aspect of the humeral cup contacting the scapula at the base of the glenoid, as depicted in Figure 1-6, is the driving mechanism for scapular notching, resulting in damage to the polyethylene humeral liner. A finite element modeling and experimental simulation found that while the contact encompasses a small area, the resulting stresses are greater than the compressive yield stress for polyethylene with the application of a 22.5 N load in impingement (Permeswaran, Goetz, Rudert, Hettrich, & Anderson, 2016). Notably, visual evidence of humeral component edge deformation, similar to that observed in *in-vivo* studies, was present after scapular notching simulation. Typically, this denting process of the humeral cup begins to present within 2 years after surgery (Oh & Choi, 2013). Additionally, the process of scapular notching results in damage to the osseous anatomy through the process of biologic notching as a result of polyethylene debris (Kohut et al., 2012). This process of debris-induced inflammation is largely mediated by macrophages (Hallab & Jacobs, 2009), whose cytokine release is increased in the presences of polyethylene debris and is enhanced with debris in higher concentrations, further stimulating bone resorption (Rader, Sterner, Jakob, Schütze, & Eulert, 1999). The bone defects are classified on a grading system based on the extent of damage relative to the inferior baseplate and screw, with damage extending beyond the screw as illustrated in Figure 1-7 being the most severe (Boileau et al., 2006; Sirveaux et al., 2004). It is the most frequently reported complication resulting from RTSA which can be identified through the visual appearance of wear on radiographic images (Farshad & Gerber, 2010). Additionally severe notching, extending beyond the inferior fixation screw can occur in the short term, in some cases as little as 8 months after implantation (Nyffeler, Werner, Simmen, & Gerber, 2004).

14
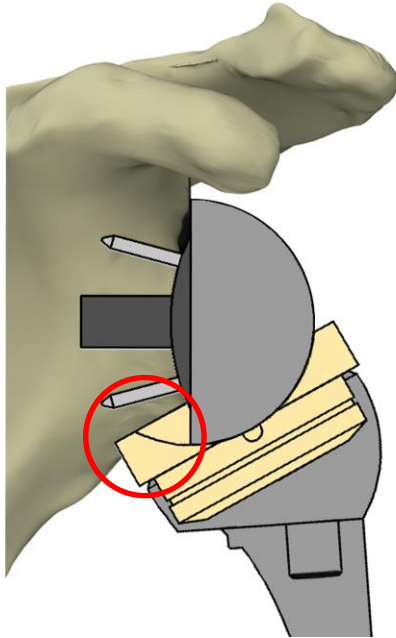
Figure 1-6: Scapular notching area of impingement in adduction highlighted
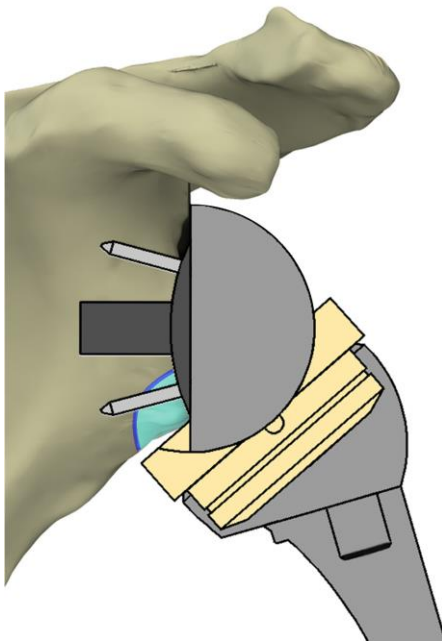
Figure 1-7: Scapular notching osseous damage extending beyond inferior fixation screw

While quite variable, radiographic studies have indicated a relatively common incidence for scapular notching, with many reporting it in 49% to 74% of included cases (Boileau et al., 2006; Boileau, Watkinson, Hatzidakis, & Balg, 2005; Ek et al., 2013; Flury et al., 2011; Lévigne et al., 2011; Nolan et al., 2011; Sirveaux et al., 2004). Moreover, a recent radiographic assessment of 476 patients reported only viewing scapular notching in 10% of patients, with the incidence being more common in those at a longer period at time of follow up (Mollon, Mahure, Roche, & Zuckerman, 2017). Similar results have been reported, with a lower incidence of scapular notching of 14% to 27%, while also only observing the least severe form of the condition (Mulieri et al., 2010; Weber-Spickschen et al., 2015; Young et al., 2009). However, damage to the inferior aspect of the glenoid progressing to the extent of exposing the baseplate screw, or at least grade three, was reported in 11% to 26% of patients included (Boileau et al., 2006, 2005; Ek et al., 2013; Flury et al., 2011; Nolan et al., 2011; Sirveaux et al., 2004). The degree of notching was also reported to increase over the course of observation (Ek et al., 2013) or was more severe in those with a longer follow up period (Mollon et al., 2017). In turn, the exposed fixation screw would exacerbate material removal from the polyethylene liner and has been observed in surgical retrieval studies. Nyffeler et al (2004) reported damage resulting from an exposed baseplate screw extending through the polyethylene cup, all the way to the metal epiphysis, encompassing an arc of 120°. Similar damage was observed in 29% of humeral cups in the retrieval study by Day et al (2012), where metal on metal contact was also evident in one case from the fracture of the screw. This also presents further compounding issues, with the introduction of metallic wear debris in addition to the loosening of the baseplate securing the glenosphere (Day et al., 2012). Alternatively, severe damage in the inferior region of the humeral cup has been reported to occur as a result of fracturing as opposed to erosion of the material (Samuelson, Cordero, & Fehringer, 2009).

The prevalence of scapular notching damage has also been reported in surgical retrieval studies, albeit in varying frequency. Notably, a study by Day et al (2012) observed evidence of boney impingement on all seven of their retrieved humeral cups in one series. However it is also of interest to note that the severity of humeral cup impingement damage

did not correlate to the scapular notching grade score indicated in each case. Therefore the amount of damage to the polyethylene cup is not necessarily directly proportional to the bone loss observed on radiographic images. The surgical retrieval studies of Nam et al (2010) and Wiater et al (2015) also indicated a high prevalence of scapular notching and inferior region damage. Specifically, the results of Nam et al (2010) indicated that inferior damage was the most prevalent and severe in the retrieved humeral components, in addition to scapular notching being reported for 46% of the cases with available radiographic images. In a similar fashion, Wiater et al (2015) observed inferior rim damage in 45% of humeral cup retrievals from the aseptic patients undergoing revisions.

1.3.3 Strategies for Reducing Scapular Notching

Due to the modular nature of RTSA systems, there are several strategies available to reduce the risk of scapular notching. Specifically these involve alterations of both the humeral and glenoid components in an attempt to increase the adduction range of motion or avoid notching altogether. Additionally, through the positioning and orientation of the implant components, specifically the glenosphere, this area can also be affected. This would include RTSA parameters such as glenosphere size (Berhouet, Garaud, & Favard, 2014; de Wilde, Poncet, Middernacht, & Ekelund, 2010; Gutiérrez, Comiskey, Luo, Pupello, & Frankle, 2008; Gutiérrez, Luo, Levy, & Frankle, 2009; Langohr, Giles, Athwal, & Johnson, 2015; Roche et al., 2009; Torrens, Guirro, Miquel, & Santana, 2016; Wiater et al., 2015), neck-shaft angle of the humeral component (de Wilde et al., 2010; Gutiérrez, Comiskey, et al., 2008; Gutiérrez et al., 2009; Oh et al., 2014; Roche et al., 2009), lateralization of the glenosphere (Berhouet et al., 2014; Cuff, Pupello, Virani, Levy, & Frankle, 2008; de Wilde et al., 2010; Gutiérrez, Comiskey, et al., 2008; Gutiérrez, Greiwe, Frankle, Siegal, & Lee, 2007; Gutiérrez et al., 2009; Langohr et al., 2015), reversing the articular component materials (Bloch et al., 2014), and the use of an eccentric or more inferiorly positioned glenosphere (Berhouet et al., 2014; de Wilde et al., 2010; Gutiérrez, Comiskey, et al., 2008; Nyffeler, Werner, & Gerber, 2005), which have all been evaluated for their efficacy through a combination of *in-silico, in-vitro,* or clinical observation studies. It is evident that in some instances, while the adduction range of motion may increase there is an accompanying degradation in other areas of performance. Nevertheless, low angles of

abduction are of particular interest based on motion tracking indicating abduction below 40° comprised a majority of the daily use for arthroplasty patients' operated shoulder (Langohr, 2015). While there are several options available to achieve these results, only the factors related to the current work will be discussed. These factors are the inferior tilt of the glenosphere and the reduced constraint of the humeral cups component.

Inferior tilting of the glenosphere is obtained through the use of reaming and bone grafts in order to orientate the glenosphere in a downward fashion Figure 1-8. As a result of this process, there is a decrease in contact area, specifically at the inferior aspect, due to the oblique cut of the glenoid (Nyffeler et al., 2005). In addition, there is an increase in the deltoid forces, relative to a neutral orientation, required for abduction range of motion (Tashjian, Burks, Zhang, & Henninger, 2015).
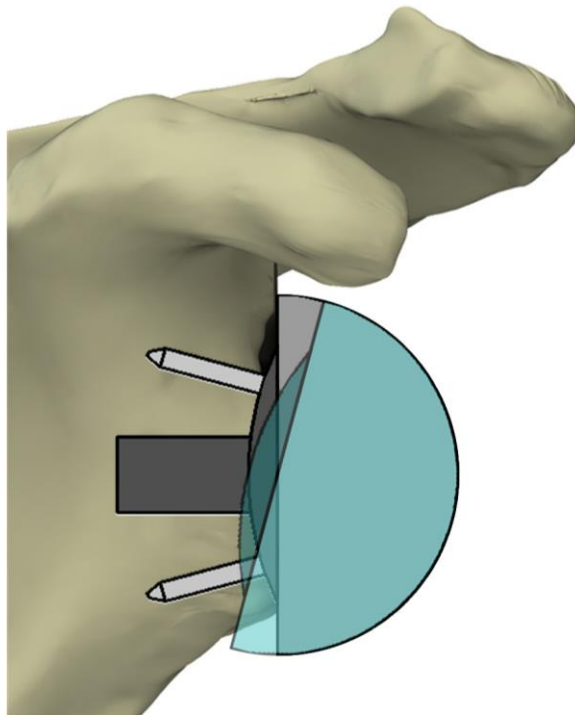
Figure 1-8: Inferiorly tilted glenosphere (overlaid in blue)

Note that only the glenosphere has been rotated for the purpose of clarity.

It has been demonstrated through the use of computer simulation (de Wilde et al., 2010; Gutiérrez, Comiskey, et al., 2008) and cadaveric studies (Berhouet et al., 2014; Nyffeler et al., 2005) that the implementation of an inferiorly tilted glenosphere increases adduction range of motion. In particular, it was reported by de Wilde et al (2010) that the reduction in adduction deficit, and therefore increased adduction range of motion, was equivalent to the angle of inclination of the glenosphere. Nevertheless, it should also be noted that in all of the above studies there were other factors investigated that were found to have a greater influence on adduction range of motion.

However, there is some controversy with regards to inferior glenosphere tilt in terms of baseplate stability and micromotion. Work lead by Gutiérrez investigated these factors through both an analogous, foam block model (2007) and computer simulation (2011). It was demonstrated that there is decreased micromotion of the base plate (Gutiérrez et al., 2007), as well as a more uniform stress distribution was found at the baseplate interface (Gutiérrez et al., 2007, 2011). Furthermore, finite element assessment by Denard et al (2016) also reported reduced baseplate stress and displacement with the implementation of an inferior glenosphere tilt. Conversely, a cadaveric shoulder simulation study by Chae et al (2015) reported increased baseplate micromotion with an inferiorly tilted glenosphere. Additionally, there was an increased rate of failure at the baseplate, with all failures occurring around the insertion site for the inferior screw, due to the decreased bone stock from reaming. In a follow-up finite element study by Chae et al (2016) also indicated adverse effects to baseplate stability. Specifically, it was determined that inferior glenosphere tilt resulted in increased micromotion, particularly in the middle and inferior third of the baseplate, increased stress in the bone-baseplate interface, and decreased contact area of the screws (Chae et al., 2016).

Nevertheless, in practice inferior glenosphere tilt has indicted success. Randelli et al (2014) reported improved joint stability with an inferior tilt in glenosphere. Of the 33 patients, with a median follow up period of 32 months, there were 3 incidences of dislocation. The average glenosphere tilt of the 30 stable patients was 10.2° inferiorly, whereas the inferior glenosphere tilt for the 3 patients with dislocations was -6.9° (superior), 2.4°, and 8.3°. However, it should be noted that the patient with 8.3° inferior

tilt experienced a traumatic dislocation in a fall, whereas the other 2 incidences were atraumatic and occurred within 2 months of the surgery.

An additional surgical follow-up study was conducted by Kempton et al (2011) to investigate if inferior glenosphere tilt influenced the radiographic presentation of scapular notching, at a minimum period of 12 months after surgery. The overall incidence of scapular notching was quite high at 71% overall, albeit greater in the neutral tilt group at 77% relative to 61% for those with an inferior tilt. However, it should be noted that when adjusting for follow-up time in the statistical analysis there was no difference detected between the two groups, further indicating the time dependent nature of the scapular notching process (Kempton et al., 2011). Moreover, other performance indicators related to scapular notching, such as range of motion, were not included in this work.

Another variable of RTSA components that can be altered to influence the adduction range of motion is the conformity, or depth, of the humeral cup component. Implants can either be shallower than the standard offering, referred to as a high mobility liner, or deeper, also described as retentive. In the case of the DePuy Delta XTEND™ range (Warsaw, IN, USA) there is a 2 mm change in relative depth between the standard humeral cup and the high mobility or retentive alternatives, while maintaining the same center of rotation, as illustrated in Figure 1-9. The increase of adduction range of motion with decreasing humeral cup depth has been illustrated through several *in-silico* simulation studies (de Wilde et al., 2010; Gutiérrez et al., 2009; Roche et al., 2009).
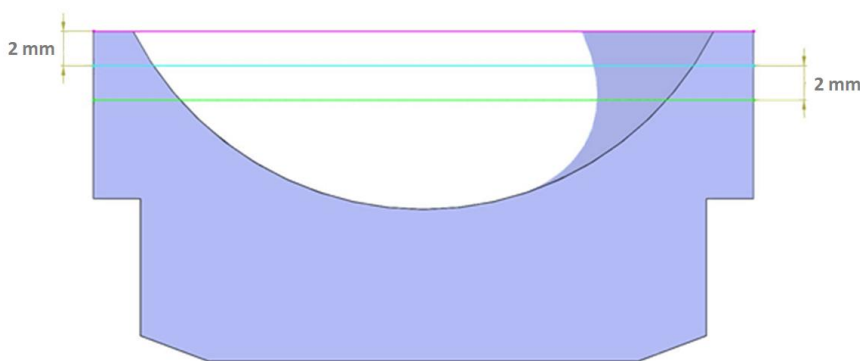
Figure 1-9: Stacked, cross-section of humeral cups with varying depth parameter

Deep (+2 mm; pink), standard (blue), and shallow (-2 mm; green) constraints indicated

However, it has also been reported that a change in humeral cup depth can affect the contact mechanics and stability of the joint replacement. Specifically Langohr et al (2016) indicated that the decrease in humeral cup depth increased maximum contact stress values and decreased the articular contact area through finite element modeling. With respect to joint stability, it has been indicated through both biaxial loading (Gutiérrez, Keller, Levy, Lee, & Zong-Ping, 2008) and cadaveric biomechanics studies (Clouthier et al., 2013; Pastor, Kraemer, Wellmann, Hurschler, & Smith, 2016) that the decreasing conformity of the humeral cup reduces the load required to elicit dislocation.

1.4 Motivation

While scapular notching has been widely reported in RTSA, with respect to scapular damage, the overall impact of the subsequent damage observed on the humeral cup has not been fully investigated. This is of particular importance as surgical retrievals have indicated extensive damage within a region that has been demonstrated to be of particular importance in the context of maximum contact stress values and subsequent material wear. Additionally, as it has also been indicated to be a progressive process, the gradual increase in material lost to scapular notching should also be included to ascertain the effects of increasing in severity. However it should be noted that the process of scapular notching has presented at different times and rates in individuals.

With the prevalence of this complication, it is important to evaluate the effect of scapular notching damage within these areas to better understand the factors which could ultimately lead to revisions being required. Beyond the damage to the implant system, this would include additional complications which can result, such as implant loosening. Currently, research within the areas of contact mechanics and wear simulation of RTSA systems has focused predominately on the analysis of fully intact implants.

Furthermore, implant configurations which have been demonstrated to increase adduction range of motion have been previously investigated for their implications on articular contact mechanics. However, these studies excluded the changes in the positioning and orientation of the components. Current research within this area has largely concentrated on the bone-implant interface, as opposed to the articular interface. Therefore it would be

beneficial to assess how some alterations in component orientation affect the implant contact mechanics from this altered perspective.

1.5   Objectives & Hypotheses

The goal of the present work is to assess the effects of notching damage of the humeral cup on the contact mechanics and subsequent articular wear of RTSA implants. Furthermore, changes in component orientation, previously demonstrated to reduce the risk for scapular notching, will also be explored for its effects on articular contact mechanics.

1.5.1   Objectives

1) To evaluate the effects of humeral cup impingement damage on the contact mechanics of RTSA implants during abduction. Specifically, this will include:

   a) Investigating the change in location of articular contact and stress distribution with the modeling of humeral cup scapular notching damage.

   b) Ascertaining if there are further implications on articular contact mechanics with the progression of the simulated defect.

2) To perform wear test on commercially available RTSA implants with simulated notching damage. Specifically this is to determine if the introduction and propagation of simulated defects of the humeral cup, representative of notching damage, affects the early wear rates of high-mobility polyethylene humeral cups.

3) To investigate the effects of glenosphere orientation on the contact mechanics of RTSA implants during abduction. Moreover, this encompasses determining the effect of inferiorly tilting the glenosphere on the articular contact area and contact stress in RTSA.

1.5.2   Hypotheses

Hypothesis 1:

a) Simulated impingement damage of the humeral cups will result in reduced contact area, with an increase in contact stress values specifically around the region of damage in the inferior quadrant.

b) Increasing scapular notching damage of the humeral cup will result in a further decrease of the articular contact mechanics parameters assessed.

Hypothesis 2:

Simulated damage from scapular notching will cause an increased in observed early wear rates, particularly located within the remaining inferior quadrant of the humeral cup.

Hypothesis 3:

Inferior tilting of the glenosphere will result in improved contact mechanics (increased contact area, decreased maximum stress values), specifically at low angles of abduction.

1.6 Thesis Overview

Chapter 2 describes the investigation of RTSA contact mechanics with increasing levels of simulated scapular notching damage of the humeral cup during abduction. Specifically, this is to ascertain the effects this damage has on articular contact area and stress as they relate to wear morphology and continued performance.

Chapter 3 describes the results of a wear test of high-mobility, 38 mm DePuy Delta XTEND™ RTSA implants with the introduction of simulated scapular notching damage of the humeral cup. Wear rates as well as surface morphology was used in analyzing the wear characteristics.

Chapter 4 investigates the effect of inferior glenosphere tilt on the articular contact mechanics of RTSA implants during abduction. Contact area and stress distribution will be used to assess the implications of this change in component orientation.

Chapter 5 offers a cumulative discussion of the above work, drawing connections between each section's conclusion highlighting the relation of aspects from separate chapters.

1.7 References

Ackland, D. C., Roshan-Zamir, S., Richardson, M., & Pandy, M. G. (2010). Moment arms of the shoulder musculature after reverse total shoulder arthroplasty. *The Journal of Bone and Joint surgery.American Volume*, *92*(5), 1221–1230. http://doi.org/10.2106/JBJS.I.00001 [doi]

Affatato, S., Bersaglia, G., Rocchi, M., Taddei, P., Fagnano, C., & Toni, A. (2005). Wear behaviour of cross-linked polyethylene assessed in vitro under severe conditions. *Biomaterials*, *26*(16), 3259–3267. http://doi.org/10.1016/j.biomaterials.2004.07.070

Berhouet, J., Garaud, P., & Favard, L. (2014). Evaluation of the role of glenosphere design and humeral component retroversion in avoiding scapular notching during reverse shoulder arthroplasty. *Journal of Shoulder and Elbow Surgery*, *23*(2), 151–158. http://doi.org/10.1016/j.jse.2013.05.009

Bistolfi, A., Turell, M. B., Lee, Y., & Bellare, A. (2009). Tensile and Tribological Properties of High-Crystallinity Radiation Crosslinked UHMWPE. *Journal of Biomedical Materials Research Part B: Applied Biomaterials*, *90*(1), 137–144. http://doi.org/10.1002/jbm.b.31265

Bloch, H. R., Budassi, P., Bischof, A., Agneskirchner, J., Domenghini, C., Frattini, M., … Castagna, A. (2014). Influence of glenosphere design and material on clinical outcomes of reverse total shoulder arthroplasty. *Shoulder & Elbow*, *6*(3), 156–164. http://doi.org/10.1177/1758573214535574

Boileau, P., Watkinson, D., Hatzidakis, A. M., & Hovorka, I. (2006). Neer Award 2005: The Grammont reverse shoulder prosthesis: Results in cuff tear arthritis, fracture sequelae, and revision arthroplasty. *Journal of Shoulder and Elbow Surgery*, *15*(5), 527–540. http://doi.org/10.1016/j.jse.2006.01.003

Boileau, P., Watkinson, D. J., Hatzidakis, A. M., & Balg, F. (2005). Grammont reverse prosthesis: Design, rationale, and biomechanics. *Journal of Shoulder and Elbow Surgery*, *14*(1), S147–S161. http://doi.org/10.1016/j.jse.2004.10.006

Brandt, J.-M., Briere, L. K., Marr, J., Macdonald, S. J., Bourne, R. B., & Medley, J. B. (2010). Biochemical comparisons of osteoarthritic human synovial fluid with calf sera used in knee simulator wear testing. *Journal of Biomedical Materials Research A*, *94A*(3), 961–971. http://doi.org/10.1002/jbm.a.32728

Brandt, J.-M., Charron, K. D. J., Zhao, L., Macdonald, S. J., & Medley, J. B. (2011). Commissioning of a displacement-controlled knee wear simulator and exploration of some issues related to the lubricant. *Journal of Engineering in Medicine*, *225*(Part H), 736–752. http://doi.org/10.1177/0954411911406061

Brandt, J.-M., Charron, K., Zhao, L., Macdonald, S. J., & Medley, J. B. (2012). Calf serum constituent fractions influence polyethylene wear and microbial growth in knee simulator testing. *Journal of Engineering in Medicine*, *226*(6), 427–440. http://doi.org/10.1177/0954411912444248

Brandt, J.-M., Vecherya, A., Guenther, L. E., Koval, S. F., Petrak, M. J., Bohm, E. R., & Wyss, U. P. (2014). Wear testing of crosslinked polyethylene : Wear rate variability and microbial contamination. *Journal of the Mechanical Behavior of Biomedical Materials*, *34*, 208–216. http://doi.org/10.1016/j.jmbbm.2014.02.016

Capello, W. N., D'Antonio, J. a., Ramakrishnan, R., & Naughton, M. (2011). Continued improved wear with an annealed highly cross-linked polyethylene. *Clinical Orthopaedics and Related Research*, *469*(3), 825–830. http://doi.org/10.1007/s11999-010-1556-5

Carpenter, S., Pinkas, D., Newton, M. D., Kurdziel, M. D., Baker, K. C., & Wiater, J. M. (2015). Wear rates of retentive versus nonretentive reverse total shoulder arthroplasty liners in an in vitro wear simulation. *Journal of Shoulder and Elbow Surgery*, *24*(9), 1372–1379. http://doi.org/10.1016/j.jse.2015.02.016

Castagna, A., Delcogliano, M., De Caro, F., Ziveri, G., Borroni, M., Gumina, S., … De Biase, C. F. (2013). Conversion of shoulder arthroplasty to reverse implants: Clinical and radiological results using a modular system. *International Orthopaedics*, *37*(7), 1297–1305. http://doi.org/10.1007/s00264-013-1907-4

Chae, S. W., Lee, H., Kim, S. M., Lee, J., Han, S., & Kim, S. (2016). Primary Stability of Inferior Tilt Fixation of the Glenoid Component in Reverse Total Shoulder Arthroplasty : A Finite Element Study. *Journal of Orthopaedic Research*, (June), 1061–1068. http://doi.org/10.1002/jor.23115

Chae, S. W., Lee, J., Han, S. H., & Kim, S. (2015). Inferior tilt fixation of the glenoid component in reverse total shoulder arthroplasty : A biomechanical study. *Orthopaedics & Traumatology: Surgery & Research*, *101*(4), 421–425. http://doi.org/10.1016/j.otsr.2015.03.009

Clouthier, A. L., Hetzler, M. A., Fedorak, G., Bryant, J. T., Deluzio, K. J., & Bicknell, R. T. (2013). Factors affecting the stability of reverse shoulder arthroplasty : a biomechanical study. *Journal of Shoulder and Elbow Surgery*, *22*(4), 439–444. http://doi.org/10.1016/j.jse.2012.05.032

Cuff, D., Pupello, D., Virani, N., Levy, J., & Frankle, M. (2008). Reverse Shoulder Arthroplasty for the Treatment of Rotator Cuff Deficiency. *The Journal of Bone and Joint Surgery*, *90–A*(6), 1244–1251. http://doi.org/10.2106/JBJS.G.00775

Culham, E., & Peat, M. (1993). Functional Anatomy of the Shoulder Complex. *Journal of Orthopedic & Sports Physical Therapy*, *18*(1), 342–350.

Day, J. S., MacDonald, D. W., Olsen, M., Getz, C., Williams, G. R., & Kurtz, S. M. (2012). Polyethylene wear in retrieved reverse total shoulder components. *Journal of Shoulder and Elbow Surgery*, *21*(5), 667–674. http://doi.org/10.1016/j.jse.2011.03.012

de Wilde, L. F., Poncet, D., Middernacht, B., & Ekelund, A. (2010). Prosthetic overhang is the most effective way to prevent scapular conflict in a reverse total shoulder prosthesis. *Acta Orthopaedica*, *81*(6), 719–726. http://doi.org/10.3109/17453674.2010.538354

Denard, P. J., Lederman, E., Parsons, B. O., & Romeo, A. A. (2016). Finite element analysis of glenoid-sided lateralization in reverse shoulder arthroplasty. *Journal of Orthopaedic Research*, *35*(7), 1548–1555. http://doi.org/10.1002/jor.23394

DesJardins, J., Aurora, A., Tanner, S. L., Pace, T. B., Acampora, K. B., & Laberge, M. (2006). Increased total knee arthroplasty ultra-high molecular weight polyethylene wear using a clinically relevant hyaluronic acid simulator lubricant. *Journal of Engineering in Medicine*, *220*(Part H), 609–623. http://doi.org/10.1243/09544119JEIM30

Dieckmann, R., Liem, D., Gosheger, G., Henrichs, M. P., Höll, S., Hardes, J., & Streitbürger, A. (2013). Evaluation of a reconstruction reverse shoulder for tumour surgery and tribological comparision with an anatomical shoulder arthroplasty. *International Orthopaedics*, *37*(3), 451–456. http://doi.org/10.1007/s00264-012-1771-7

Ek, E. T. H., Neukom, L., Catanzaro, S., & Gerber, C. (2013). Reverse total shoulder arthroplasty for massive irreparable rotator cuff tears in patients younger than 65 years old: Results after five to fifteen years. *Journal of Shoulder and Elbow Surgery*, *22*(9), 1199–1208. http://doi.org/10.1016/j.jse.2012.11.016

Farshad, M., & Gerber, C. (2010). Reverse total shoulder arthroplasty-from the most to the least common complication. *International Orthopaedics*, *34*(8), 1075–1082. http://doi.org/10.1007/s00264-010-1125-2

Flury, M. P., Frey, P., Goldhahn, J., Schwyzer, H. K., & Simmen, B. R. (2011). Reverse shoulder arthroplasty as a salvage procedure for failed conventional shoulder replacement due to cuff failure-midterm results. *International Orthopaedics*, *35*(1), 53–60. http://doi.org/10.1007/s00264-010-0990-z

Gutiérrez, S., Comiskey, C. A., Luo, Z.-P., Pupello, D. R., & Frankle, M. A. (2008). Range of Impingement-Free Abduction and Adduction Deficit After Reverse Shoulder Arthroplasty. *The Journal of Bone and Joint Surgery-American Volume*, *90*(12), 2606–2615. http://doi.org/10.2106/JBJS.H.00012

Gutiérrez, S., Greiwe, R. M., Frankle, M. A., Siegal, S., & Lee, W. E. (2007). Biomechanical comparison of component position and hardware failure in the reverse shoulder prosthesis. *Journal of Shoulder and Elbow Surgery*, *16*(3 SUPPL.), 9–12. http://doi.org/10.1016/j.jse.2005.11.008

Gutiérrez, S., Keller, T. S., Levy, J. C., Lee, W. E. I., & Zong-Ping, L. (2008). Hierarchy of Stability Factors in Reverse Shoulder Arthroplasty Hierarchy of Stability Factors in Reverse Shoulder Arthroplasty. *Clinical Orthopaedics and Related Research*, *446*(3), 670–676. http://doi.org/10.1007/s11999-007-0096-0

Gutiérrez, S., Luo, Z. P., Levy, J., & Frankle, M. A. (2009). Arc of motion and socket depth in reverse shoulder implants. *Clinical Biomechanics*, *24*(6), 473–479. http://doi.org/10.1016/j.clinbiomech.2009.02.008

Gutiérrez, S., Walker, M., Willis, M., Pupello, D. R., & Frankle, M. A. (2011). Effects of tilt and glenosphere eccentricity on baseplate/bone interface forces in a computational model, validated by a mechanical model, of reverse shoulder arthroplasty. *Journal of Shoulder and Elbow Surgery*, *20*(5), 732–739. http://doi.org/10.1016/j.jse.2010.10.035

Haider, H., Sperling, J., & Throckmorton, T. (2013). A Method For Wear Testing Of Reverse Shoulder Arthroplasty Systems. *Bone & Joint Journal Orthopaedic Proceedings Supplement*, *95–B*(SUPP 34), 607.

Halder, A. M., Itoi, E., & An, K.-N. (2000). Anatomy and Biomechanics of the Shoulder. *Orthopedic Clinics of North America*, *31*(2), 159–176.

Hallab, N. J., & Jacobs, J. J. (2009). Biologic effects of implant debris. *Bulletin of the NYU Hospital for Joint Diseases*, *67*(2), 182–188.

Inman, V. T., Saunders, J. B. deC. M., & Abbott, L. C. (1996). Observations on the Function of the Shoulder Joint. 1944. *Clinical Orthopaedics and Related Research*, *330*, 3–12.

Kempton, L. B., Balasubramaniam, M., Ankerson, E., & Wiater, J. M. (2011). A radiographic analysis of the effects of glenosphere position on scapular notching following reverse total shoulder arthroplasty. *Journal of Shoulder and Elbow Surgery*, *20*(6), 968–974. http://doi.org/10.1016/j.jse.2010.11.026

Kilgour, A., & Elfick, A. (2009). Influence of crosslinked polyethylene structure on wear of joint replacements. *Tribology International*, *42*(11–12), 1582–1594. http://doi.org/10.1016/j.triboint.2008.11.011

Kohut, G., Dallmann, F., & Irlenbusch, U. (2012). Wear-induced loss of mass in reversed total shoulder arthroplasty with conventional and inverted bearing materials. *Journal of Biomechanics*, *45*(3), 469–473. http://doi.org/10.1016/j.jbiomech.2011.11.055

Langohr, G. D. G. (2015). *Fundamentals of the Biomechanical Characteristics Related to the Loading of Reverse Total Shoulder Arthroplasty Implants and the Development of a Wear Simulation Strategy*.

Langohr, G. D. G., Athwal, G. S., Johnson, J. A., & Medley, J. B. (2016). Wear simulation strategies for reverse shoulder arthroplasty implants. *Journal of Engineering in Medicine*, *230*(5), 458–469. http://doi.org/10.1177/0954411916642801

Langohr, G. D. G., Giles, J. W., Athwal, G. S., & Johnson, J. A. (2015). The effect of glenosphere diameter in reverse shoulder arthroplasty on muscle force, joint load, and range of motion. *Journal of Shoulder and Elbow Surgery*, *24*(6), 972–979. http://doi.org/10.1016/j.jse.2014.10.018

Langohr, G. D. G., Willing, R., Medley, J. B., Athwal, G. S., & Johnson, J. A. (2016). Contact mechanics of reverse total shoulder arthroplasty during abduction: The effect of neck-shaft angle, humeral cup depth, and glenosphere diameter. *Journal of Shoulder and Elbow Surgery*, *25*(4), 589–597. http://doi.org/10.1016/j.jse.2015.09.024

Lévigne, C., Garret, J., Boileau, P., Alami, G., Favard, L., & Walch, G. (2011). Scapular notching in reverse shoulder arthroplasty: Is it important to avoid it and how? *Clinical Orthopaedics and Related Research*, *469*(9), 2512–2520. http://doi.org/10.1007/s11999-010-1695-8

Marieb, E. N. (2012). *Essentials of Human Anatomy and Physiology* (10th ed.). San Francisco: Pearson.

McCalden, R. W., MacDonald, S. J., Rorabeck, C. H., Bourne, R. B., Chess, D. G., & Charron, K. D. (2009). Wear Rate of Highly Cross-Linked Polyethylene in Total Hip Arthroplasty. *Journal of Bone and Joint Surgery*, *91A*(4), 773–782. http://doi.org/10.2106/JBJS.H.00244

McMahon, P. J., Debski, R. E., Thompson, W. O., Warner, J. J. P., Fu, F. H., & Woo, S. L. (1995). Shoulder muscle forces and tendon excursions during glenohumeral abduction in the scapular plane. *Journal of Shoulder and Elbow Surgery*, *4*(3), 199–208.

Mollon, B., Mahure, S. A., Roche, C. P., & Zuckerman, J. D. (2017). Impact of scapular notching on clinical outcomes after reverse total shoulder arthroplasty: an analysis of 476 shoulders. *Journal of Shoulder and Elbow Surgery*, *26*(7), 1253–1261. http://doi.org/10.1016/j.jse.2016.11.043

Muh, S. J., Streit, J. J., Wanner, J. P., Lenarz, C. J., Shishani, Y., Rowland, D. Y., … Gobezie, R. (2013). Early follow-up of reverse total shoulder arthroplasty in patients sixty years of age or younger. *The Journal of Bone and Joint Surgery. American Volume*, *95*(20), 1877–83. http://doi.org/10.2106/JBJS.L.10005

Mulieri, P., Dunning, P., Klein, S., Pupello, D., & Frankle, M. (2010). Reverse shoulder arthroplasty for the treatment of irreparable rotator cuff tear without glenohumeral arthritis. *The Journal of Bone and Joint Surgery. American Volume*, *92*(15), 2544–56. http://doi.org/10.2106/JBJS.I.00912

Nam, D., Kepler, C. K., Nho, S. J., Craig, E. V, Warren, R. F., & Wright, T. M. (2010). Observations on retrieved humeral polyethylene components from reverse total shoulder arthroplasty. *Journal of Shoulder and Elbow Surgery*, *19*(7), 1003–1012. http://doi.org/10.1016/j.jse.2010.05.014

Nolan, B. M., Ankerson, E., & Wiater, M. J. (2011). Reverse total shoulder arthroplasty improves function in cuff tear arthropathy. *Clinical Orthopaedics and Related Research*, *469*(9), 2476–2482. http://doi.org/10.1007/s11999-010-1683-z

Nyffeler, R. W., Werner, C. M. L., & Gerber, C. (2005). Biomechanical relevance of glenoid component positioning in the reverse Delta III total shoulder prosthesis. *Journal of Shoulder and Elbow Surgery*, *14*(5), 524–528. http://doi.org/10.1016/j.jse.2004.09.010

Nyffeler, R. W., Werner, C. M. L., Simmen, B. R., & Gerber, C. (2004). Analysis of a retrieved Delta III total shoulder prosthesis. *The Journal of Bone and Joint Surgery*, *86*(8), 1187–1191. http://doi.org/10.1302/0301-620X.86B8.15228

Oh, J. H., & Choi, J. H. (2013). Current Concepts of Arthroplasty for the Treatment of Massive Rotator Cuff Tears. *Journal of the Korean Orthopaedic Association*, *48*, 78–87. http://doi.org/10.4055/jkoa.2013.48.1.78

Oh, J. H., Shin, S. J., McGarry, M. H., Scott, J. H., Heckmann, N., & Lee, T. Q. (2014). Biomechanical effects of humeral neck-shaft angle and subscapularis integrity in reverse total shoulder arthroplasty. *Journal of Shoulder and Elbow Surgery*, *23*(8), 1091–1098. http://doi.org/10.1016/j.jse.2013.11.003

Oonishi, H., Kim, S. C., Takao, Y., Kyomoto, M., Iwamoto, M., & Ueno, M. (2006). Wear of highly cross-linked polyethylene acetabular cup in Japan. *The Journal of Arthroplasty*, *21*(7), 944–949. http://doi.org/10.1016/j.arth.2006.03.009

Pastor, M., Kraemer, M., Wellmann, M., Hurschler, C., & Smith, T. (2016). Anterior stability of the reverse shoulder arthroplasty depending on implant configuration and rotator cuff condition. *Archives of Orthopaedic and Trauma Surgery*, *136*(11), 1513–1519. http://doi.org/10.1007/s00402-016-2560-3

Peers, S., Moravek, J. E., Budge, M. D., Newton, M. D., Kurdziel, M. D., Baker, K. C., & Wiater, J. M. (2015). Wear rates of highly cross-linked polyethylene humeral liners subjected to alternating cycles of glenohumeral flexion and abduction. *Journal of Shoulder and Elbow Surgery*, *24*(1), 143–149. http://doi.org/10.1016/j.jse.2014.05.001

Permeswaran, V. N., Goetz, J. E., Rudert, M. J., Hettrich, C. M., & Anderson, D. D. (2016). Cadaveric validation of a finite element modeling approach for studying scapular notching in reverse shoulder arthroplasty. *Journal of Biomechanics*, *49*(13), 3069–3073. http://doi.org/10.1016/j.jbiomech.2016.07.007

Pruitt, L. A. (2005). Deformation , yielding , fracture and fatigue behavior of conventional and highly cross-linked ultra high molecular weight polyethylene. *Biomaterials*, *26*, 905–915. http://doi.org/10.1016/j.biomaterials.2004.03.022

Pruitt, L. A., Ansari, F., Kury, M., Mehdizah, A., Patten, E. W., Huddlestein, J., … Ries, M. D. (2013). Clinical trade-offs in cross-linked ultrahigh-molecular-weight polyethylene used in total joint arthroplasty. *Journal of Biomedical Materials Research Part B: Applied Biomaterials*, *10B*(3), 476–484. http://doi.org/10.1002/jbm.b.32887

Rader, C. P., Sterner, T., Jakob, F., Schütze, N., & Eulert, J. (1999). Cytokine response of human macrophage-like cells after contact with polyethylene and pure titanium particles. *Journal of Arthroplasty*, *14*(7), 840–848. http://doi.org/10.1016/S0883-5403(99)90035-9

Randelli, P., Randelli, F., Arrigoni, P., Ragone, V., Masuzzo, P., Cabitza, P., & Banfi, G. (2014). Optimal glenoid component inclination in reverse shoulder arthroplasty . How to improve implant stability. *Musculoskeletal Surgery*, *98*, 15–18. http://doi.org/10.1007/s12306-014-0324-1

Reinders, J., Sonntag, R., & Kretzer, J. P. (2015). Synovial Fluid Replication in Knee Wear Testing : An Investigation of the Fluid Volume. *Journal of Orthopa*, (January), 92–97. http://doi.org/10.1002/jor.22736

Roche, C., Flurin, P. H., Wright, T., Crosby, L. A., Mauldin, M., & Zuckerman, J. D. (2009). An evaluation of the relationships between reverse shoulder design parameters and range of motion, impingement, and stability. *Journal of Shoulder and Elbow Surgery*, *18*(5), 734–741. http://doi.org/10.1016/j.jse.2008.12.008

Samuelson, E. M., Cordero, G. X., & Fehringer, E. V. (2009). Fracture of a Reverse Total Shoulder Arthroplasty Retentive Liner. *Orthopedics*, *32*(3), 2–6. http://doi.org/10.3928/01477447-20090301-25

Scholes, S. C., & Joyce, T. J. (2013). In vitro tests of substitute lubricants for wear testing orthopaedic biomaterials. *Journal of Engineering in*, *227*(6), 693–703. http://doi.org/10.1177/0954411913481549

Schwenke, T., Kaddick, C., Schneider, E., & Wimmer, M. A. (2005). Fluid composition impacts standardized testing protocols in ultrahigh molecular weight polyethylene knee wear testing. *Journal of Engineering in Medicine*, *219*(Part H), 457–464. http://doi.org/10.1243/095441105X34392

Sharkey, N. A., Marder, R. A., & Hanson, P. B. (1994). The Entire Rotator Cuff Contributes to Elevation of the Arm. *Journal of Orthopaedic Research*, *12*(5), 699–708.

Sirveaux, F., Favard, L., Oudet, D., Huquet, D., Walch, G., & Molé, D. (2004). Grammont inverted total shoulder arthroplasty in the treatment of glenohumeral osteoarthritis with massive rupture of the cuff. *The Journal of Bone and Joint Surgery*, *86*(3), 388–395. http://doi.org/10.1302/0301-620X.86B3.14024

Smith, S. L., Li, B. L., Buniya, A., Lin, S. H., Scholes, S. C., Johnson, G., & Joyce, T. J. (2015). In vitro wear testing of a contemporary design of reverse shoulder prosthesis. *Journal of Biomechanics*, *48*(12), 3072–3079. http://doi.org/10.1016/j.jbiomech.2015.07.022

Tashjian, R. Z., Burks, R. T., Zhang, Y., & Henninger, H. B. (2015). Reverse total shoulder arthroplasty: A biomechanical evaluation of humeral and glenosphere hardware configuration. *Journal of Shoulder and Elbow Surgery*, *24*(3), e68–e77. http://doi.org/10.1016/j.jse.2014.08.017

Terrier, A., Merlini, F., Farron, A., & Pioletti, D. P. (2009). Reverse shoulder arthroplasty: polyethylene wear. *Computer Methods in Biomechanics and Biomedical Engineering*, *12*(sup1), 247–248. http://doi.org/10.1080/10255840903097855

Torrens, C., Guirro, P., Miquel, J., & Santana, F. (2016). Influence of glenosphere size on the development of scapular notching: a prospective randomized study. *Journal of Shoulder and Elbow Surgery*, *25*(11), 1735–1741. http://doi.org/10.1016/j.jse.2016.07.006

Vaupel, Z. M., Baker, K. C., Kurdziel, M. D., & Wiater, J. M. (2012). Wear simulation of reverse total shoulder arthroplasty systems: effect of glenosphere design. *Journal of Shoulder and Elbow Surgery*, *21*(10), 1422–1429. http://doi.org/10.1016/j.jse.2011.10.024

Wang, A., Essner, A., & Schmidig, G. (2003). The Effects of Lubricant Composition on in Vitro Wear Testing of Polymeric Acetabular Components. *Journal of Biomedical Materials Research Part B: Applied Biomaterials*, *68B*(1), 45–52. http://doi.org/10.1002/jbm.b.10077

Weber-Spickschen, T. S., Alfke, D., & Agneskirchner, J. D. (2015). The use of a modular system to convert an anatomical total shoulder arthroplasty to a reverse shoulder arthroplasty: Clinical and radiological results. *Bone and Joint Journal*, *97B*(12), 1662–1667. http://doi.org/10.1302/0301-620X.97B12.35176

Werner, B. S., Boehm, D., & Gohlke, F. (2013). Revision to reverse shoulder arthroplasty with retention of the humeral component. *Acta Orthopaedica*, *84*(5), 473–478. http://doi.org/10.3109/17453674.2013.842433

Wiater, B. P., Baker, E. A., Salisbury, M. R., Koueiter, D. M., Baker, K. C., Nolan, B. M., & Wiater, J. M. (2015). Elucidating trends in revision reverse total shoulder arthroplasty procedures: a retrieval study evaluating clinical, radiographic, and functional outcomes data. *Journal of Shoulder and Elbow Surgery*, *24*(12), 1915–1925. http://doi.org/10.1016/j.jse.2015.06.004

Wirth, M. A., Klotz, C., Deffenbaugh, D. L., McNulty, D., Richards, L., & Tipper, J. L. (2009). Cross-linked glenoid prosthesis: a wear comparison to conventional glenoid prosthesis with wear particulate analysis. *Journal of Shoulder and Elbow Surgery*, *18*(1), 130–137. http://doi.org/10.1016/j.jse.2008.06.015

Yanagawa, T., Goodwin, C. J., Shelburne, K. B., Giphart, J. E., Torry, M. R., & Pandy, M. G. (2008). Contributions of the Individual Muscles of the Shoulder to Glenohumeral Joint Stability. *Journal of Biomechanical Engineering*, *130*(April 2008), 021024.1-021024.9. http://doi.org/10.1115/1.2903422

Young, S. W., Everts, N. M., Ball, C. M., Astley, T. M., & Poon, P. C. (2009). The SMR reverse shoulder prosthesis in the treatment of cuff-deficient shoulder conditions. *Journal of Shoulder and Elbow Surgery*, *18*(4), 622–626. http://doi.org/10.1016/j.jse.2009.01.017

Chapter 2

Effects of Scapular Notching Polyethylene Damage on the Contact Mechanics

OVERVIEW: While the observed incidence of scapular notching and its osseous damage is well reported in literature as documented in Chapter 1, there is very little described on the implications on reverse total shoulder arthroplasty (RTSA) implant performance. With the inferior region of the intact humeral cup having been demonstrated to be of particular importance in RTSA contact mechanics, the repercussions of damage from scapular notching in this region is of great concern. Therefore, the purpose of the present finite element study was to investigate the effects simulated notching damage has on articular contact mechanics.[1]

---

[1] A portion of the work covered in Chapter 1 is included within the introduction as part of the Integrated-Article format.

2.1   Introduction

As the name would imply, reverse total shoulder arthroplasty (RTSA) involves reversing the native geometry of the glenohumeral joint. RTSA can effectively treat several shoulder conditions, including those with severe rotator cuff tears in addition to the revision of failed shoulder arthroplasty (Castagna et al., 2013; Flury et al., 2011; Muh et al., 2013; Weber-Spickschen et al., 2015; Werner et al., 2013). However, these systems are not without their issues, with scapular notching being the most frequently arising complication (Farshad & Gerber, 2010). Nevertheless it's reported incidence has been quite variable, being observed to occur in 10% to 74% of cases of radiographic studies (Boileau et al., 2006, 2005; Ek et al., 2013; Flury et al., 2011; Lévigne et al., 2011; Mollon et al., 2017; Mulieri et al., 2010; Nolan et al., 2011; Sirveaux et al., 2004; Weber-Spickschen et al., 2015; Young et al., 2009), in addition to 45% to 100% of humeral cups included in surgical retrieval analysis studies (Day et al., 2012; Nam et al., 2010; Wiater et al., 2015).

Scapular notching occurs when the inferior aspect of the humeral cup component impinging against the scapula during adduction resulting in damage to the polyethylene component, as the stress values of the small area in contact exceeds the material's yield stress (Permeswaran et al., 2016). The resulting volumetric changes of the humeral cup along the inferior aspect progress and become quite severe, as depicted in Figure 2-1. Subsequent deposits of polyethylene debris result in the biologic notching of the scapula (Kohut et al., 2012) through macrophage mediated bone resorption, which increases in response to the concentration of polyethylene particulates (Hallab & Jacobs, 2009; Rader et al., 1999). RTSA implants are highly modular providing several strategies for altering the component geometry and placement which can serve to reduce the risk of scapular notching through a reduction in adduction deficit, as illustrated through several computer model and biomechanical studies.

Figure 2-1: Retrieved humeral cup with advanced defect from scapular notching highlighted (red outline)

Scapular notching is identified using radiographs and graded using the system described by Sirveaux et al (2004). This system is based on the extent of damage relative to the implant landmarks, with bone removal extending beyond the inferior fixation screw to the baseplate being classified as the most severe, as depicted in Figure 1-7 (Boileau et al., 2006; Sirveaux et al., 2004). Similarly, the extent of damage to the humeral cup can also be assessed upon retrieval. It has been reported by Day et al (2012) that impingement damage encompassed an 87° to 226° arc of the humeral cup surface, with a mean value of 136°. A comparable region of impingement damage was also reported by Nyffeler et al (2004), who observed damage covering 120° of the single humeral cup reported. The depth of the impingent scar has been reported to range between 0.1 mm and 4.7 mm, with a mean of 2.1 mm (Day et al., 2012). It should be noted that the most severe cases of humeral cup damage observed by Day et al (2012), as well as the single case investigated by Nyffeler et al (2004), contact with the locking screw had occurred to the extent of metal-on-metal contact with the rim of the epiphysis holding the humeral cup.

This inferomedial region of the humeral cup has been indicated to be a particularly important region with respect to articular contact. It has been demonstrated through finite element modelling to be the region of contact and the location of maximum contact stress values (Langohr, Willing, et al., 2016; Terrier et al., 2009), as well as the region with the most pronounce wear in simulation studies (Carpenter et al., 2015; Langohr, 2015; Langohr, Athwal, et al., 2016). Therefore, the objective of the present study was to evaluate the effect of the severity of scapular notching impingement damage on contact

mechanics through the use of finite element analysis. This will provide further understanding as to the implications of progressing impingement damage, given the importance of this region in RTSA articular contact mechanics. We hypothesized that increased scapular notching damage will result in a decreased articular contact area and an increased maximum contact stress that has shifted to the new inferior boundary formed at the notch margin.

2.2   Materials & Methods

2.2.1   Finite Element Modeling

A finite element model of a reverse total shoulder prosthesis, comprised of a 38 mm diameter glenosphere and standard depth (8.75 mm) humeral cup, was constructed in Abaqus v6.14 (Simulia Corp, Providence, RI, USA). The geometry and parameters for this model is based on that of previously published work in assessing the effect of implant design parameters (Langohr, Willing, et al., 2016), and consisted of only these two components in order to focus on their interactions. The humeral cup component was assigned linear elastic ultra-high-molecular-weight polyethylene (UHMWPE) material properties (E = 650 MPa, $v = 0.44$) (Kurtz et al., 2002; Pruitt, 2005), with three levels of simulated scapular notching damage being applied to the intact component. Alternatively, the glenosphere component was assigned cobalt-chrome (CoCr) material properties (E = 210 GPa, $v = 0.3$). The two components were meshed using linear hexahedral elements (C3D8R), with an average side length of approximately 0.3 mm (Figure 2-2), however the total number of elements varied for the assemblies. This resulted in a range of 220,000-450,000 elements for the assemblies (800,000-1,500,000 degrees of freedom), due to the alterations in the humeral cup geometry from the introduction and propagation of scapular notching damage. The back (non-articular) faces of each component were rigidly constrained, while surface-to-surface discretization was utilized in penalty-based contact with a coefficient of friction set at 0.04 (Godest, Beaugonin, Haug, Taylor, & Gregson, 2002; Willing & Kim, 2009) for the articular surface.
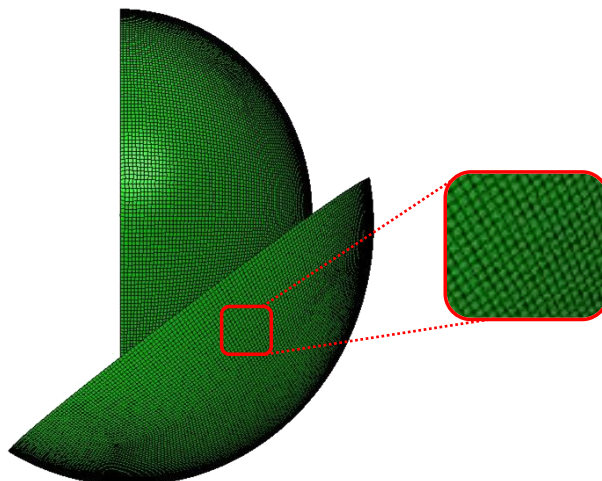
Figure 2-2: Component mesh for finite element model, highlighted within insert

Models of the humeral cup component with simulated defects from scapular notching damage were constructed in SolidWorks (v24.2, Dassault Systèmes, Waltham, MA, USA) Figure 2-3. The extent of damage for the levels of notching defects included were based on the values reported in the retrievals analyzed by Day et al (2012). The simulated defect models and their respective parameters (depth, width, and arc of articular surface encompassed) can be found in Figure 2-3. It should be noted that while these reflect the depth values progressing from the mean of the observations from Day et al (2012), the defects included are not as wide due to limitations in meshing. However, the most severe defect does encompass an arc within the range reported by Day et al (2012).

The glenosphere component remained in a fixed position while the humeral cup component articulated against it at humeroscapular abduction angles of 10° to 55° at 5° increments. The joint load profiles applied for the seven specimens (n = 7) included, as depicted in Figure 2-4, were discretized from previous works using instrumented reverse total shoulder prosthesis (Giles, Langohr, Johnson, & Athwal, 2015; Langohr et al., 2015) in a custom shoulder simulator (Giles, Ferreira, Athwal, & Johnson, 2014). However, the anterior-posterior load contributions were not included in the present model, due to the smaller relative magnitude compared to the compressive and shear components.

A)

Load Angle (∅) with respect to Glenosphere

Load Angle (θ) with respect to Humeral Cup

Joint Reaction Forces

10°-55° Humeroscapular Abduction Angle

B)

Intact Defect 1

Defect 2 Defect 3

Defect 1:
• 2 mm deep
• 14 mm wide **(53° arc)**

Defect 2:
• 3 mm deep
• 21 mm wide **(84° arc)**

Defect 3:
• 4 mm deep
• 23 mm wide **(94° arc)**
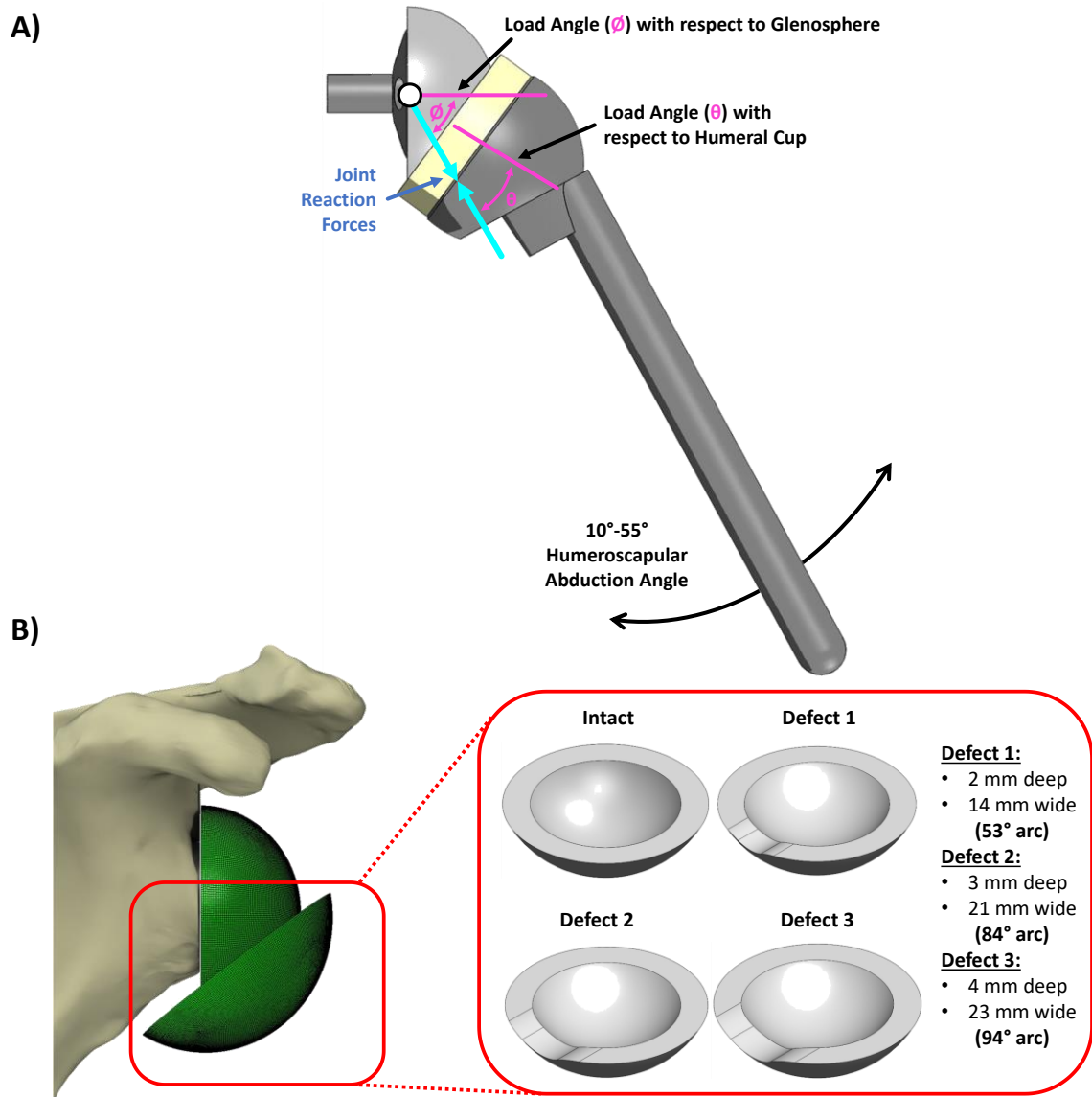
Figure 2-3: (A) Finite element model loading and boundary conditions with (B) simulated scapular notching defect conditions and parameters indicated

Note the scapula has been included in (B) for orientation purposes but was not included in the constructed model.
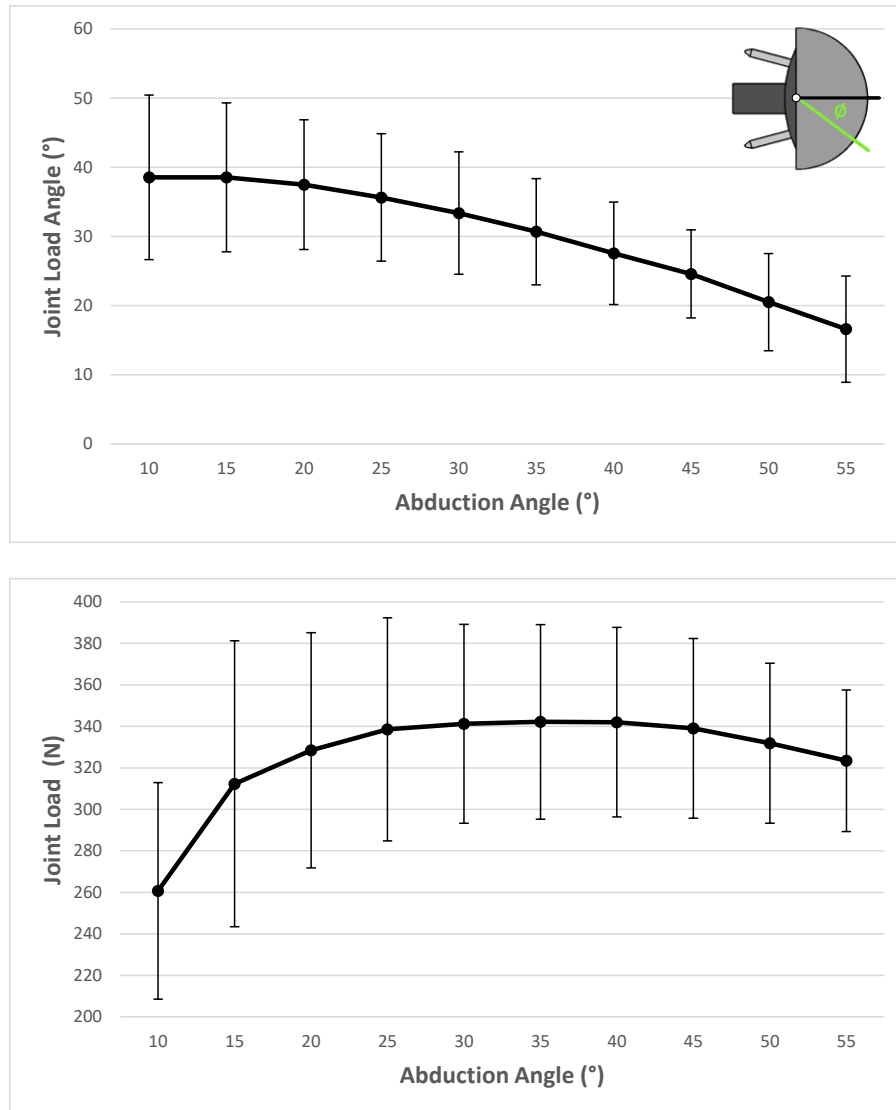
Figure 2-4: Joint load profiles simulated in finite element models

Mean joint load angle (±1 std dev; top), with respect to glenosphere (Ø), and mean joint load magnitudes (±1 std dev).

2.2.2   Testing Protocol & Outcome Variables

Finite element analysis for each of the seven specimen loading data was conducted for the intact humeral cup, as well as the three levels of simulated scapular notching with increasing severity. Only the interactions between the two components were analyzed, and osseous based factors such as scapular impingement were not considered. Maximum contact stress values of the humeral cup and the articular contact area were recorded for each angle of abduction in order to assess the contact mechanics, and was visualized using

stress distribution maps. A two-way repeated measures ANOVA ($\alpha = 0.05$) was conducted in SPSS (V25, IBM Corporation, Armonk, NY, USA) to evaluate each of the outcome variables, where level of defect and angle of abduction where the independent variables.

2.3 Results

As shown in Figure 2-5, both abduction angle and level of notching defect were found to have a significant effect on mean contact area ($p = 0.018$ and $p < 0.001$, respectively). This is visibly apparent with contact area increasing throughout lower angles of abduction, as well as the increase of notching resulting in decreased contact area beyond 25° abduction of the range tested. The intact state was found to be significantly different from all defect levels ($p < 0.001$ for all three stages of notching), resulting in a 6% (54.25 ± 28.27 mm^2), 7% (73.03 ± 28.27 mm^2), and 9% (90.76 ± 41.35 mm^2) decrease in contact area for each respective simulated defect relative to the intact state when observed across all angles of abduction tested. Each level of defect was also found to be significantly different from each other ($p \leq 0.013$ for all). While a significant relation between notching defect and abduction angle was determined ($p < 0.001$), no significance was observed between abduction levels ($p \geq 0.293$ for all).

From the maximum contact stress values (Figure 2-6), the progression of notching defect was found to have a significant effect ($p < 0.001$) as well as to have a significant relation with the angle of abduction ($p < 0.001$). Furthermore the intact state was found to differ significantly from all levels of simulated notching defect ($p < 0.001$ for all), resulting in a 32% (0.33 ± 0.20 MPa), 33% (0.31 ± 0.15 MPa), and 51% (0.48 ± 0.33 MPa) increase in maximum contact stress for each respective defect relative to the intact state when observed across all angles of abduction tested. However, unlike the trends noted for contact area, the severity of notching defect was not observed to have a significant effect between the different levels of notching defects ($p \geq 0.124$ between all stages of notching defect). Additionally, the angle of abduction was not observed to significantly affect the maximum contact stress ($p = 0.493$). In most cases the maximum contact stress was located on the most inferior region of contact or the inferior boundary of the humeral cup, be it the intact inferiomedial edge or more superior at the margin of the notch (Figure 2-7).
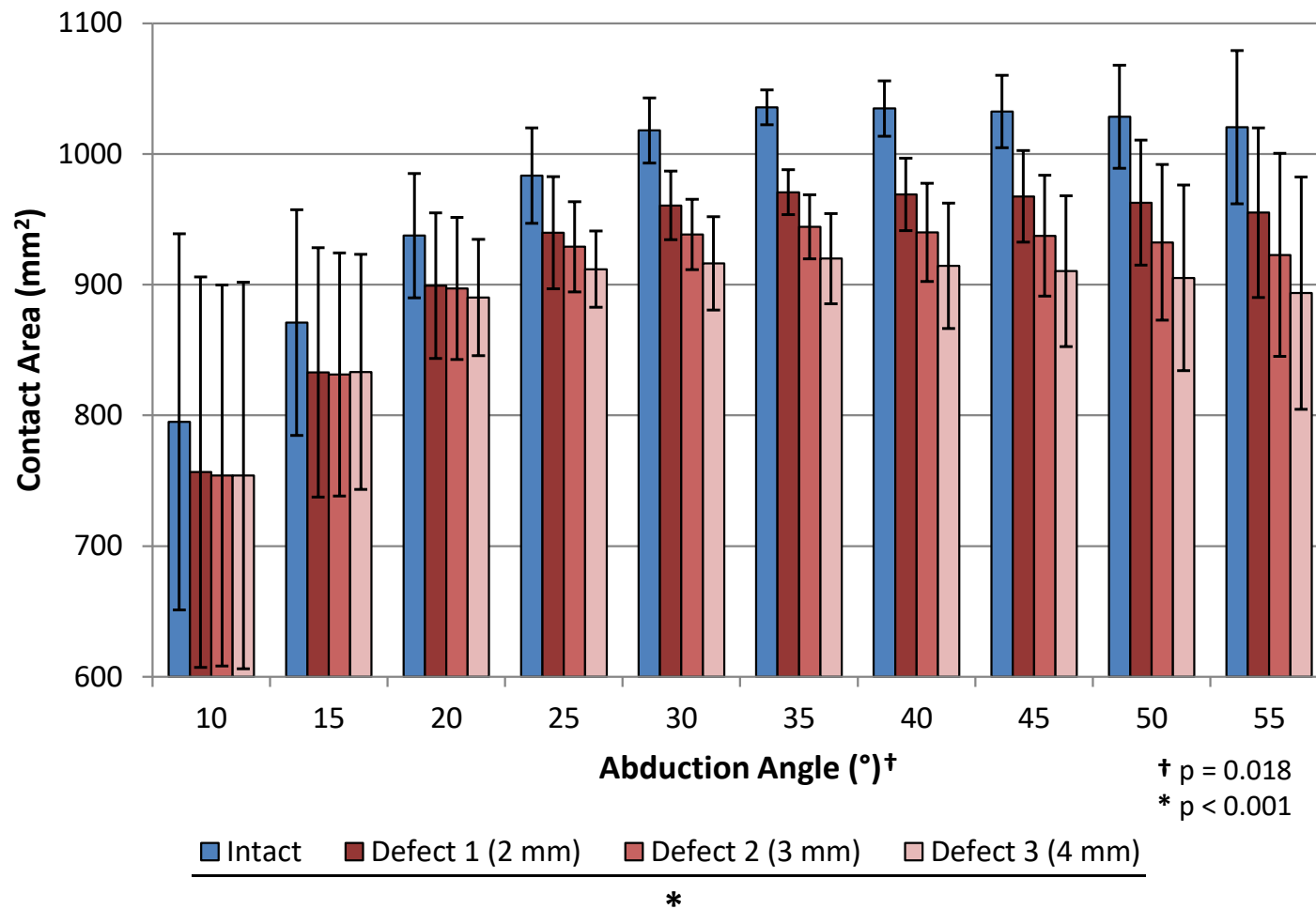
Figure 2-5: Mean contact area plot with increasing scapular notching damage

For all specimens investigated (±1 std dev) with intact humeral cup (blue) and progressive scapular notching depth (red).
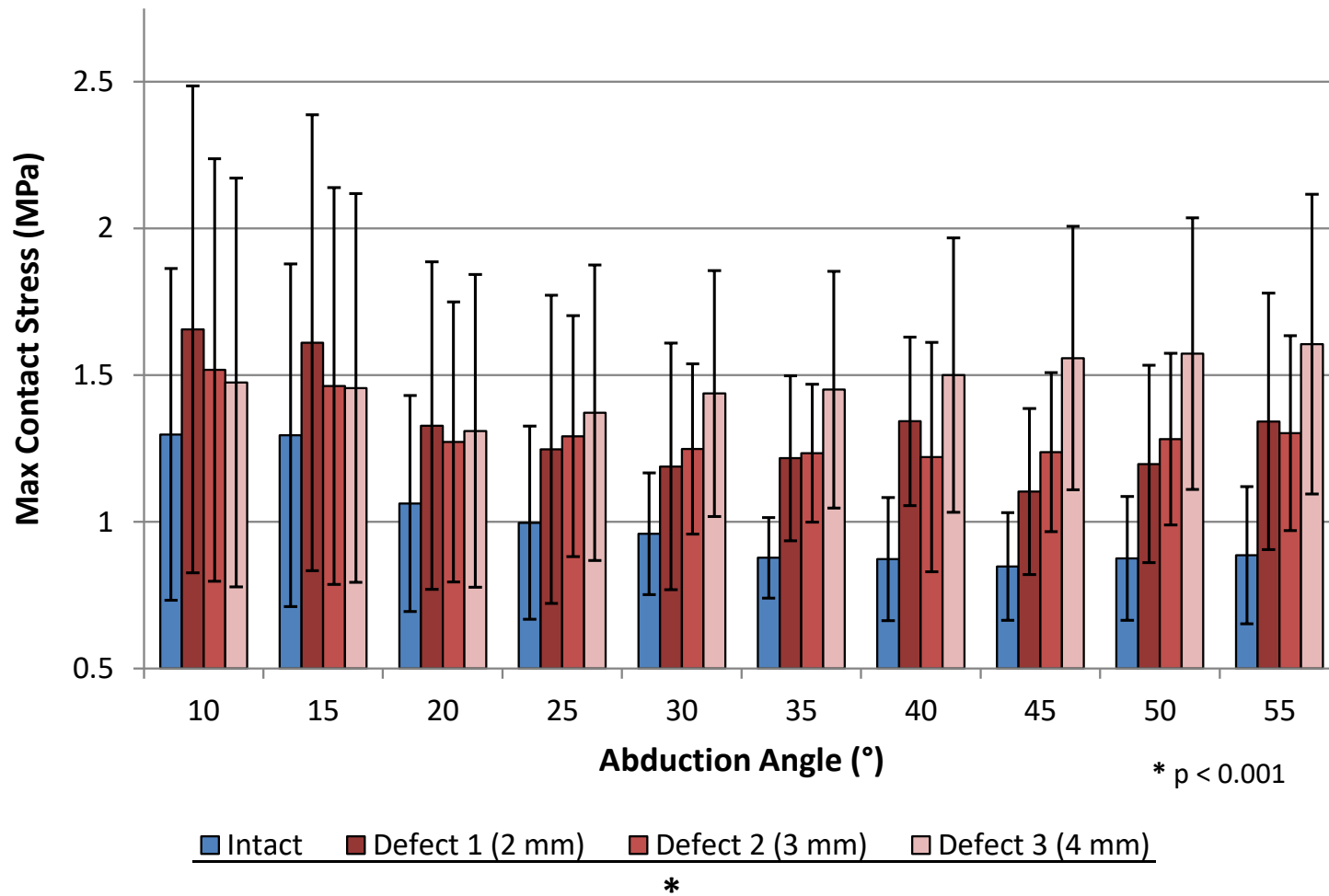
Figure 2-6: Mean maximum contact stress plot with increasing scapular notching damage

For all specimens investigated (±1 std dev) with intact humeral cup (blue) and progressive scapular notching depth (red).
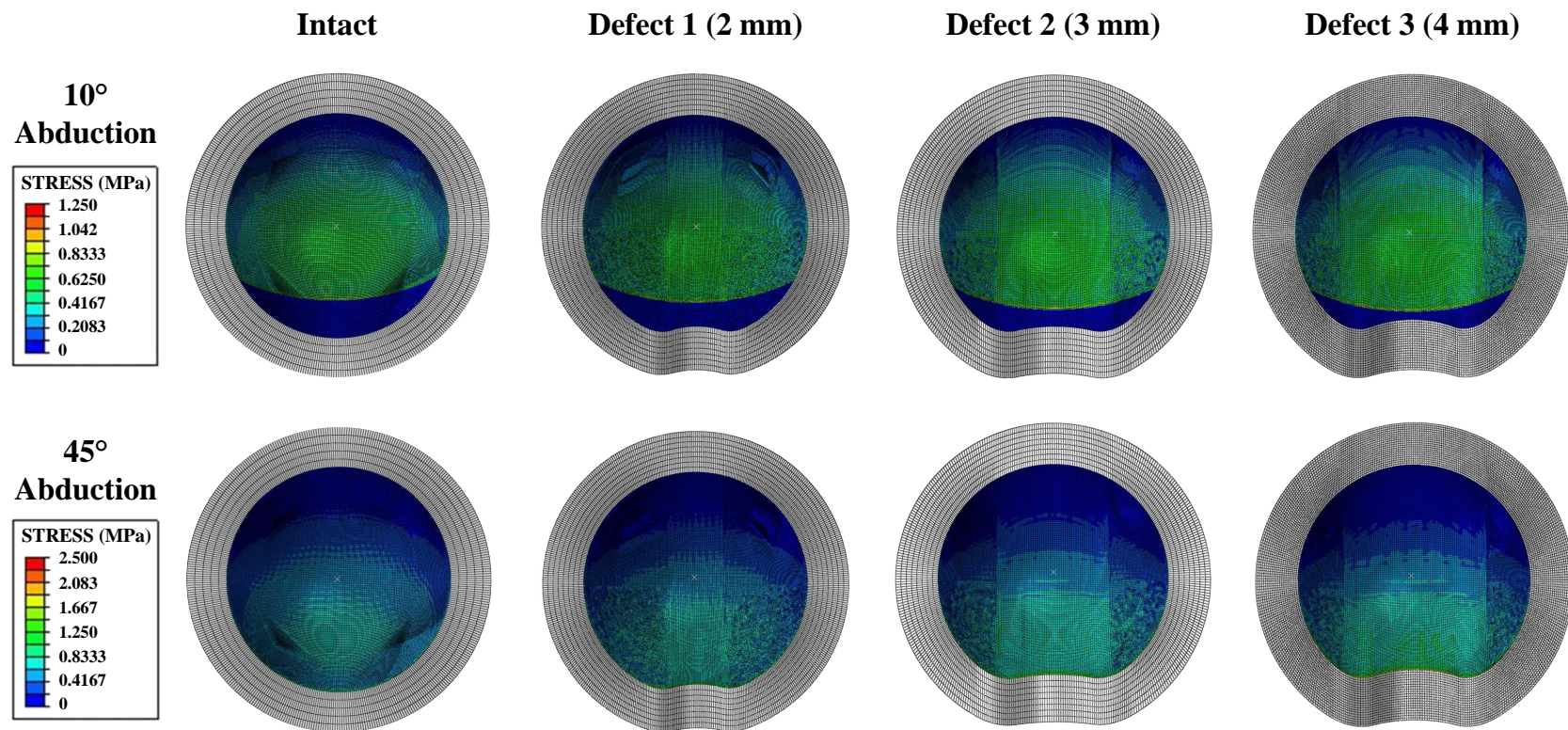
Figure 2-7: Humeral cup contact stress distribution maps for 10° and 45° abduction

All normalized to the same scale for each respective abduction angle for the intact and all notched states (indicated by depth parameter).

2.4 Discussion

As hypothesized, the simulation of progressive scapular notching humeral cup defects resulted in a deterioration of the assessed contact mechanic parameters. This was speculated by Langohr et al (2016), as the inferior edge of the humeral cup was indicated to play a crucial role in the performance of RTSA systems. This has been demonstrated to be the region of maximum contact stresses in finite element studies (Langohr, Willing, et al., 2016; Terrier et al., 2009). Of specific interest, the effects of scapular notching damage and its progression was largely only viewed beginning at 25° humeroscapular abduction. Until this point, the region of notching was not yet fully in contact with the glenosphere, due to the overhang of the humeral cup behind the medial edge of the glenosphere at low angles of abduction. This can be visualized in the stress distribution maps taken at 10° abduction (Figure 2-7), wherein the inferior aspect of the humeral cup is not yet under stress regardless of the extent of notching.

It is possible that through the degradation of contact mechanics from further damage of the humeral cup from scapular notching would result in an accompanying increase in wear within a region demonstrated to most frequently present with wear (Nam et al., 2010). Compounding this issue is that in addition to the articular wear debris, the resultant polyethylene particulate from the impingement damage which is generated in a greater proportion relative to abrasive wear (Kohut et al., 2012) would contribute to the biologic notching process and implant loosening. Subsequently, the overall integrity and longevity of the implant would be compromised. This is further exemplified in RTSA retrieval analysis, wherein damage resulting from scapular notching was visibly apparent in implants that had seen relatively little use, some less than fifteen months, indicating the fairly rapid onset of this damage mechanism (Day et al., 2012; Nyffeler et al., 2004). Furthermore, the resulting metallic particulate generated from contact between the inferior fixation screws and the epiphysis holding the humeral cup, as previously reported (Day et al., 2012; Nyffeler et al., 2004), would only serve to compound these aforementioned complications. It should be noted that while the depth parameters simulated for scapular notching humeral cup defects reflect that of the range described by Day et al (2012), the

arc of articular surface encompassed by the damage is less severe (Day et al., 2012; Nyffeler et al., 2004). Therefore if the trends of the current work continue to hold true, the effects of scapular notching damage on articular contact mechanics may actually be more severe than that observed.

Even though the results indicating an increased risk of articular polyethylene wear as a result of the increased contact stress this may not actually be the case. A wear simulation study which included a single specimen with simulated notching found little change in the wear rates between the intact and notched states (Langohr, Athwal, et al., 2016). While it is possible that the simulated impingement damage had not progressed to an extent of significantly altering the contact mechanics, this is of particular interest to note given the results of the present work.

Scapular notching is associated with a deterioration in clinical function in comparison to those without notching presenting in radiographic evaluation (Ek et al., 2013). Specifically, those with scapular notching have demonstrated decreased strength and active abduction (Lévigne et al., 2011; Mollon et al., 2017), as well as an increased overall complication rate (Mollon et al., 2017). While there were no increase of reported pain in either study (Lévigne et al., 2011; Mollon et al., 2017), the reduced function of the joint, especially given that notching was more common in active patients (Lévigne et al., 2011), highlights the undesirable consequences of this process.

Further complicating this matter would be the implications on activities of daily living and commonly employed ranges of motion for the shoulder. The distribution of shoulder abduction-adduction motion has been observed to be a bimodal distribution with one central peak around 0° humerothoracic abduction and a secondary peak near the extent of recorded motion when using motion tracking, however these tended to vary depending on the occupational or recreational tasks (Kirking, El-Gohary, & Kwon, 2016). Overall, the mean 50th and 95th percentile values for abduction were 5.6° and 128.4° humerothoracic abduction respectively (Kirking et al., 2016). Furthermore, in a motion tracking study of shoulder arthroplasty patients, including those with RTSA, found that abduction angles below 80° humerothoracic abduction comprised $98 \pm 26\%$ of daily motion for the operated

shoulder, which was not observed to significantly differ from the non-operated side (Langohr, 2015). The range of motion represented an average of 1910 ± 373 motions per hour of the operated shoulder (Langohr, 2015). All encompassed, this would indicate that the range of abduction wherein scapular notching damage could affect contact mechanics (above 25° humeroscapular abduction) are frequently experienced in occupational and recreational tasks, as well as the daily lives of shoulder arthroplasty recipients.

This study has a number of strengths, one of the main ones being the use of multiple physiologically relevant loading profiles encompassing a wide arc of abduction based on previous *in-vitro* studies. Subsequent statistical analysis was then able to be performed to better elucidate trends that were apparent from the finite element models. Secondly, a very refined mesh was utilized in the finite element models, specifically those of the notched humeral cups. Although three increments of simulated defects from scapular notching were included, this in no way completely encompasses all scapular notching damage. With this being an extremely individualistic process, with factors such as anatomy geometry, activity level, as well as implant configuration and position influencing its initiation and progression, it would be impossible to replicate all manners of damage presentation.

Furthermore, one limitation of the present work is the inherent differences in element distribution due to the differences in component geometry. This is illustrated through the difference in stress appearance throughout the central aspects of the cups in Figure 2-7. It should be noted that there was an attempt to avoid this complication, through the use of inserts added onto a base model of the most damaged specimen, thereby maintaining the same initial mesh and only adding new sections. However this setup resulted in stress values concentrated along the seam of the multiple components comprising the humeral cup, and was therefore not deemed a viable approach.

2.5   Conclusions

Overall, simulated scapular notching damage to the humeral cup was found to negatively affect RTSA articular contact mechanics through the use of finite element modelling. Specifically this was an increase in maximum contact stress values and a decrease in contact area, both of which were further degraded with the increasing severity of the simulated damage.   It should be noted that this was predominantly viewed at humeroscapular angles of abduction above 25° due to the inferior overhang of the humeral cup behind the medial aspect of the glenosphere at low angles of abduction. As a result the inferior aspect of the humeral cup with the impingement damage was not in contact with the glenosphere. It is possible that the deterioration in contact mechanics can also contribute to accelerated articular wear rates from the elevated stress values, as well as other related complications such as component loosening from the generation of polyethylene debris.

2.6   References

Boileau, P., Watkinson, D., Hatzidakis, A. M., & Hovorka, I. (2006). Neer Award 2005: The Grammont reverse shoulder prosthesis: Results in cuff tear arthritis, fracture sequelae, and revision arthroplasty. *Journal of Shoulder and Elbow Surgery*, *15*(5), 527–540. http://doi.org/10.1016/j.jse.2006.01.003

Boileau, P., Watkinson, D. J., Hatzidakis, A. M., & Balg, F. (2005). Grammont reverse prosthesis: Design, rationale, and biomechanics. *Journal of Shoulder and Elbow Surgery*, *14*(1), S147–S161. http://doi.org/10.1016/j.jse.2004.10.006

Carpenter, S., Pinkas, D., Newton, M. D., Kurdziel, M. D., Baker, K. C., & Wiater, J. M. (2015). Wear rates of retentive versus nonretentive reverse total shoulder arthroplasty liners in an in vitro wear simulation. *Journal of Shoulder and Elbow Surgery*, *24*(9), 1372–1379. http://doi.org/10.1016/j.jse.2015.02.016

Castagna, A., Delcogliano, M., De Caro, F., Ziveri, G., Borroni, M., Gumina, S., … De Biase, C. F. (2013). Conversion of shoulder arthroplasty to reverse implants: Clinical and radiological results using a modular system. *International Orthopaedics*, *37*(7), 1297–1305. http://doi.org/10.1007/s00264-013-1907-4

Day, J. S., MacDonald, D. W., Olsen, M., Getz, C., Williams, G. R., & Kurtz, S. M. (2012). Polyethylene wear in retrieved reverse total shoulder components. *Journal of Shoulder and Elbow Surgery*, *21*(5), 667–674. http://doi.org/10.1016/j.jse.2011.03.012

Ek, E. T. H., Neukom, L., Catanzaro, S., & Gerber, C. (2013). Reverse total shoulder arthroplasty for massive irreparable rotator cuff tears in patients younger than 65 years old: Results after five to fifteen years. *Journal of Shoulder and Elbow Surgery*, *22*(9), 1199–1208. http://doi.org/10.1016/j.jse.2012.11.016

Farshad, M., & Gerber, C. (2010). Reverse total shoulder arthroplasty-from the most to the least common complication. *International Orthopaedics*, *34*(8), 1075–1082. http://doi.org/10.1007/s00264-010-1125-2

Flury, M. P., Frey, P., Goldhahn, J., Schwyzer, H. K., & Simmen, B. R. (2011). Reverse shoulder arthroplasty as a salvage procedure for failed conventional shoulder replacement due to cuff failure-midterm results. *International Orthopaedics*, *35*(1), 53–60. http://doi.org/10.1007/s00264-010-0990-z

Giles, J. W., Ferreira, L. M., Athwal, G. S., & Johnson, J. A. (2014). Development and Performance Evaluation of a Multi-PID Muscle Loading Driven In Vitro Active-Motion Shoulder Simulator and Application to Assessing Reverse Total Shoulder Arthroplasty. *Journal of Biomechanical Engineering*, *136*(12), 121007. http://doi.org/10.1115/1.4028820

Giles, J. W., Langohr, G. D. G., Johnson, J. A., & Athwal, G. S. (2015). Implant Design Variations in Reverse Total Shoulder Arthroplasty Influence the Required Deltoid Force and Resultant Joint Load. *Clinical Orthopaedics and Related Research*, *473*(11), 3615–3626. http://doi.org/10.1007/s11999-015-4526-0

Godest, A. C., Beaugonin, M., Haug, E., Taylor, M., & Gregson, P. J. (2002). Simulation of a knee joint replacement during a gait cycle using explicit finite element analysis. *Journal of Biomechanics*, *35*(2), 267–275. http://doi.org/10.1016/S0021-9290(01)00179-8

Hallab, N. J., & Jacobs, J. J. (2009). Biologic effects of implant debris. *Bulletin of the NYU Hospital for Joint Diseases*, *67*(2), 182–188.

Kirking, B., El-Gohary, M., & Kwon, Y. (2016). The feasibility of shoulder motion tracking during activities of daily living using inertial measurement units. *Gait and Posture*, *49*, 47–53. http://doi.org/10.1016/j.gaitpost.2016.06.008

Kohut, G., Dallmann, F., & Irlenbusch, U. (2012). Wear-induced loss of mass in reversed total shoulder arthroplasty with conventional and inverted bearing materials. *Journal of Biomechanics*, *45*(3), 469–473. http://doi.org/10.1016/j.jbiomech.2011.11.055

Kurtz, S. M., Villarraga, M. L., Herr, M. P., Bergstrom, J. S., Rimmac, C. M., & Edidin, A. A. (2002). Thermomechanical behavior of virgin and highly crosslinked ultra-high molecular weight polyethylene used in total joint replacements. *Biomaterials*, *23*, 3681–3697.

Langohr, G. D. G. (2015). *Fundamentals of the Biomechanical Characteristics Related to the Loading of Reverse Total Shoulder Arthroplasty Implants and the Development of a Wear Simulation Strategy*.

Langohr, G. D. G., Athwal, G. S., Johnson, J. A., & Medley, J. B. (2016). Wear simulation strategies for reverse shoulder arthroplasty implants. *Journal of Engineering in Medicine*, *230*(5), 458–469. http://doi.org/10.1177/0954411916642801

Langohr, G. D. G., Giles, J. W., Athwal, G. S., & Johnson, J. A. (2015). The effect of glenosphere diameter in reverse shoulder arthroplasty on muscle force, joint load, and range of motion. *Journal of Shoulder and Elbow Surgery*, *24*(6), 972–979. http://doi.org/10.1016/j.jse.2014.10.018

Langohr, G. D. G., Willing, R., Medley, J. B., Athwal, G. S., & Johnson, J. A. (2016). Contact mechanics of reverse total shoulder arthroplasty during abduction: The effect of neck-shaft angle, humeral cup depth, and glenosphere diameter. *Journal of Shoulder and Elbow Surgery*, *25*(4), 589–597. http://doi.org/10.1016/j.jse.2015.09.024

Lévigne, C., Garret, J., Boileau, P., Alami, G., Favard, L., & Walch, G. (2011). Scapular notching in reverse shoulder arthroplasty: Is it important to avoid it and how? *Clinical Orthopaedics and Related Research*, *469*(9), 2512–2520. http://doi.org/10.1007/s11999-010-1695-8

Mollon, B., Mahure, S. A., Roche, C. P., & Zuckerman, J. D. (2017). Impact of scapular notching on clinical outcomes after reverse total shoulder arthroplasty: an analysis of 476 shoulders. *Journal of Shoulder and Elbow Surgery*, *26*(7), 1253–1261. http://doi.org/10.1016/j.jse.2016.11.043

Muh, S. J., Streit, J. J., Wanner, J. P., Lenarz, C. J., Shishani, Y., Rowland, D. Y., … Gobezie, R. (2013). Early follow-up of reverse total shoulder arthroplasty in patients sixty years of age or younger. *The Journal of Bone and Joint Surgery. American Volume*, *95*(20), 1877–83. http://doi.org/10.2106/JBJS.L.10005

Mulieri, P., Dunning, P., Klein, S., Pupello, D., & Frankle, M. (2010). Reverse shoulder arthroplasty for the treatment of irreparable rotator cuff tear without glenohumeral arthritis. *The Journal of Bone and Joint Surgery. American Volume*, *92*(15), 2544–56. http://doi.org/10.2106/JBJS.I.00912

Nam, D., Kepler, C. K., Nho, S. J., Craig, E. V, Warren, R. F., & Wright, T. M. (2010). Observations on retrieved humeral polyethylene components from reverse total shoulder arthroplasty. *Journal of Shoulder and Elbow Surgery*, *19*(7), 1003–1012. http://doi.org/10.1016/j.jse.2010.05.014

Nolan, B. M., Ankerson, E., & Wiater, M. J. (2011). Reverse total shoulder arthroplasty improves function in cuff tear arthropathy. *Clinical Orthopaedics and Related Research*, *469*(9), 2476–2482. http://doi.org/10.1007/s11999-010-1683-z

Nyffeler, R. W., Werner, C. M. L., Simmen, B. R., & Gerber, C. (2004). Analysis of a retrieved Delta III total shoulder prosthesis. *The Journal of Bone and Joint Surgery*, *86*(8), 1187–1191. http://doi.org/10.1302/0301-620X.86B8.15228

Permeswaran, V. N., Goetz, J. E., Rudert, M. J., Hettrich, C. M., & Anderson, D. D. (2016). Cadaveric validation of a finite element modeling approach for studying scapular notching in reverse shoulder arthroplasty. *Journal of Biomechanics*, *49*(13), 3069–3073. http://doi.org/10.1016/j.jbiomech.2016.07.007

Pruitt, L. A. (2005). Deformation , yielding , fracture and fatigue behavior of conventional and highly cross-linked ultra high molecular weight polyethylene. *Biomaterials*, *26*, 905–915. http://doi.org/10.1016/j.biomaterials.2004.03.022

Rader, C. P., Sterner, T., Jakob, F., Schütze, N., & Eulert, J. (1999). Cytokine response of human macrophage-like cells after contact with polyethylene and pure titanium particles. *Journal of Arthroplasty*, *14*(7), 840–848. http://doi.org/10.1016/S0883-5403(99)90035-9

Sirveaux, F., Favard, L., Oudet, D., Huquet, D., Walch, G., & Molé, D. (2004). Grammont inverted total shoulder arthroplasty in the treatment of glenohumeral osteoarthritis with massive rupture of the cuff. *The Journal of Bone and Joint Surgery*, *86*(3), 388–395. http://doi.org/10.1302/0301-620X.86B3.14024

Terrier, A., Merlini, F., Farron, A., & Pioletti, D. P. (2009). Reverse shoulder arthroplasty: polyethylene wear. *Computer Methods in Biomechanics and Biomedical Engineering*, *12*(sup1), 247–248. http://doi.org/10.1080/10255840903097855

Weber-Spickschen, T. S., Alfke, D., & Agneskirchner, J. D. (2015). The use of a modular system to convert an anatomical total shoulder arthroplasty to a reverse shoulder arthroplasty: Clinical and radiological results. *Bone and Joint Journal*, *97B*(12), 1662–1667. http://doi.org/10.1302/0301-620X.97B12.35176

Werner, B. S., Boehm, D., & Gohlke, F. (2013). Revision to reverse shoulder arthroplasty with retention of the humeral component. *Acta Orthopaedica*, *84*(5), 473–478. http://doi.org/10.3109/17453674.2013.842433

Wiater, B. P., Baker, E. A., Salisbury, M. R., Koueiter, D. M., Baker, K. C., Nolan, B. M., & Wiater, J. M. (2015). Elucidating trends in revision reverse total shoulder arthroplasty procedures: a retrieval study evaluating clinical, radiographic, and functional outcomes data. *Journal of Shoulder and Elbow Surgery*, *24*(12), 1915–1925. http://doi.org/10.1016/j.jse.2015.06.004

Willing, R., & Kim, I. Y. (2009). A holistic numerical model to predict strain hardening and damage of UHMWPE under multiple total knee replacement kinematics and experimental validation. *Journal of Biomechanics*, *42*(15), 2520–2527. http://doi.org/10.1016/j.jbiomech.2009.07.008

Young, S. W., Everts, N. M., Ball, C. M., Astley, T. M., & Poon, P. C. (2009). The SMR reverse shoulder prosthesis in the treatment of cuff-deficient shoulder conditions. *Journal of Shoulder and Elbow Surgery*, *18*(4), 622–626. http://doi.org/10.1016/j.jse.2009.01.017

Chapter 3

Simulator Wear of Conventional Polyethylene, High-Mobility Humeral Cups with Simulated Notching Damage

OVERVIEW: Scapular notching is a process affecting reverse total shoulder arthroplasty (RTSA) systems, wherein the geometry of the humeral cup articular surface becomes compromised. As demonstrated in the previous chapter, the simulated scapular notching damage degraded contact mechanics parameters, relative to the intact state. While it is recognized that the use of a high-mobility humeral cup can serve to reduce the risk for developing scapular notching, it comes at the price of less favourable contact mechanics, specifically decreased contact area and increased maximum contact stress values when compared to their standard depth counterpart. Therefore, the purpose of the present wear simulation study was to assess the early wear rates of RTSA systems with high-mobility humeral cups, and observe if changes occur as a result of introducing and propagation simulated scapular notching damage. This was accomplished through the use of gravimetric analysis. A companion finite element analysis was also included.[2]

---

[2] A portion of the work covered in Chapter 1 is included within the introduction, in addition to the methods covered in Chapter 2 for the finite element modelling, as part of the Integrated-Article format.

3.1 Introduction

Reverse total shoulder arthroplasty (RTSA) has been demonstrated to be an effective treatment for several shoulder conditions, in addition to the revision of failed shoulder arthroplasty, which encompasses reversing the native geometry of the glenohumeral joint (Castagna et al., 2013; Flury et al., 2011; Muh et al., 2013; Weber-Spickschen et al., 2015; Werner et al., 2013). However, this ball-in-socket implant system has exhibited wear on the polyethylene primarily within the inferior quadrant of the humeral cup, being attributed to both articular surface wear at the interface with the glenosphere, as well as damage from scapular impingement on the inferiomedial edge (Day et al., 2012; Nam et al., 2010). Both of these processes generate polyethylene debris deposits, which can contribute to the progression of osseous damage to the area around the glenoid, resulting in loosening of the baseplate component (Hallab & Jacobs, 2009; Kohut et al., 2012; Rader et al., 1999; Vaupel et al., 2012). An additional complication this presents is the possibility of eventual dislocation, as a result of the loss of the inferiomedial aspect of the humeral cup. However, even before such a drastic result, this region is the location of peak contact stress values based on analysis with finite element models (Langohr, Willing, et al., 2016; Terrier et al., 2009).

As previously described in Section 1.3.1, there have been many studies on the wear testing of RTSA systems. However, currently there are no accepted testing standards which has subsequently resulting in the varied methods and simulator conditions of these experiments, as outlined in Table 1-1. Subsequently there have been a wide range of results reported for wear rates, from 9.93 mm^3/MC (Dieckmann et al., 2013) to 201.1 mm^3/MC (Langohr, 2015) for standard, conventional polyethylene humeral cups. However, other than a single specimen trial conducted by Langohr et al (2016), research within this area has focused on intact RTSA components and the effects of scapular notching impingement damage have not been included. Scapular notching is the most frequently reported RTSA complication (Farshad & Gerber, 2010) and it progresses over time (Ek et al., 2013). In some cases revisions must be performed within a relatively short timeframe (Day et al., 2012; Nyffeler et al., 2004), for reasons including component loosening, pain, and impingement (Day et al., 2012). Nevertheless, no major change in wear rate was observed

after the damage to the articular surface was introduced for this single specimen (Langohr, Athwal, et al., 2016). This is of particular interest given the results of the previous chapter, wherein the initiation and progression of humeral cup scapular notching damage significantly affected the observed contact mechanics parameters.

Furthermore, there are several strategies with respect to the geometry of RTSA components which can serve to reduce the risk for developing scapular notching. One such example is the use of a high-mobility humeral cup, which has been demonstrated though *in-silico* evaluation to reduce the adduction deficit (de Wilde et al., 2010; Gutiérrez et al., 2009; Roche et al., 2009). Additionally, the use of this design has also been reported to result in decreasing contact area and increasing maximum contact stress values, relative to its standard depth counterpart in finite element modelling (Langohr, Willing, et al., 2016). While the application of a retentive humeral cups was assessed in wear testing by Carpenter et al (2015), reporting an increase in wear rate with the deeper cups, the use of high mobility humeral cups have not been assessed in wear simulation studies. However, it is of interest to note that deep humeral cups have been demonstrated to have increased contact area and reduced maximum contact stress values relative to the standard offering through the use of finite element analysis (Langohr, Willing, et al., 2016).

Therefore the purpose of the present study was to further assess the wear of a clinically available high-mobility RTSA implant, both with and without the presence of simulated defects from scapular notching. We hypothesized that there will be an increase in early wear rates, specifically within the remaining inferior quadrant of the humeral cup, with the introduction and progression of simulated scapular notching.

3.2   Materials & Methods

3.2.1   Wear Simulation Strategy

As developed by Langohr et al (2016), a modified orbital bearing hip wear simulator (MATCO, La Canada, CA, USA; model MMED EW08) was utilized in performing the wear testing (Figure 3-1). This simulator is configured for five wear test stations, as well as three load soak stations. The glenospheres, mounted on custom fixtures within lubricant on the drive block, underwent a biaxial rocking motion of ±22.5° at a rate of 1.134 Hz,

while the accompanying humeral cups were mounted above, attached to the vertical shafts of the hydraulic cylinders. The physiological equivalent of this motion would be ±22.5° flexion-extension and 30-97.5° scapulothoracic adduction-abduction, combined in a circumduction motion that is repeated every cycle (Figure 3-2). Following Langohr et al (2016), a load profile with a 900 N peak was applied to the implant couples of all stations, including those of the load soak controls. This load profile was representative of the loads experience in a reversed arthroplasty shoulder from holding a 0.5 kg mass in hand according to Masjedi & Johnson (2010).
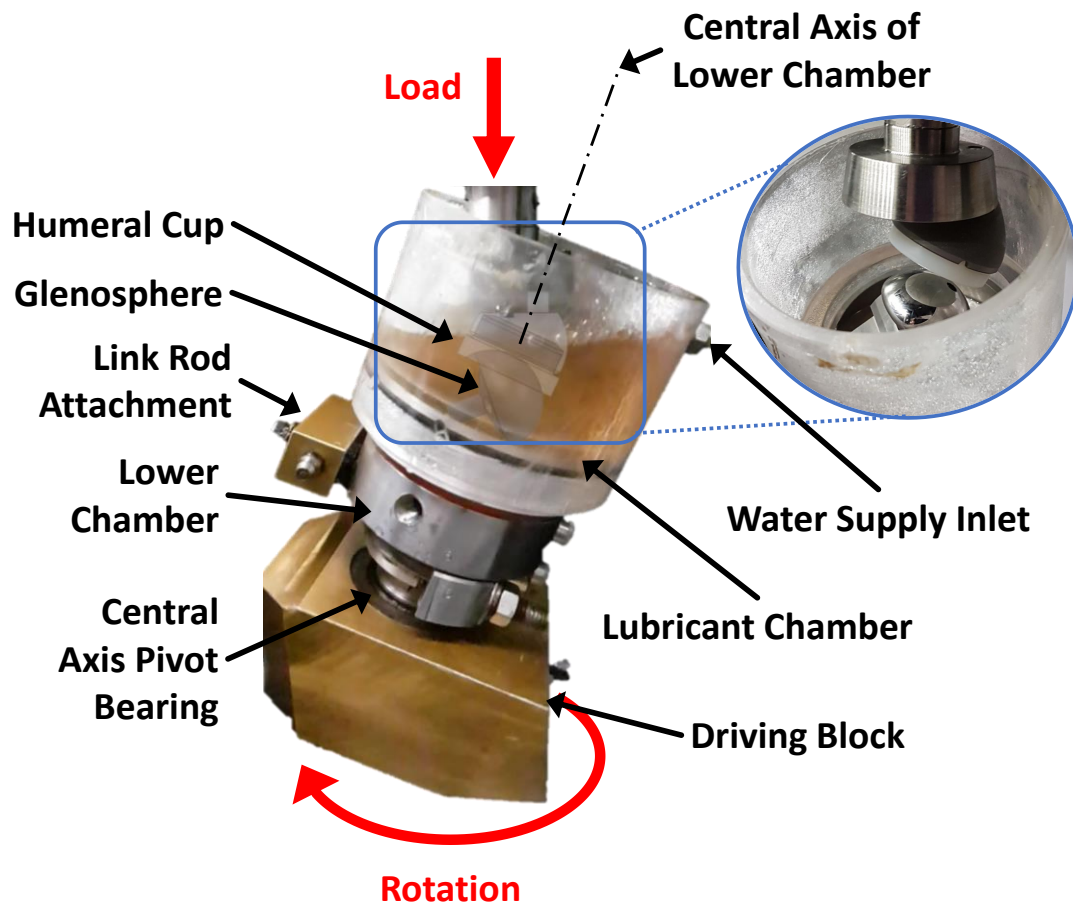
Figure 3-1: Single station of the modified MATCO simulator, with inlay highlighting RTSA component alignment

0% Cycle
Abd-Add = 30°
Flex-Ext = 0°

25% Cycle
Abd-Add = 63.75°
Flex-Ext = -22.5°

50% Cycle
Abd-Add = 97.5°
Flex-Ext = 0°

75% Cycle
Abd-Add = 63.75°
Flex-Ext = +22.5°
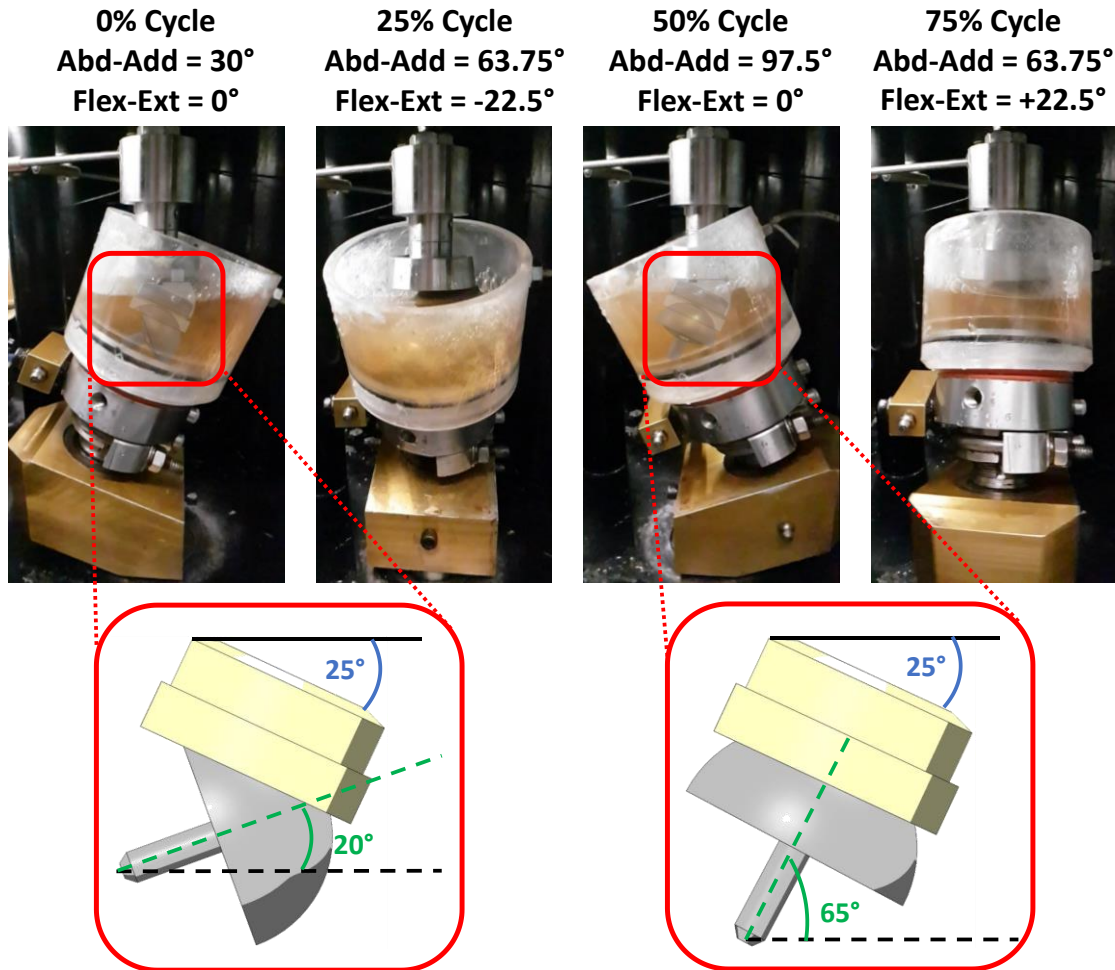
Figure 3-2: Range of motion elicited by the modified MATCO RTSA wear simulator

Inserts of the resulting humeral cup and glenosphere angles at the limits of abduction corresponding to 0% and 50% of the circumduction cycle are also depicted.

3.2.2   Simulation Protocols

Wear testing of five coupled RTSA implants was performed in three stages, each comprised of 0.25 Mc for a total of 0.75 Mc (1 Mc = 10^6 cycles), in the wear simulator as previously described. In total, the wear simulation comprised of eight commercially available, high-mobility conventional polyethylene RTSA implants (Delta XTEND; DePuy, Warsaw, IN, US) and matching standard glenosphere (38 mm diameter system).

Following Langohr et al (2016), the lubricant used in the present work was alpha calf fraction serum without iron (HyClone; GE Healthcare Life Sciences, South Logan, UT, USA) diluted to a total protein concentration of 30 g/L with phosphate buffer solution (PBS, VWR International, ON, CAN). Additionally research grade sodium hyaluronate (HA) was added at a concentration of 1.5 g/L as well as 5 mL of antimycotic antibiotic (Invitrogen Inc., ON, CAN) per 500 mL of lubricant to suppress bacterial growth (Appendix B). This formulation was determined to be an excellent substitute for synovial fluid in wear testing, with respect to the lubricant biochemistry and wear rate magnitudes in the application of knee implant wear (Brandt et al., 2010; Brandt, Mahmoud, Koval, MacDonald, & Medley, 2013). During wear testing the lubricant temperature was maintained at approximately 37° C, with de-ionized water being introduced to each chamber at a slow, controlled flow rate to replenish water volume lost to evaporation.

The first stage (0-0.25 Mc) consisted of the intact state, while the second and third states were with simulated defects from scapular notching which were introduced and subsequently increased. At the 0.25 Mc mark of testing this involved the removal of material using a rotary cutting tool. A template was applied to each specimen in order to achieve a cut profile as outlined in pink in Figure 3-3, wherein the simulated defect applied was 1 mm deep and 10 mm wide. This process was repeated at 0.5 Mc, wherein the replicated damage was increased to 2 mm deep and 12 mm wide (Figure 3-3; green line). The depth parameters were selected based off of the observations by Day et al (2012) for standard depth humeral cups where the notching scar depth ranged from 0.1 mm to 4.7 mm (mean: 2.1 mm). However the damage was narrower than that reported by Day et al (2012) due to the uncertainty of disarticulation when mounted on the simulator. This was of particular concern given that decreased depth of the humeral cup has been demonstrated to decrease the load required to elicit disarticulation (Clouthier et al., 2013; Gutiérrez, Keller, et al., 2008; Pastor et al., 2016).
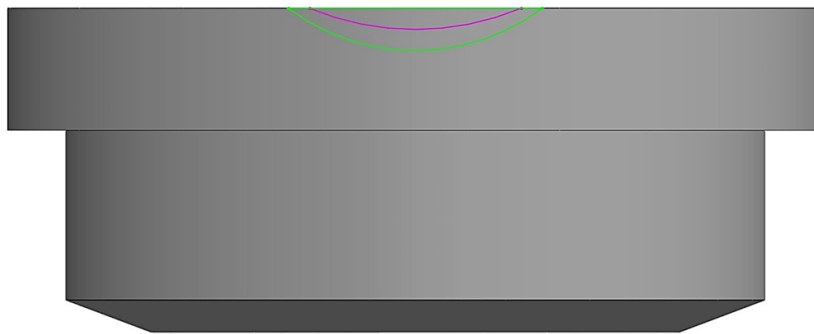
Figure 3-3: Cut profiles for inferior aspect of humeral cups simulating notching damage

Outlines indicate the first (pink line) and second (green line) stages of simulated notching imparted on the high-mobility humeral cup.

At both 0.1 Mc and 0.25 Mc of the first two stages of testing, the humeral cups were removed from the wear simulator, where the cleaning and mass measurement protocol (Table 3-1) was conducted using a Mettler Toledo AX205 Analytical Balance (Columbus, OH, USA) with a precision of 0.01 mg. Alternatively, for the third stage of testing (0.5-0.75 Mc) there was no stop at the 0.1 Mc point as the trends for the observed wear rates were approximately linear throughout the entire 0.25 Mc of each of the previous stages. The mass of the humeral cups was recorded three times and averaged to determine the mass loss relative to the initially recorded values. Even though the humeral cups were presoaked for several months and were probably close to saturation, this process was also repeated for the three load soak controls to account for any fluid uptake which would serve to occlude the true wear rates.

Again following Langohr et al (2016), the average increases in mass of the load soaks controls were applied to the mass differences recorded for each of wear test specimens to determine their "real" change in mass. This value was then converted to volumetric wear in mm^3, by dividing by the density of polyethylene (0.935 mg/mm^3). The wear rate of each specimen, reported in mm^3/Mc, was also calculated for each specimen, excluding the origin point, as suggested by ISO 14242-2 (International Organization for Standardization, 2000) for the first two stages of testing (0.1-0.25 Mc of each respective stage). However, for the third stage of testing (0.5-0.75 Mc) the wear rate was obtained from the linear fit between the start and end points.

Table 3-1: Protocol for cleaning and mass measurement of wear test and load soak control specimens

Steps are adapted from Langohr, Athwal, et al. (2016).

STEP	DESCRIPTION
1)	Rinse with de-ionized water to remove loose contaminants
2)	Scrub with a soft brush (to remove adhered contaminants) and rinse with de-ionized water
3)	Clean in an ultrasonic cleaner in individual containers of a 2% solution of Liqui-NOX® detergent (Alconox, Inc., White Plains, NY, USA) for 10 minutes
4)	Rinse with de-ionized water
5)	Clean in an ultrasonic cleaner in individual containers of de-ionized water for 5 minutes
6)	Soak in isopropyl alcohol for 5 minutes to remove residual surface water and then dry in a stream of nitrogen gas
7)	Allow to air dry and acclimatize next to the balance for 10 minutes
8)	Calibrate the balance using the automatic calibration feature and tare the scale
9)	Measure the mass of the two manual calibration "weights" (20 g and 100 g)
10)	Successively measure the mass of each specimen once
11)	Repeat step 10 two more times to obtain three measurements for each
12)	Average the three mass measurements for each specimen. If all three measured values of a particular specimen are not in the range of 0.2 mg repeat steps 8-12
13)	Measure the mass of the manual calibration "weights" to ensure that they are within 0.2 mg of the value determined in step 9

The aforementioned cleaning and weighing protocol was also repeated after the simulated notching defect was conducted at the 0.25 Mc and 0.5 Mc of testing. Fresh lubricant solution was used at the start of each of these stages as well.   The wear rates of the intact and notched humeral cups were also compared using repeated measures analysis of variance (ANOVA, α = 0.05) conducted in SPSS (V25, IBM Corporation, Armonk, NY, USA).

It should be noted that surface scanning of the humeral cups was conducted before testing and at every stoppage of the first 0.5 Mc. However, this was excluded from the current work as the surface deviations were found to be within the extent of accuracy for the laser scanner used. Further information about this protocol and its results can be found in Appendix C.

3.2.3   Finite Element Companion Study

An accompanying finite element model was developed in Abaqus v6.14 (Simulia Corp, Providence, RI, USA) to investigate the effects of simulated notching damage on contact areas and peak contact stresses of the high-mobility humeral cups, under the loading conditions imposed by the wear simulator. Following the same methodologies as utilized in the previous chapter's study (Section 2.2), the loading and abduction angles were altered to reflect the conditions of 30° and 97.5° abduction with a 900 N joint load, as applied by the simulator on a high-mobility humeral cup (inlays of Figure 3-2). The finite element analysis was performed on a high-mobility humeral cup that was notched in the same manner as in the second and third stages of the wear testing (1 mm deep and 10 mm wide; 2 mm deep and 12 mm wide; Figure 3-4). The contact area and the maximum contact stress values were predicted and visualized through stress distribution maps of the cup surfaces.

High-Mobility Cup	Level 1 Notch	Level 2 Notch
Intact State	**1 mm deep ~ 10 mm wide**	**2 mm deep ~ 12 mm wide**
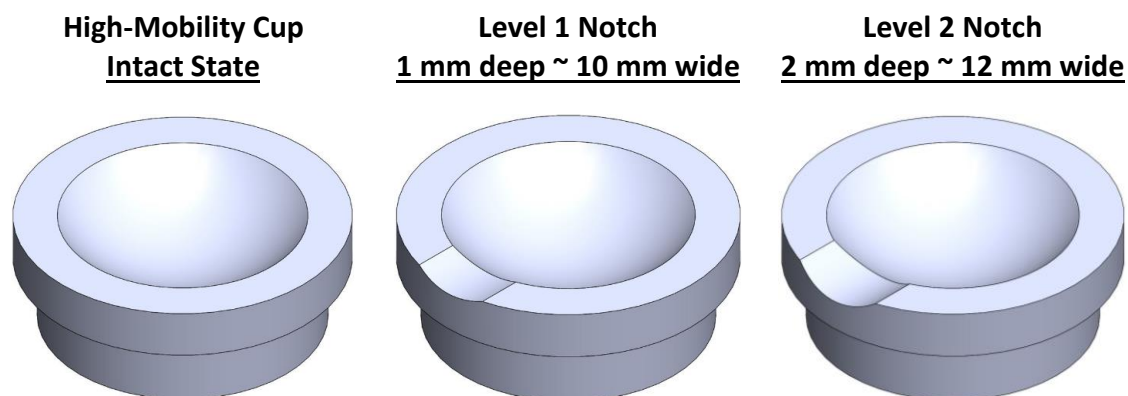
Figure 3-4: Isometric views of intact and notched high-mobility humeral cup models for companion study

3.3   Results

3.3.1   Wear Simulation Trials

All of the humeral cups showed visual signs of wear from articulation at the initial 0.1 Mc assessment and progressed when re-assessed at 0.25 Mc. While difficult to illustrate in the photographs, the humeral cups were orientated in a way to best display these regions where wear zones are estimated and indicated in the outlines of Figure 3-5. For the intact humeral cup a polished region (indicated by the white dashed line) encompassed all but a small portion of the superior region, which appeared to remain as the new condition. Located centrally within the polished region, there was a small area that was less polished, and appeared marked or scuffed in appearance, for all wear specimens (encircled in red dashed line). This aspect would approximately correspond to the articular contact region for locking bolt hole of the glenosphere component.

With the introduction of a simulated defect from scapular notching (margin of cut indicated in green dotted line Figure 3-6), a secondary wear band at the inferior aspect (margin indicated by a blue dashed line) developed to varying extents based on visual inspection. In one humeral cup (specimen 3) this region appeared as no longer polished and was flat and scuffed in appearance, whereas this band appeared relatively less polished or scuffed in appearance for the others. Additionally there appeared to be a more gradual slope on the articular surface at the margin of the applied cut, relative to its appearance when first

established. The centrally located area of marking within the polished region also enlarged (circled in a red dashed line), with some regions developing more superiorly, such as that seen in humeral cup 1. The margin of the polished region (white dashed line) also appeared to be more gradual in profile, relative to that seen in the intact state.

With the third stage of testing, similar visual trends as the previous stage were apparent, albeit further developed, as depicted in Figure 3-7. Around the cut margin (indicated by green dashed line) at the inferior aspect of the articular surface there was a more gradual inclination, in a thin band, as was observed with the less severe notch. However, the secondary wear area (indicated by blue dashed line) had progressed to encompass between a quarter and a third of the articular surface, which was visibly differentiable under certain lighting conditions by its less polished appearance with almost vertical (inferior-superior) scuffing. The centrally located markings (indicated by red dashed line), visible since the first trial, were still apparent. Additionally, the margins of the polished region (indicated by the white dashed line) did not appear to visibly progress much from the last stage of testing, possibly implying that the recorded wear was predominantly occurring within the secondary inferior wear region that developed.

The average wear rates of the humeral cups were 31.19 ± 3.73 mm^3/Mc for the intact state, whereas the defect states were 29.68 ± 5.40 mm^3/Mc and 22.52 ± 2.07 mm^3/Mc for each state tested (Figure 3-8). Damage from scapular notching was found to have a significant effect on the reported wear rates ($p = 0.044$). However, no significant differences were observed between any of the tested conditions ($p \geq 0.066$).

All glenospheres exhibited light surface scratching within the articular contact zone, to varying degrees (Figure 3-5, Figure 3-6, and Figure 3-7). Specifically, glenosphere of station 2 and 4 exhibited a few deeper scratches after the second stage of testing.

Wear Station	Humeral Cup Appearance	Glenosphere Appearance
1		
2		
3		
4		
5		
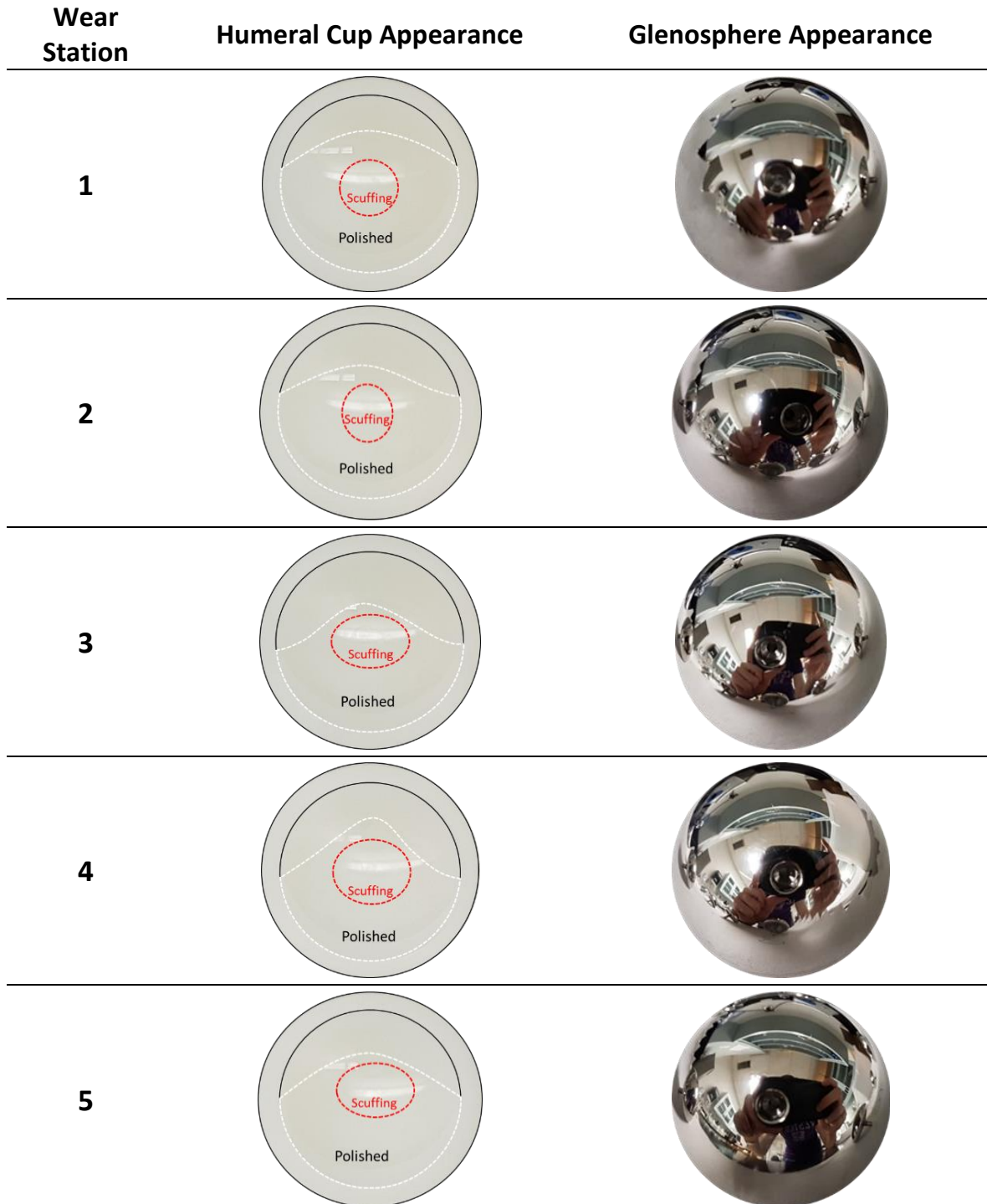
Figure 3-5: Appearance of the worn, intact humeral cups (left) and glenospheres (right) of all wear test specimens after the first stage of testing (0 – 0.25 Mc)

Dashed white lines denote wear region, whereas blue and red dashed lines indicate visual changes within this region. The specimens are orientated with the superior aspect towards the top.

Wear Station	Humeral Cup Appearance	Glenosphere Appearance
1		
2		
3		
4		
5		
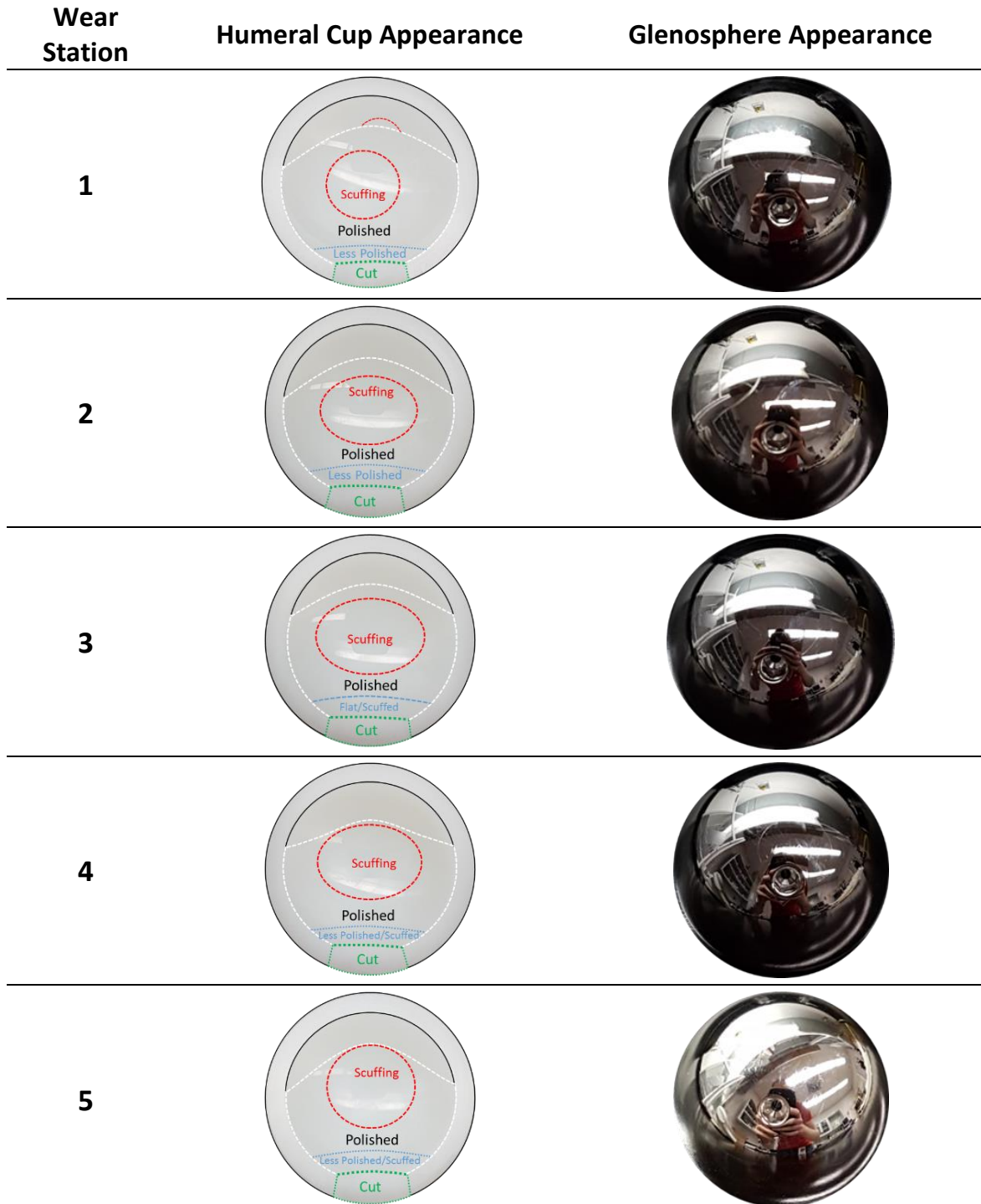
Figure 3-6: Appearance of the worn humeral cups with simulated notching defects (left) and glenospheres (right) of all wear test specimens, after the second stage of testing (0.25 – 0.5 Mc)

Dashed white lines denote wear region, whereas blue and red dashed lines indicate visual changes within this region. The specimens are orientated with the superior aspect towards the top.

Wear Station	Humeral Cup Appearance	Glenosphere Appearance
1	Polished / Scuffing / Less Polished/Scuffed / Cut	
2	Scuffing / Polished / Less Polished/Scuffed / Cut	
3	Scuffing / Polished / Less Polished/Scuffed / Cut	
4	Scuffing / Polished / Less Polished/Scuffed / Cut	
5	Scuffing / Polished / Less Polished/Scuffed / Cut	

Figure 3-7: Appearance of the worn humeral cups with simulated notching defects (left) and glenospheres (right) of all wear test specimens, after the third stage of testing (0.5 – 0.75 Mc)

Dashed white lines denote wear region, whereas blue and red dashed lines indicate visual changes within this region. The specimens are orientated with the superior aspect towards the top.
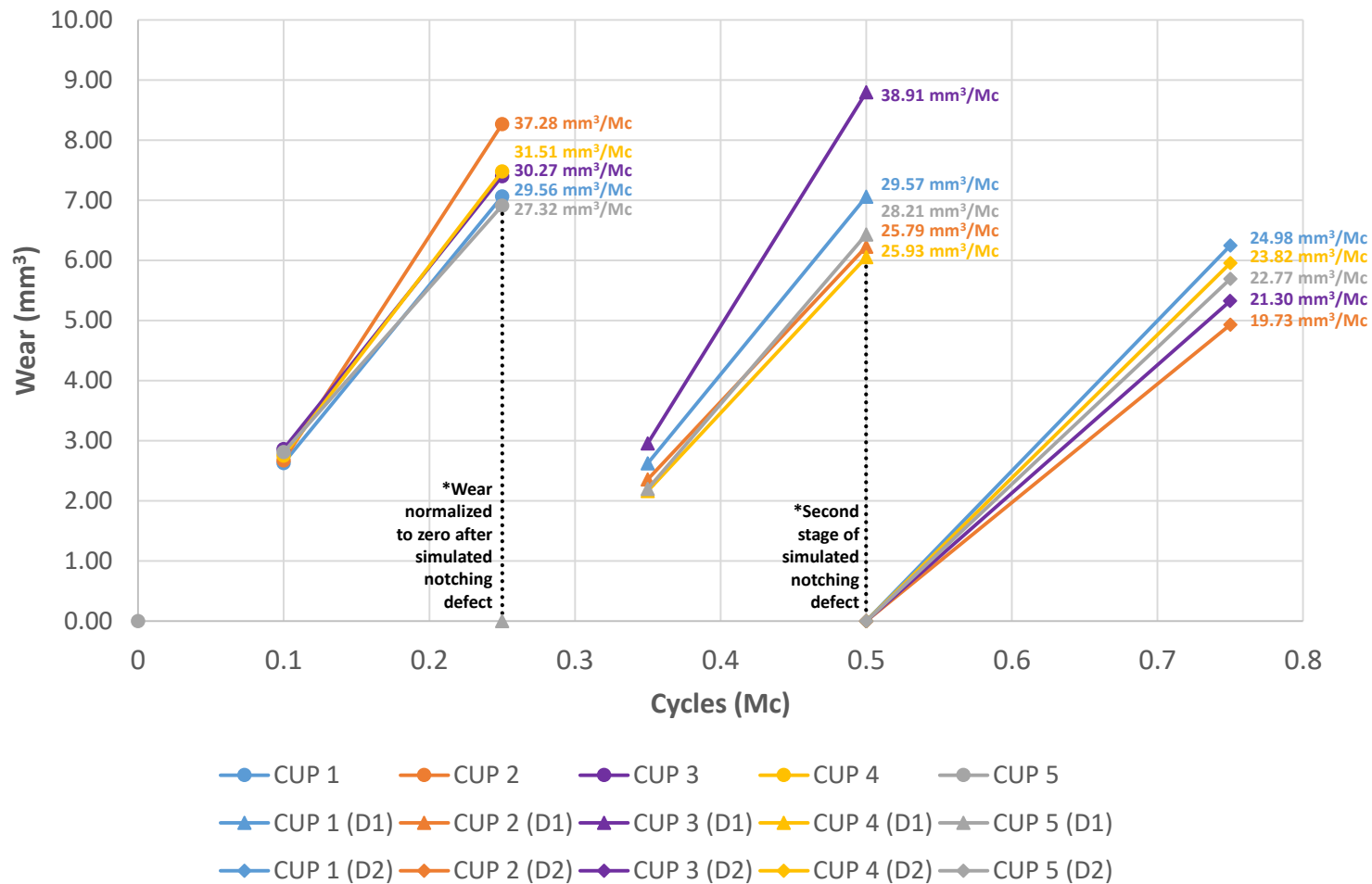
Figure 3-8: Wear rates of the humeral cup in each station with their respective linear assumed wear rate for each stage of testing

Note that "D1" and "D2" represent the first and second stage of simulated notching defect respectively.

3.3.2   Finite Element Companion Study

As anticipated, the introduction and progression of notching damage to the humeral cups resulted in the reduction of articular contact area, as depicted in Figure 3-9. However the maximum contact stress values remained fairly consistent between the intact and the first notched states. However with the second notch state there was an increase in the maximum contact stress v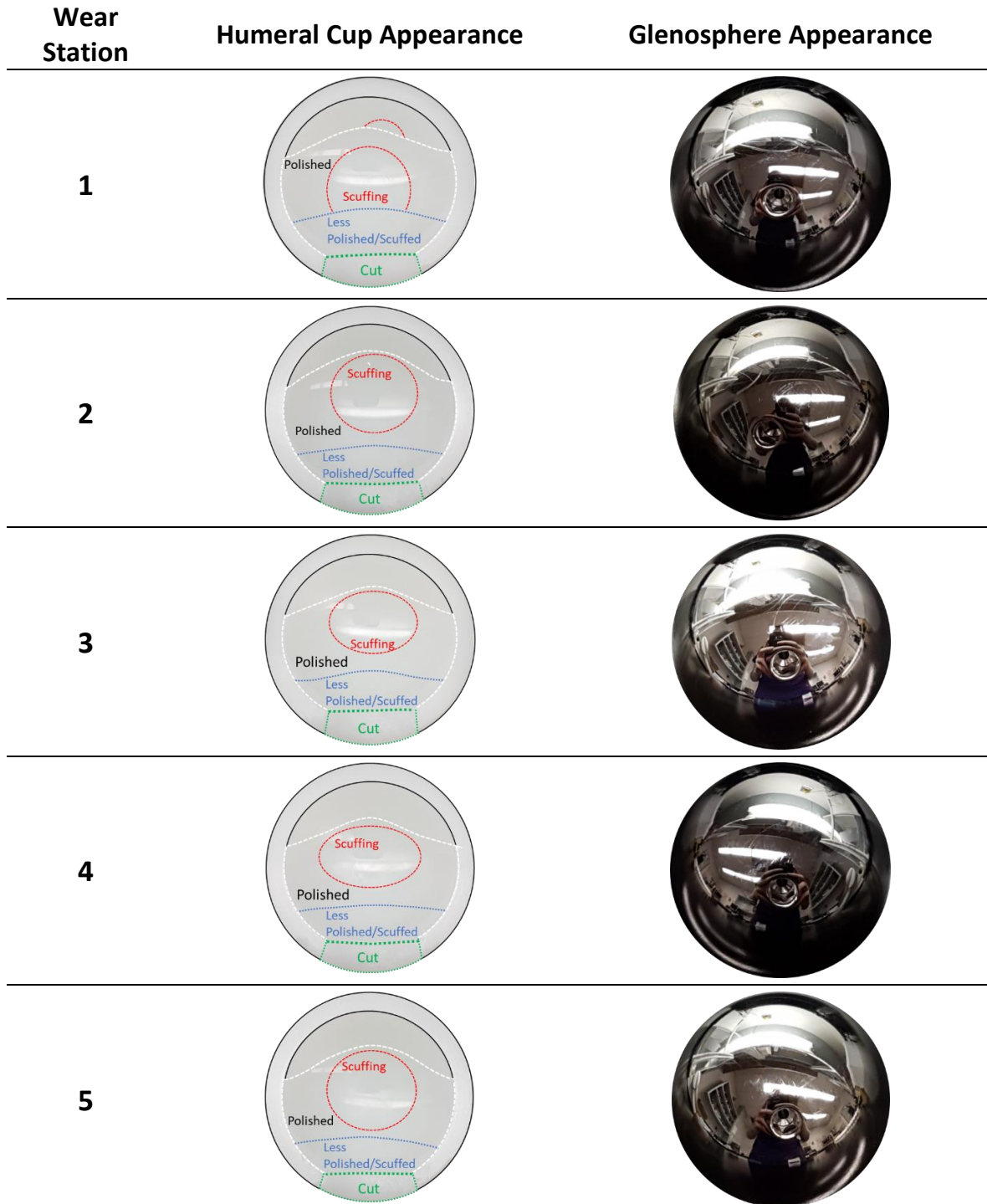alues for both 30° and 97.5° abduction. However in all cases the maximum contact stress remains below that of the yield stress value for polyethylene (Kurtz et al., 2002; Pruitt, 2005). When viewing the stress distribution maps (Figure 3-10), it would appear that the initial notch had not yet encroached on the region of maximum contact stress for the 30° abduction simulation, which was a narrow band in the inferior aspect of the humeral cup. While greater overall stress values are apparent on the notched 97.5° stress distribution map, the first notch had not yet progressed to an extent where the maximum contact stress value was affected. However, the second stage of notching had progressed to where this was no longer the case, resulting in the increased stress as indicated with the separate stress scale used for its stress distribution diagrams (Figure 3-10). In the case of all simulations, the maximum contact stress values were located at the inferior most edge of contact, be it on the articular surface, inferior edge of the cup, or margin of the applied cut.
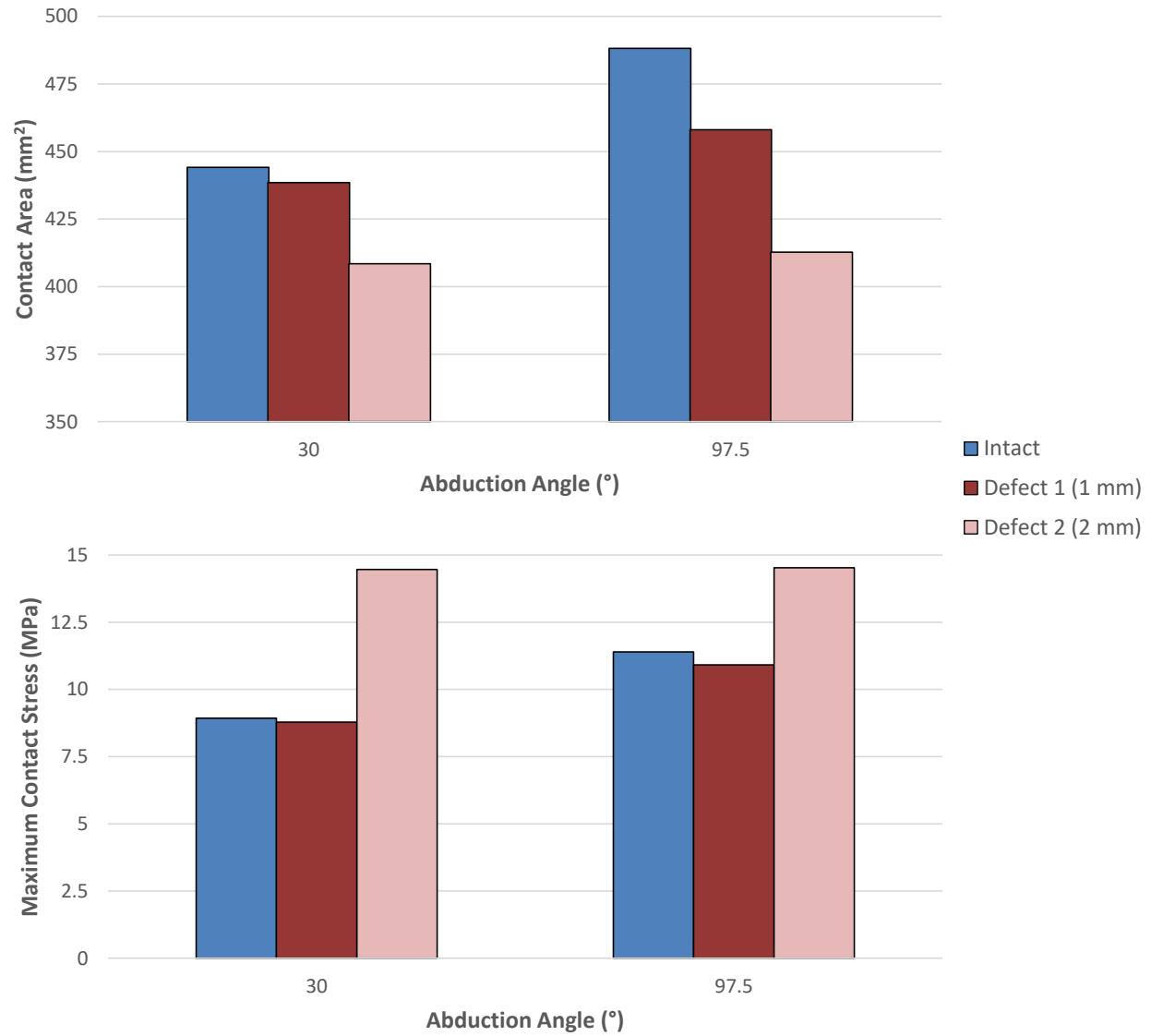
Figure 3-9: Finite element companion study contact area (top) and maximum contact stress (bottom)

This is conducted for wear simulator minimum & maximum abduction angles for intact and notched states.
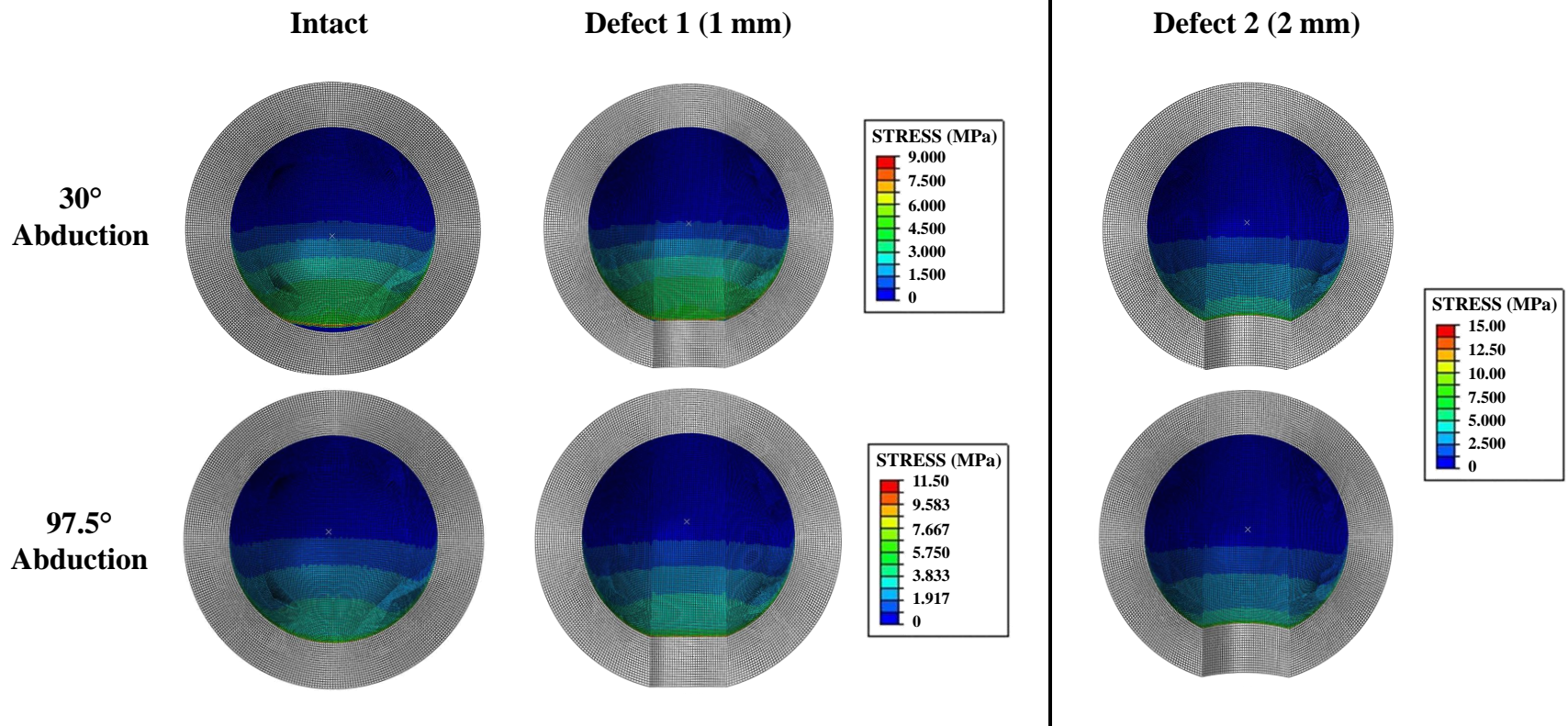
Figure 3-10: Humeral cup contact stress distribution maps for minimum & maximum abduction angles of the wear simulator for the intact and simulated notching defect states

Note that a different scale for both abduction angles is used for the stress distributions in the more severe notching defect state.

3.4 Discussion

High-mobility humeral cups were developed to increase adduction range of motion (de Wilde et al., 2010; Gutiérrez et al., 2009; Roche et al., 2009), but demonstrate unfavourable effects on articular contact mechanics. Specifically, the decrease in cup depth has also been shown to effect joint stability, wherein for both biaxial (Gutiérrez, Keller, et al., 2008) and cadaveric biomechanics studies (Clouthier et al., 2013; Pastor et al., 2016) the decreasing conformity of the humeral cup reduced the load required for dislocation. In addition, by employing a finite element model Langohr et al (2016) found that the use of high-mobility humeral cups increased maximum contact stress and decreased articular contact area relative to a standard depth cup. Despite this, the reported wear rates remained relatively low in magnitude, compared to those in literature, at 31.19 ± 3.73 mm^3/Mc for the intact state. While lower wear rates have been previously reported for standard depth humeral cups, experiment protocols have widely differed, including the use of different lubricating solutions and/or less severe loading parameters (Dieckmann et al., 2013; Kohut et al., 2012; Smith et al., 2015). This lower wear rate for the high-mobility humeral cup also continues the trend reported by Carpenter et al (2015), wherein the decreasing conformity of the humeral was reported to decrease the wear rates when comparing deep to standard depth components. It is possible that while the increased contact stress would increase abrasive wear, the decrease in wear from the decreased contact area had an overall greater effect, resulting in the net effect observed.

An unanticipated finding from the present work was that the introduction of simulated scapular notching defect to the humeral cup did not significantly increase the observed early wear rates from the first stage of testing. This is further characterized in the finite element model wherein the first stage of notching defect did not seem to affect the maximum contact stress, even with the decrease in contact area. Conversely, there was a small decrease in the wear rates with the second stage of notching damage relative to the previous states, albeit not determined to be significantly different from the other test conditions. However, this wear visually appeared to be occurring predominantly within the inferior region. This is due to the overall region of visible wear not changing, whereas there was the visible progression of the secondary inferior wear region. In terms of the

finite element model, the second stage of notching defect resulted in a greater maximum contact stress value, specifically in the inferior margin with the maximum located at the cut interface. As previously described, it is possible that the effect of the increased contact stress had not progressed to an extent relative to the decreased contact area to result in a net increase of wear rate. However, in the long term, it is possible that fatigue wear could occur resulting in catastrophic damage to the implant, especially considering the increasing stresses imparted if scapular notching damage was to progress. This would be further emphasized in the application of different humeral cup materials, such as highly cross-linked polyethylene which has a reduced resistance to fatigue crack propagation (Pruitt et al., 2013).

It should be noted that similar results were reported in a single specimen wear test by Langohr et al (2016), wherein the introduction of notching damage of the humeral cup did not drastically effect the wear rate. However, in the case of that study, as well as the present work, even though material was removed from the humeral cup the resulting polyethylene debris was not retained within the lubricating media. As was the case for the estimated polyethylene removed from scapular notching by Kohut et al (2012), it was also found in the present work that the simulated scapular notching defects resulted in a much greater change in mass, and therefore greater amount of potential debris, than that seen from articular wear in simulation trials.

One limitation of the current work is the limited number of cycles tested relative to most of that seen in literature for RTSA wear simulation, although it should be noted that Kohut et al (2012) had only tested for a duration of only 0.5 Mc. However the presentation of scapular notching damage of the humeral cup presents fairly rapidly, being observed in surgical retrievals that were *in-vivo* for less than 15 months in some cases (Day et al., 2012; Nyffeler et al., 2004). It is very possible that the scapular notching damage would necessitate intervention being required before articular wear damage became problematic. Herein lies the difficulty in defining the equivalent duration of time simulated by in the wear test, as there are wide estimates on the activity level of the shoulder, depending on how a cycle is defined. Characterizing a cycle as abduction angles greater than 60° would approximate to 1.5 Mc/year, whereas increasing the motion to 80° abduction reduces this

value to 0.33 Mc/year (Langohr, 2015). Therefore the duration of the current work would approximate to between 6 and 27 months of use, comparable to that of observed retrieval cases with visible humeral cup notching damage in literature.

3.5 Conclusions

The present study describes the wear testing of RTSA implant system with a high-mobility humeral cup component and simulated scapular notching defects being introduced. Simulated notching damage was found to significantly affect the observed wear rates of the polyethylene humeral cups. However, contrary to the hypothesis, the increase of scapular notching damage resulted in a decrease of early wear rates relative to the intact state, albeit not observed to be significantly different. It should be noted that the wear appeared visually to be concentrated within a secondary wear region that developed in the inferior aspect, for a testing period representative of the time of implantation for retrieved RTSA components exhibiting scapular notching damage.

3.6 References

Brandt, J.-M., Briere, L. K., Marr, J., Macdonald, S. J., Bourne, R. B., & Medley, J. B. (2010). Biochemical comparisons of osteoarthritic human synovial fluid with calf sera used in knee simulator wear testing. *Journal of Biomedical Materials Research A*, *94A*(3), 961–971. http://doi.org/10.1002/jbm.a.32728

Brandt, J.-M., Mahmoud, K. K., Koval, S. F., MacDonald, S. J., & Medley, J. B. (2013). Antimicrobial agents and low-molecular weight polypeptides affect polyethylene wear in knee simulator testing. *Tribology International*, *65*, 97–104. http://doi.org/10.1016/j.triboint.2013.02.019

Carpenter, S., Pinkas, D., Newton, M. D., Kurdziel, M. D., Baker, K. C., & Wiater, J. M. (2015). Wear rates of retentive versus nonretentive reverse total shoulder arthroplasty liners in an in vitro wear simulation. *Journal of Shoulder and Elbow Surgery*, *24*(9), 1372–1379. http://doi.org/10.1016/j.jse.2015.02.016

Castagna, A., Delcogliano, M., De Caro, F., Ziveri, G., Borroni, M., Gumina, S., … De Biase, C. F. (2013). Conversion of shoulder arthroplasty to reverse implants: Clinical and radiological results using a modular system. *International Orthopaedics*, *37*(7), 1297–1305. http://doi.org/10.1007/s00264-013-1907-4

Clouthier, A. L., Hetzler, M. A., Fedorak, G., Bryant, J. T., Deluzio, K. J., & Bicknell, R. T. (2013). Factors affecting the stability of reverse shoulder arthroplasty : a biomechanical study. *Journal of Shoulder and Elbow Surgery*, *22*(4), 439–444. http://doi.org/10.1016/j.jse.2012.05.032

Day, J. S., MacDonald, D. W., Olsen, M., Getz, C., Williams, G. R., & Kurtz, S. M. (2012). Polyethylene wear in retrieved reverse total shoulder components. *Journal of Shoulder and Elbow Surgery*, *21*(5), 667–674. http://doi.org/10.1016/j.jse.2011.03.012

de Wilde, L. F., Poncet, D., Middernacht, B., & Ekelund, A. (2010). Prosthetic overhang is the most effective way to prevent scapular conflict in a reverse total shoulder prosthesis. *Acta Orthopaedica*, *81*(6), 719–726. http://doi.org/10.3109/17453674.2010.538354

Dieckmann, R., Liem, D., Gosheger, G., Henrichs, M. P., Höll, S., Hardes, J., & Streitbürger, A. (2013). Evaluation of a reconstruction reverse shoulder for tumour surgery and tribological comparision with an anatomical shoulder arthroplasty. *International Orthopaedics*, *37*(3), 451–456. http://doi.org/10.1007/s00264-012-1771-7

Ek, E. T. H., Neukom, L., Catanzaro, S., & Gerber, C. (2013). Reverse total shoulder arthroplasty for massive irreparable rotator cuff tears in patients younger than 65 years old: Results after five to fifteen years. *Journal of Shoulder and Elbow Surgery*, *22*(9), 1199–1208. http://doi.org/10.1016/j.jse.2012.11.016

Farshad, M., & Gerber, C. (2010). Reverse total shoulder arthroplasty-from the most to the least common complication. *International Orthopaedics*, *34*(8), 1075–1082. http://doi.org/10.1007/s00264-010-1125-2

Flury, M. P., Frey, P., Goldhahn, J., Schwyzer, H. K., & Simmen, B. R. (2011). Reverse shoulder arthroplasty as a salvage procedure for failed conventional shoulder replacement due to cuff failure-midterm results. *International Orthopaedics*, *35*(1), 53–60. http://doi.org/10.1007/s00264-010-0990-z

Gutiérrez, S., Keller, T. S., Levy, J. C., Lee, W. E. I., & Zong-Ping, L. (2008). Hierarchy of Stability Factors in Reverse Shoulder Arthroplasty Hierarchy of Stability Factors in Reverse Shoulder Arthroplasty. *Clinical Orthopaedics and Related Research*, *446*(3), 670–676. http://doi.org/10.1007/s11999-007-0096-0

Gutiérrez, S., Luo, Z. P., Levy, J., & Frankle, M. A. (2009). Arc of motion and socket depth in reverse shoulder implants. *Clinical Biomechanics*, *24*(6), 473–479. http://doi.org/10.1016/j.clinbiomech.2009.02.008

Hallab, N. J., & Jacobs, J. J. (2009). Biologic effects of implant debris. *Bulletin of the NYU Hospital for Joint Diseases*, *67*(2), 182–188.

International Organization for Standardization. (2000). Implants for surgery - Wear of total hip-joint prostheses - Part 2: Methods of measurement. In *ISO 14242-2*.

Kohut, G., Dallmann, F., & Irlenbusch, U. (2012). Wear-induced loss of mass in reversed total shoulder arthroplasty with conventional and inverted bearing materials. *Journal of Biomechanics*, *45*(3), 469–473. http://doi.org/10.1016/j.jbiomech.2011.11.055

Kurtz, S. M., Villarraga, M. L., Herr, M. P., Bergstrom, J. S., Rimmac, C. M., & Edidin, A. A. (2002). Thermomechanical behavior of virgin and highly crosslinked ultra-high molecular weight polyethylene used in total joint replacements. *Biomaterials*, *23*, 3681–3697.

Langohr, G. D. G. (2015). *Fundamentals of the Biomechanical Characteristics Related to the Loading of Reverse Total Shoulder Arthroplasty Implants and the Development of a Wear Simulation Strategy*.

Langohr, G. D. G., Athwal, G. S., Johnson, J. A., & Medley, J. B. (2016). Wear simulation strategies for reverse shoulder arthroplasty implants. *Journal of Engineering in Medicine*, *230*(5), 458–469. http://doi.org/10.1177/0954411916642801

Langohr, G. D. G., Willing, R., Medley, J. B., Athwal, G. S., & Johnson, J. A. (2016). Contact mechanics of reverse total shoulder arthroplasty during abduction: The effect of neck-shaft angle, humeral cup depth, and glenosphere diameter. *Journal of Shoulder and Elbow Surgery*, *25*(4), 589–597. http://doi.org/10.1016/j.jse.2015.09.024

Masjedi, M., & Johnson, G. R. (2010). Glenohumeral contact forces in reversed anatomy shoulder replacement. *Journal of Biomechanics*, *43*(13), 2493–2500. http://doi.org/10.1016/j.jbiomech.2010.05.024

Muh, S. J., Streit, J. J., Wanner, J. P., Lenarz, C. J., Shishani, Y., Rowland, D. Y., … Gobezie, R. (2013). Early follow-up of reverse total shoulder arthroplasty in patients sixty years of age or younger. *The Journal of Bone and Joint Surgery. American Volume*, *95*(20), 1877–83. http://doi.org/10.2106/JBJS.L.10005

Nam, D., Kepler, C. K., Nho, S. J., Craig, E. V, Warren, R. F., & Wright, T. M. (2010). Observations on retrieved humeral polyethylene components from reverse total shoulder arthroplasty. *Journal of Shoulder and Elbow Surgery*, *19*(7), 1003–1012. http://doi.org/10.1016/j.jse.2010.05.014

Nyffeler, R. W., Werner, C. M. L., Simmen, B. R., & Gerber, C. (2004). Analysis of a retrieved Delta III total shoulder prosthesis. *The Journal of Bone and Joint Surgery*, *86*(8), 1187–1191. http://doi.org/10.1302/0301-620X.86B8.15228

Pastor, M., Kraemer, M., Wellmann, M., Hurschler, C., & Smith, T. (2016). Anterior stability of the reverse shoulder arthroplasty depending on implant configuration and rotator cuff condition. *Archives of Orthopaedic and Trauma Surgery*, *136*(11), 1513–1519. http://doi.org/10.1007/s00402-016-2560-3

Pruitt, L. A. (2005). Deformation , yielding , fracture and fatigue behavior of conventional and highly cross-linked ultra high molecular weight polyethylene. *Biomaterials*, *26*, 905–915. http://doi.org/10.1016/j.biomaterials.2004.03.022

Pruitt, L. A., Ansari, F., Kury, M., Mehdizah, A., Patten, E. W., Huddlestein, J., … Ries, M. D. (2013). Clinical trade-offs in cross-linked ultrahigh-molecular-weight polyethylene used in total joint arthroplasty. *Journal of Biomedical Materials Research Part B: Applied Biomaterials*, *10B*(3), 476–484. http://doi.org/10.1002/jbm.b.32887

Rader, C. P., Sterner, T., Jakob, F., Schütze, N., & Eulert, J. (1999). Cytokine response of human macrophage-like cells after contact with polyethylene and pure titanium particles. *Journal of Arthroplasty*, *14*(7), 840–848. http://doi.org/10.1016/S0883-5403(99)90035-9

Roche, C., Flurin, P. H., Wright, T., Crosby, L. A., Mauldin, M., & Zuckerman, J. D. (2009). An evaluation of the relationships between reverse shoulder design parameters and range of motion, impingement, and stability. *Journal of Shoulder and Elbow Surgery*, *18*(5), 734–741. http://doi.org/10.1016/j.jse.2008.12.008

Smith, S. L., Li, B. L., Buniya, A., Lin, S. H., Scholes, S. C., Johnson, G., & Joyce, T. J. (2015). In vitro wear testing of a contemporary design of reverse shoulder prosthesis. *Journal of Biomechanics*, *48*(12), 3072–3079. http://doi.org/10.1016/j.jbiomech.2015.07.022

Terrier, A., Merlini, F., Farron, A., & Pioletti, D. P. (2009). Reverse shoulder arthroplasty: polyethylene wear. *Computer Methods in Biomechanics and Biomedical Engineering*, *12*(sup1), 247–248. http://doi.org/10.1080/10255840903097855

Vaupel, Z. M., Baker, K. C., Kurdziel, M. D., & Wiater, J. M. (2012). Wear simulation of reverse total shoulder arthroplasty systems: effect of glenosphere design. *Journal of Shoulder and Elbow Surgery*, *21*(10), 1422–1429. http://doi.org/10.1016/j.jse.2011.10.024

Weber-Spickschen, T. S., Alfke, D., & Agneskirchner, J. D. (2015). The use of a modular system to convert an anatomical total shoulder arthroplasty to a reverse shoulder arthroplasty: Clinical and radiological results. *Bone and Joint Journal*, *97B*(12), 1662–1667. http://doi.org/10.1302/0301-620X.97B12.35176

Werner, B. S., Boehm, D., & Gohlke, F. (2013). Revision to reverse shoulder arthroplasty with retention of the humeral component. *Acta Orthopaedica*, *84*(5), 473–478. http://doi.org/10.3109/17453674.2013.842433

Chapter 4

Effect of Inferior Glenosphere Tilt on the Contact Mechanics

OVERVIEW: Inferior tilting of the glenosphere is a strategy that can be applied during reverse total shoulder arthroplasty (RTSA) to improve adduction range of motion, thereby potentially reducing the risk of scapular notching. While the effects at the bone-baseplate interface have been previously assessed in literature, the purpose of the present finite element study was to investigate the effect that this change in component orientation has on articular contact mechanics during abduction, utilizing multiple physiologically relevant joint load profiles. While it is recognized that there are a wide range of implant parameters that can affect the contact mechanics of the RTSA glenohumeral articulation, glenosphere tilting was selected herein as a clinically viable intraoperative option that does not need changes to implant design parameters.[3,4]

---

[3] A portion of the work covered in Chapter 1 is included within the introduction, in addition to the methods covered in Chapter 2 for the finite element modelling, as part of the Integrated-Article format.

[4] A version of this work was presented as part of the 2017 Canadian Orthopaedic Research Society Annual Meeting: Griffiths, M.W., Langohr, G.D.G., Athwal, G.S., Johnson, J.A. (2017) Inferior Glenosphere Tilt Improves Reverse Shoulder Arthroplasty Contact Mechanics. *Canadian Orthopaedic Research Society Annual Meeting*, June 15-18, Ottawa, Ontario

4.1 Introduction

Reverse total shoulder arthroplasty (RTSA) is an effective treatment of severe rotator cuff arthropathies and proximal humeral fractures, as well as the revision of failed shoulder arthroplasty (Boileau et al., 2006; Castagna et al., 2013; Ek et al., 2013; Flury et al., 2011; Muh et al., 2013; Mulieri et al., 2010; Nolan et al., 2011; Weber-Spickschen et al., 2015; Young et al., 2009). However, scapular notching is still a common finding with this joint replacement system, as documented in Section 1.3.2. This process is initiated when the inferior aspect of the humeral cup component impinges against the scapula during adduction, with damage to the polyethylene humeral cup resulting, as the material's yield stress is exceeded over the small area of contact (Permeswaran et al., 2016). Subsequent polyethylene debris deposits on the scapula then initiate a biologic notching process (Kohut et al., 2012), with macrophage mediated bone resorption increasing in response to the concentration of polyethylene debris (Hallab & Jacobs, 2009; Rader et al., 1999).

Scapular notching is the most frequently reported complication of RTSA systems (Farshad & Gerber, 2010). However, its observed incidence is quite variable, being reported in 10% to 74% of cases in radiographic assessment studies (Boileau et al., 2006, 2005; Ek et al., 2013; Flury et al., 2011; Lévigne et al., 2011; Mollon et al., 2017; Mulieri et al., 2010; Nolan et al., 2011; Sirveaux et al., 2004; Weber-Spickschen et al., 2015; Young et al., 2009), with an increase in degree of notching being observed over time (Ek et al., 2013). Furthermore, damage to the humeral cup as a result of scapular notching has also been reported in 45% to 100% of surgical retrieval studies (Day et al., 2012; Nam et al., 2010; Wiater et al., 2015).

With RTSA being a highly modular system, there are several strategies in the geometry and placement of components which can reduce the risk of scapular notching, mainly through increasing adduction range of motion. One such example is the inferior tilting of the glenosphere, where a downward tilt of the glenosphere is achieved through the use of reaming and bone grafts, as depicted in Figure 4-1. This has been demonstrated to increase the adduction range of motion in both computer simulation (de Wilde et al., 2010; Gutiérrez, Comiskey, et al., 2008) and cadaveric biomechanical studies (Berhouet et al., 2014; Nyffeler et al., 2005). This increase in adduction range of motion comes as a result

of the oblique cut of the glenoid, wherein there is a decrease in the osseous surface area, specifically along the inferior aspect (Nyffeler et al., 2005). Clinically it has been indicated that inferior glenosphere tilt results in an overall improvement joint stability, with a reduction in the incidence of atraumatic dislocations (Randelli et al., 2014).

While the effects on shoulder range of motion and implications for the bone-baseplate and bone-screw interfaces have been previously explored, the influence of glenosphere tilt has not been investigated for factors with respect to articular contact mechanics. Therefore, the objective of the current study was to evaluate the effects of glenosphere tilt on the contact mechanics of RTSA at multiple angles of abduction utilizing finite element analysis, in the absence of scapular impingement and baseplate micromotion. It is hypothesized that the inferior tilting of the glenosphere will result in improved contact mechanics, specifically at low angles of abduction, as a result of the decreased inferior overhang of the humeral cup.
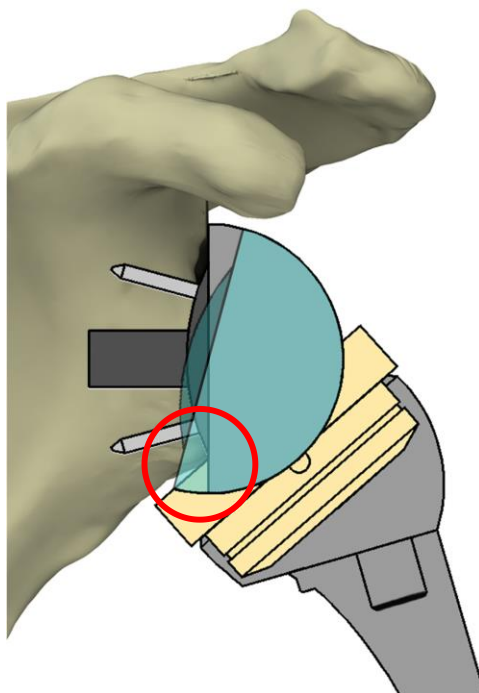

Figure 4-1: Inferiorly tilted glenosphere, with reduced humeral cup overhang indicated

Note that only the glenosphere has been rotated (overlayed in blue) for the purpose of clarity.

4.2   Materials & Methods

4.2.1   Finite Element Modeling

Similar to that employed in Chapter 2, finite element models of a reverse total shoulder prosthesis were constructed in Abaqus v6.12 (Simulia Corp, Providence, RI, USA), based on the geometry and simulation parameters of a previously published model used in assessing the effect of implant design considerations (Langohr, Willing, et al., 2016). The implant system parameters modeled for the current work were representative of a reverse total shoulder prostheses with a humeral neck-shaft angle of 155°, glenosphere diameter of 38 mm, and a conventional humeral cup depth of 8.75 mm, while varying the angle of glenosphere tilt as depicted in Figure 4-2. This simplified model consisted of only the hemispherical glenosphere and humeral cup components, in order to focus on their interactions. The humeral cup component was assigned linear elastic ultra-high-molecular-weight polyethylene (UHMWPE) material properties (E = 650 MPa, v = 0.44) (Kurtz et al., 2002; Pruitt, 2005), whereas the glenosphere was assigned cobalt-chrome (CoCr) material properties (E = 210 GPa, v = 0.3). Both components were meshed with linear hexahedral elements (C3D8R), with an average side length of approximately 0.3 mm. All encompassed, this resulted in approximately 220,000 elements for the assembly (approximately 800,000 degrees of freedom). Surface-to-surface discretization of the articular faces was utilized in penalty-based contact, with a coefficient of friction set at 0.04 (Godest et al., 2002; Willing & Kim, 2009), while the back faces of each component were rigidly constrained.

Alteration of the glenosphere tilt was achieved through rotating this implant about its anterior-posterior axis while maintaining the same center of rotation, as depicted in Figure 4-2-B. This was done in order to achieve a 5° superior glenosphere tilt, as well as a 5°, 10°, and 15° inferior tilt, in addition to the (0°) neutral tilt. The glenosphere component remained in a fixed position, while the humeral cup component articulated against it at various angles of humeroscapular abduction. The joint load profiles for the seven specimens (n = 7) included, as utilized in the work of Chapter 2 (Figure 2-4), were discretized from previous works using an instrumented reverse total shoulder prosthesis (Giles et al., 2015; Langohr et al., 2015) in a custom shoulder simulator (Giles et al., 2014).

This was conducted for humeroscapular abduction angles of 10° to 55° at 5° increments. It should be noted that anterior-posterior load contributions were not included in the present model, due to the smaller relative magnitude compared to the compressive and shear components.

4.2.2   Testing Protocol & Outcome Variables

For each of the seven specimen loading data included, finite element analyses were conducted at the 5 angles of glenosphere tilt (5° superior to 15° inferior at 5° intervals). These simulations focused on modelling contact mechanics absent of the osseous anatomy, thereby excluding factors such as scapular impingement and baseplate displacement. The parameters for investigating the contact mechanics were the maximum contact stress of the humeral cup and articular surface contact area, at each abduction angle. A two-way repeated measures ANOVA ($\alpha = 0.05$) was conducted in SPSS (V25, IBM Corporation, Armonk, NY, USA) to evaluate each of the outcome variables, where level of defect and angle of abduction where the independent variables.

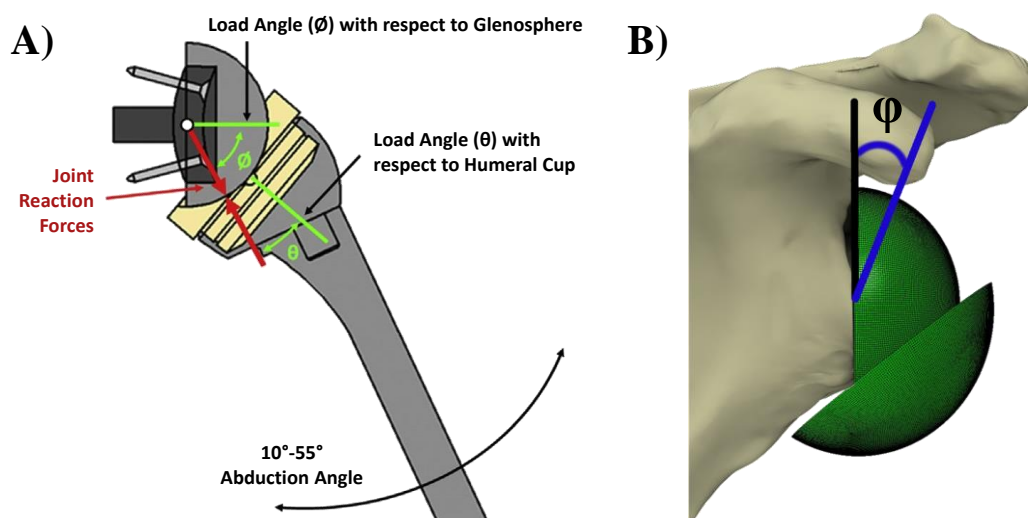**Figure 4-2: (A) Finite element model loading and boundary conditions with (B) angle of inferior glenosphere tilt (φ) indicated**

Note the scapula has been included in (B) for orientation purposes but was not included in the constructed model.

4.3   Results

As abduction angle increased, there was a corresponding increase in mean contact area (Figure 4-3). Angle of abduction was found to have a significant effect on mean contact area (p = 0.014), as was the case for the angle of glenosphere tilt (p = 0.012). The latter was predominately visible at the lower angles of abduction investigated, with an inferior tilt of the glenosphere resulting in an increased contact area. This was exemplified through the average increase in contact area of 14% (114.73 $\pm$ 82.14 mm^2) between the 5° superior and 15° inferior glenosphere tilts at 10° abduction. However, above 30° abduction the influence of glenosphere tilt is less prominent in the mean contact area values, with altering the glenosphere orientation from 5° superior to 15° inferior only resulting in an average increase in joint contact area of 5% (45.31 $\pm$ 64.24 mm^2) when observed across all angles of abduction tested.

Conversely, while mean maximum contact stress values decreased with increased abduction angle (Figure 4-4), no significant effect was observed (p = 0.155). Additionally, the angle of glenosphere tilt was also found to have no significant effect on mean maximum contact stress (p = 0.242). Overall, increasing inferior glensophere tilt from 5° superior to 15° inferior only resulted in an average decrease of maximum contact stress values of 3% (0.04 $\pm$ 0.16 MPa). The location of maximum contact stress differed among the specimens simulated, as the joint load angle varied for any given angle of abduction, but was typically observed in the inferior most (Figure 4-5) or superior most (Figure 4-6) region of contact.
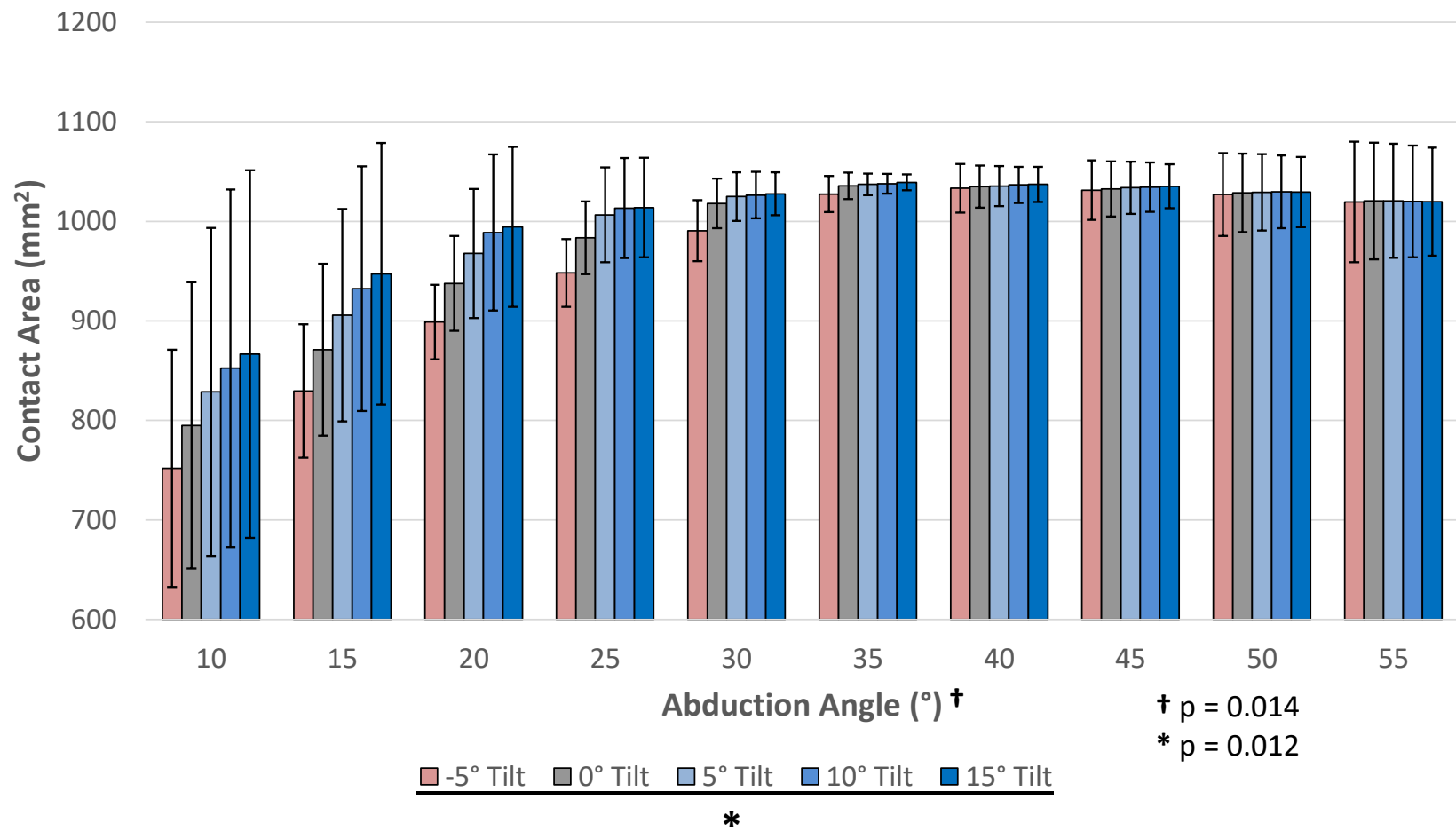
Figure 4-3: Mean contact area with increasing inferior glenosphere tilt

For all specimens investigated (±1 std dev) with superior glenosphere tilt (red; -5°), neutral glenosphere tilt (grey; 0°), and inferior glenosphere tilt (blue; 5°, 10°, & 15°).
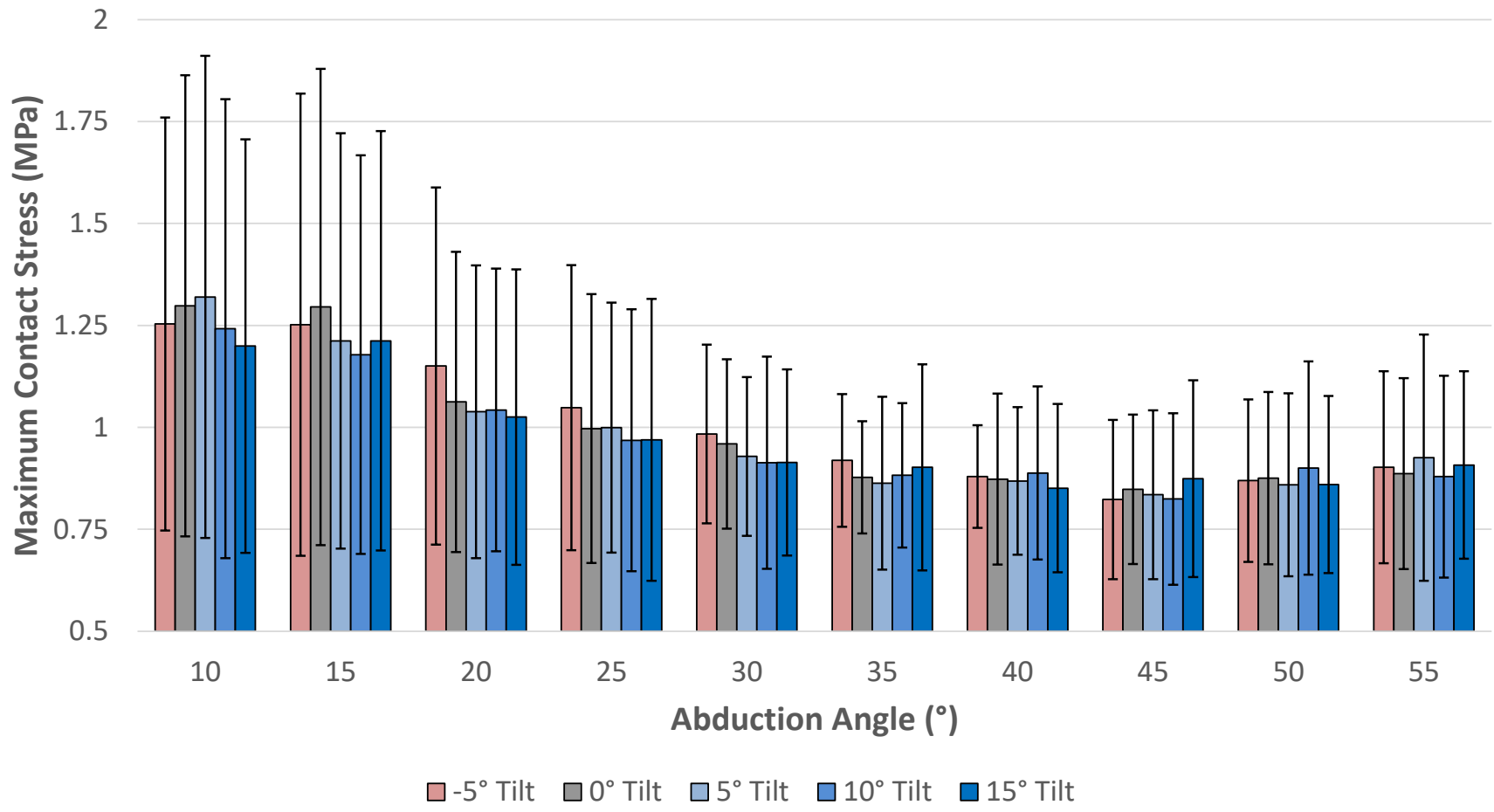
Figure 4-4: Mean maximum contact stress with increasing inferior glenosphere tilt

For all specimens investigated (±1 std dev) with superior glenosphere tilt (-5°; red), neutral glenosphere tilt (0°; grey), and inferior glenosphere tilt (5°, 10°, & 15°; blue).
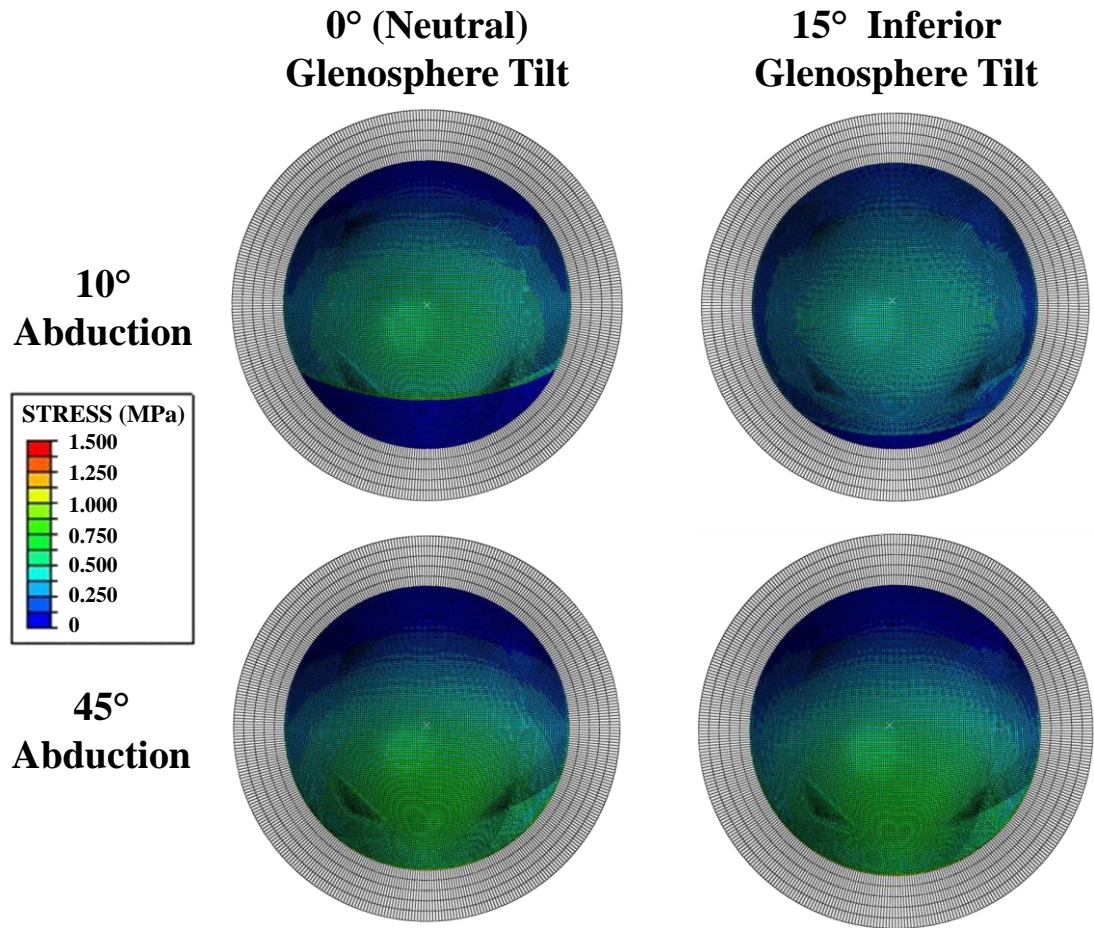
Figure 4-5: Humeral cup contact stress distribution maps for 10° and 45° abduction, with a neutral and 15° inferior glenosphere tilt (inferomedial)

Note the inferomedially located maximum contact stress and that all stress values have been normalized to the same scale.
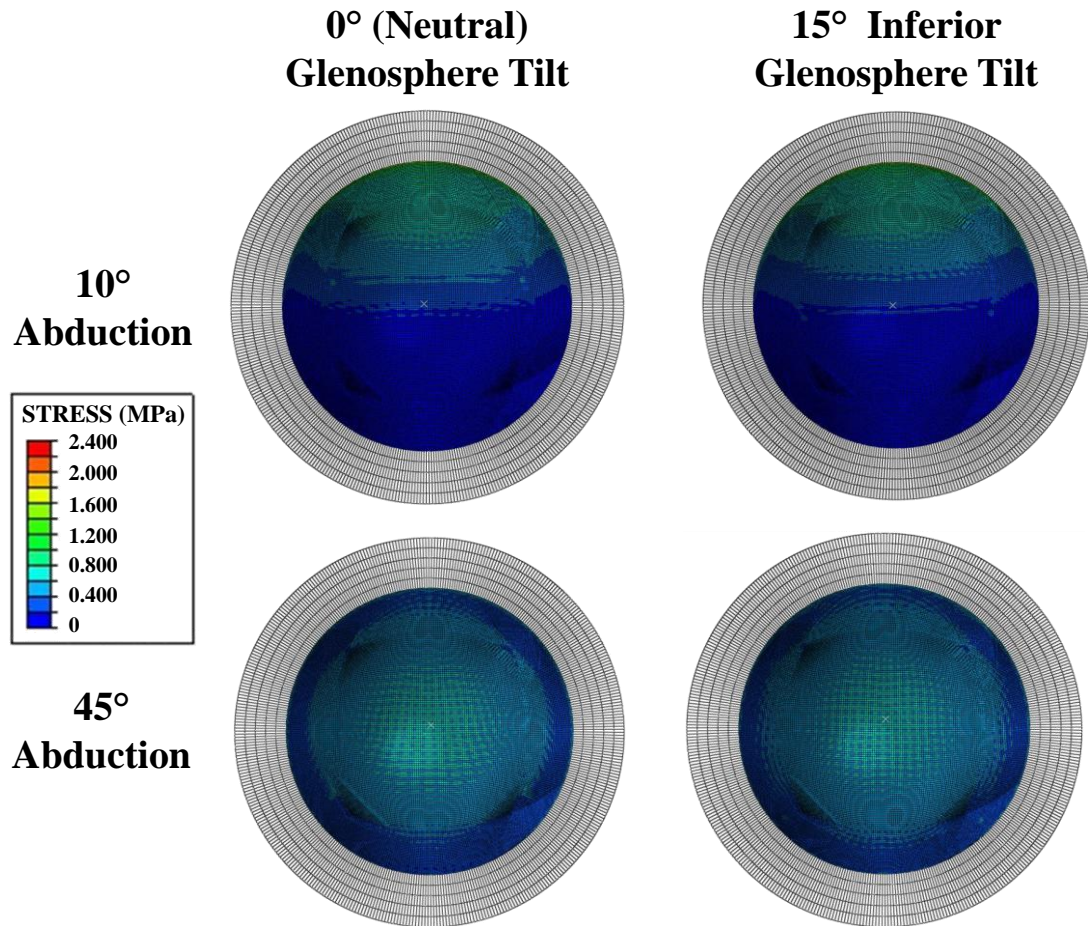
Figure 4-6: Humeral cup contact stress distribution maps for 10° and 45° abduction, with a neutral and 15° inferior glenosphere tilt (superomedial)

Note the superomedially located maximum contact stress and that all stress values have been normalized to the same scale.

4.4 Discussion

The implementation of an inferiorly tilted glenosphere in RTSA has been demonstrated to reduce the risk of scapular notching through the increase of adduction range of motion (Berhouet et al., 2014; de Wilde et al., 2010; Gutiérrez, Comiskey, et al., 2008; Nyffeler et al., 2005). However, it should be noted that while there is an increase in adduction range of motion, inferior glenosphere tilt has been shown to not affect the incidence of scapular notching relative to a neutral tilt in a surgical radiographic follow-up study, when adjusting for the time since implantation (Kempton et al., 2011). While there have been some previous studies on the effects of baseplate stability and displacement, there are conflicting results with some indicating improvement in these areas (Denard et al., 2016; Gutiérrez et al., 2007, 2011) whereas others indicate a deterioration and even increased risk of failure (Chae et al., 2016, 2015). Although previous work has investigated the effect of implant design parameters on articular contact mechanics (Langohr, Willing, et al., 2016), the present work is, to the authors' best knowledge, the first to assess the effect of implant orientation within this area.

When viewing the humeral cup contact patches, it can be discerned that the inferior tilting of the glenosphere also translated the contact area inferiorly. This was predominantly evident at lower angles of abduction and is especially prevalent in the 10° abduction stress distribution maps of Figure 4-5. Here it can be seen that the inferior tilting of the glenosphere increased contact area by reducing the area of non-contact at the inferior aspect of the humeral cup, due to the initial overhang behind the medial aspect of the glenosphere, as highlighted in Figure 4-1. A similar trend was observed by Langohr et al (2016) with the decrease of neck-shaft angle, wherein changing the neck-shaft angle from 155° to 135° resulted in an inferior movement of the contact area. However, the decrease in angle of this parameter also came with an accompanying decrease in joint contact area and increased maximum contact stress (Langohr, Willing, et al., 2016). Therefore it serves to reason that decreasing the neck-shaft angle from 155°, as tested in the present study, to 135° would mitigate the positive effects that inferior glenosphere tilt had on articular contact area.

Furthermore, the effect of altering glenosphere tilt was found to have less of an improvement for the contact area and maximum stress values relative to the parameters

tested by Langohr et al (2016). Only one factor investigated generated a percent change within a comparable range for that observed in the present work, whereas all others previously investigated demonstrated a much more pronounce impact. Namely increasing the depth to a deep humeral cup yielded an increase in contact area of 12% but only a reduction in maximum contact stress of 2% (Langohr, Willing, et al., 2016). Although this impact on contact mechanics is comparable to the effect viewed with inferior glenosphere tilt, the more conforming humeral cups would serve to decrease the adduction range of motion (de Wilde et al., 2010; Gutiérrez et al., 2009; Roche et al., 2009), thereby resulting in a possible increased risk for propagating scapular notching.

It should be noted that while the maximum stress values were well below that of the yield strength for UHMWPE (Kurtz et al., 2002; Pruitt, 2005), there were a variety of contact patches and locations for the maximum contact stress value on the humeral cup not previously observed. Previous finite element studies reported both the area of articular contact and location of maximum contact stress being located inferomedially (Langohr, Willing, et al., 2016; Terrier et al., 2009), which is also the most common location to see humeral cup damage in retrievals (Nam et al., 2010). While some of the joint load profiles discretized from cadaveric loading used in the present study corroborated these results (Figure 4-5), others presented with both the area of articular contact and maximum contact stress being located superomedially (Figure 4-6). However, it should be noted that while damage to the humeral cup in the superior region has been reported in surgical retrievals, it also occurred in the lowest observed incidence (Nam et al., 2010). Nevertheless, this would indicate that there are several possible articular contact profiles possible which could influence the effect of RTSA implant parameters on contact mechanics being investigated in finite element studies. Furthermore, displacement of the baseplate in inferiorly tilted glenospheres, whether predominantly in the middle and lower third (Chae et al., 2016) or more uniform across the baseplate (Gutiérrez et al., 2007) could alter the relative glenosphere position and orientation, albeit on the scale of micrometers, thereby effecting the articular contact response.

While the effects of inferior glenosphere tilt were predominantly noted at low angles of abduction, this is an extremely crucial range of motion. Through motion tracking, it has

been indicated that the operated shoulder of arthroplasty recipients' most common range of humeral-thoracic abduction is between 0° and 60°, encompassing 88% ± 26% of daily motion recorded (Langohr, 2015). Therefore, it serves to reason that improving the articular contact mechanics at low angles of abduction, without impeding performance at greater ranges of motion, would be beneficial in order to extend the longevity of the implant, beyond the reduced risk of scapular notching inferior glenosphere tilt already provides. Moreover, these results also provide further understanding as to the decreased risk of atraumatic dislocation with a 10° glenosphere tilt viewed by Randelli et al (2014), through the positive effects on articular contact mechanic parameters. It has also been speculated that improved articular contact mechanics, specifically a reduction in the maximum contact stress values, will result in decreased inferior polyethylene damage independent of scapular notching (Langohr, Willing, et al., 2016).

4.5   Conclusions

This work provides new insights with respect to the effects of inferior glenosphere tilt at the articular surface, in terms of joint contact area and maximum contact stress. Increasing inferior tilt was found to increase joint contact area, specifically at low angles of abduction, with no observed effect on maximum contact stress values. This was accomplished through the reduction in the inferior overhang of the humeral cup behind the medial plane of the glenosphere. Overall, this would suggest that an inferiorly tilted glenosphere can improve articular contact mechanics within a frequently utilized range of motion. Additionally, the use of multiple physiologically relevant joint load profiles demonstrated different regions of maximum contact stress not previously observed, indicating that each individual may have a different articular contact response to the alterations of RTSA implant parameters.

4.6 References

Berhouet, J., Garaud, P., & Favard, L. (2014). Evaluation of the role of glenosphere design and humeral component retroversion in avoiding scapular notching during reverse shoulder arthroplasty. *Journal of Shoulder and Elbow Surgery*, *23*(2), 151–158. http://doi.org/10.1016/j.jse.2013.05.009

Boileau, P., Watkinson, D., Hatzidakis, A. M., & Hovorka, I. (2006). Neer Award 2005: The Grammont reverse shoulder prosthesis: Results in cuff tear arthritis, fracture sequelae, and revision arthroplasty. *Journal of Shoulder and Elbow Surgery*, *15*(5), 527–540. http://doi.org/10.1016/j.jse.2006.01.003

Boileau, P., Watkinson, D. J., Hatzidakis, A. M., & Balg, F. (2005). Grammont reverse prosthesis: Design, rationale, and biomechanics. *Journal of Shoulder and Elbow Surgery*, *14*(1), S147–S161. http://doi.org/10.1016/j.jse.2004.10.006

Castagna, A., Delcogliano, M., De Caro, F., Ziveri, G., Borroni, M., Gumina, S., … De Biase, C. F. (2013). Conversion of shoulder arthroplasty to reverse implants: Clinical and radiological results using a modular system. *International Orthopaedics*, *37*(7), 1297–1305. http://doi.org/10.1007/s00264-013-1907-4

Chae, S. W., Lee, H., Kim, S. M., Lee, J., Han, S., & Kim, S. (2016). Primary Stability of Inferior Tilt Fixation of the Glenoid Component in Reverse Total Shoulder Arthroplasty : A Finite Element Study. *Journal of Orthopaedic Research*, (June), 1061–1068. http://doi.org/10.1002/jor.23115

Chae, S. W., Lee, J., Han, S. H., & Kim, S. (2015). Inferior tilt fixation of the glenoid component in reverse total shoulder arthroplasty : A biomechanical study. *Orthopaedics & Traumatology: Surgery & Research*, *101*(4), 421–425. http://doi.org/10.1016/j.otsr.2015.03.009

Day, J. S., MacDonald, D. W., Olsen, M., Getz, C., Williams, G. R., & Kurtz, S. M. (2012). Polyethylene wear in retrieved reverse total shoulder components. *Journal of Shoulder and Elbow Surgery*, *21*(5), 667–674. http://doi.org/10.1016/j.jse.2011.03.012

de Wilde, L. F., Poncet, D., Middernacht, B., & Ekelund, A. (2010). Prosthetic overhang is the most effective way to prevent scapular conflict in a reverse total shoulder prosthesis. *Acta Orthopaedica*, *81*(6), 719–726. http://doi.org/10.3109/17453674.2010.538354

Denard, P. J., Lederman, E., Parsons, B. O., & Romeo, A. A. (2016). Finite element analysis of glenoid-sided lateralization in reverse shoulder arthroplasty. *Journal of Orthopaedic Research*, *35*(7), 1548–1555. http://doi.org/10.1002/jor.23394

Ek, E. T. H., Neukom, L., Catanzaro, S., & Gerber, C. (2013). Reverse total shoulder arthroplasty for massive irreparable rotator cuff tears in patients younger than 65 years old: Results after five to fifteen years. *Journal of Shoulder and Elbow Surgery*, *22*(9), 1199–1208. http://doi.org/10.1016/j.jse.2012.11.016

Farshad, M., & Gerber, C. (2010). Reverse total shoulder arthroplasty-from the most to the least common complication. *International Orthopaedics*, *34*(8), 1075–1082. http://doi.org/10.1007/s00264-010-1125-2

Flury, M. P., Frey, P., Goldhahn, J., Schwyzer, H. K., & Simmen, B. R. (2011). Reverse shoulder arthroplasty as a salvage procedure for failed conventional shoulder replacement due to cuff failure-midterm results. *International Orthopaedics*, *35*(1), 53–60. http://doi.org/10.1007/s00264-010-0990-z

Giles, J. W., Ferreira, L. M., Athwal, G. S., & Johnson, J. A. (2014). Development and Performance Evaluation of a Multi-PID Muscle Loading Driven In Vitro Active-Motion Shoulder Simulator and Application to Assessing Reverse Total Shoulder Arthroplasty. *Journal of Biomechanical Engineering*, *136*(12), 121007. http://doi.org/10.1115/1.4028820

Giles, J. W., Langohr, G. D. G., Johnson, J. A., & Athwal, G. S. (2015). Implant Design Variations in Reverse Total Shoulder Arthroplasty Influence the Required Deltoid Force and Resultant Joint Load. *Clinical Orthopaedics and Related Research*, *473*(11), 3615–3626. http://doi.org/10.1007/s11999-015-4526-0

Godest, A. C., Beaugonin, M., Haug, E., Taylor, M., & Gregson, P. J. (2002). Simulation of a knee joint replacement during a gait cycle using explicit finite element analysis. *Journal of Biomechanics*, *35*(2), 267–275. http://doi.org/10.1016/S0021-9290(01)00179-8

Gutiérrez, S., Comiskey, C. A., Luo, Z.-P., Pupello, D. R., & Frankle, M. A. (2008). Range of Impingement-Free Abduction and Adduction Deficit After Reverse Shoulder Arthroplasty. *The Journal of Bone and Joint Surgery-American Volume*, *90*(12), 2606–2615. http://doi.org/10.2106/JBJS.H.00012

Gutiérrez, S., Greiwe, R. M., Frankle, M. A., Siegal, S., & Lee, W. E. (2007). Biomechanical comparison of component position and hardware failure in the reverse shoulder prosthesis. *Journal of Shoulder and Elbow Surgery*, *16*(3 SUPPL.), 9–12. http://doi.org/10.1016/j.jse.2005.11.008

Gutiérrez, S., Luo, Z. P., Levy, J., & Frankle, M. A. (2009). Arc of motion and socket depth in reverse shoulder implants. *Clinical Biomechanics*, *24*(6), 473–479. http://doi.org/10.1016/j.clinbiomech.2009.02.008

Gutiérrez, S., Walker, M., Willis, M., Pupello, D. R., & Frankle, M. A. (2011). Effects of tilt and glenosphere eccentricity on baseplate/bone interface forces in a computational model, validated by a mechanical model, of reverse shoulder arthroplasty. *Journal of Shoulder and Elbow Surgery*, *20*(5), 732–739. http://doi.org/10.1016/j.jse.2010.10.035

Hallab, N. J., & Jacobs, J. J. (2009). Biologic effects of implant debris. *Bulletin of the NYU Hospital for Joint Diseases*, *67*(2), 182–188.

Kempton, L. B., Balasubramaniam, M., Ankerson, E., & Wiater, J. M. (2011). A radiographic analysis of the effects of glenosphere position on scapular notching following reverse total shoulder arthroplasty. *Journal of Shoulder and Elbow Surgery*, *20*(6), 968–974. http://doi.org/10.1016/j.jse.2010.11.026

Kohut, G., Dallmann, F., & Irlenbusch, U. (2012). Wear-induced loss of mass in reversed total shoulder arthroplasty with conventional and inverted bearing materials. *Journal of Biomechanics*, *45*(3), 469–473. http://doi.org/10.1016/j.jbiomech.2011.11.055

Kurtz, S. M., Villarraga, M. L., Herr, M. P., Bergstrom, J. S., Rimmac, C. M., & Edidin, A. A. (2002). Thermomechanical behavior of virgin and highly crosslinked ultra-high molecular weight polyethylene used in total joint replacements. *Biomaterials*, *23*, 3681–3697.

Langohr, G. D. G. (2015). *Fundamentals of the Biomechanical Characteristics Related to the Loading of Reverse Total Shoulder Arthroplasty Implants and the Development of a Wear Simulation Strategy*.

Langohr, G. D. G., Giles, J. W., Athwal, G. S., & Johnson, J. A. (2015). The effect of glenosphere diameter in reverse shoulder arthroplasty on muscle force, joint load, and range of motion. *Journal of Shoulder and Elbow Surgery*, *24*(6), 972–979. http://doi.org/10.1016/j.jse.2014.10.018

Langohr, G. D. G., Willing, R., Medley, J. B., Athwal, G. S., & Johnson, J. A. (2016). Contact mechanics of reverse total shoulder arthroplasty during abduction: The effect of neck-shaft angle, humeral cup depth, and glenosphere diameter. *Journal of Shoulder and Elbow Surgery*, *25*(4), 589–597. http://doi.org/10.1016/j.jse.2015.09.024

Lévigne, C., Garret, J., Boileau, P., Alami, G., Favard, L., & Walch, G. (2011). Scapular notching in reverse shoulder arthroplasty: Is it important to avoid it and how? *Clinical Orthopaedics and Related Research*, *469*(9), 2512–2520. http://doi.org/10.1007/s11999-010-1695-8

Mollon, B., Mahure, S. A., Roche, C. P., & Zuckerman, J. D. (2017). Impact of scapular notching on clinical outcomes after reverse total shoulder arthroplasty: an analysis of 476 shoulders. *Journal of Shoulder and Elbow Surgery*, *26*(7), 1253–1261. http://doi.org/10.1016/j.jse.2016.11.043

Muh, S. J., Streit, J. J., Wanner, J. P., Lenarz, C. J., Shishani, Y., Rowland, D. Y., … Gobezie, R. (2013). Early follow-up of reverse total shoulder arthroplasty in patients sixty years of age or younger. *The Journal of Bone and Joint Surgery. American Volume*, *95*(20), 1877–83. http://doi.org/10.2106/JBJS.L.10005

Mulieri, P., Dunning, P., Klein, S., Pupello, D., & Frankle, M. (2010). Reverse shoulder arthroplasty for the treatment of irreparable rotator cuff tear without glenohumeral arthritis. *The Journal of Bone and Joint Surgery. American Volume*, *92*(15), 2544–56. http://doi.org/10.2106/JBJS.I.00912

Nam, D., Kepler, C. K., Nho, S. J., Craig, E. V, Warren, R. F., & Wright, T. M. (2010). Observations on retrieved humeral polyethylene components from reverse total shoulder arthroplasty. *Journal of Shoulder and Elbow Surgery*, *19*(7), 1003–1012. http://doi.org/10.1016/j.jse.2010.05.014

Nolan, B. M., Ankerson, E., & Wiater, M. J. (2011). Reverse total shoulder arthroplasty improves function in cuff tear arthropathy. *Clinical Orthopaedics and Related Research*, *469*(9), 2476–2482. http://doi.org/10.1007/s11999-010-1683-z

Nyffeler, R. W., Werner, C. M. L., & Gerber, C. (2005). Biomechanical relevance of glenoid component positioning in the reverse Delta III total shoulder prosthesis. *Journal of Shoulder and Elbow Surgery*, *14*(5), 524–528. http://doi.org/10.1016/j.jse.2004.09.010

Permeswaran, V. N., Goetz, J. E., Rudert, M. J., Hettrich, C. M., & Anderson, D. D. (2016). Cadaveric validation of a finite element modeling approach for studying scapular notching in reverse shoulder arthroplasty. *Journal of Biomechanics*, *49*(13), 3069–3073. http://doi.org/10.1016/j.jbiomech.2016.07.007

Pruitt, L. A. (2005). Deformation , yielding , fracture and fatigue behavior of conventional and highly cross-linked ultra high molecular weight polyethylene. *Biomaterials*, *26*, 905–915. http://doi.org/10.1016/j.biomaterials.2004.03.022

Rader, C. P., Sterner, T., Jakob, F., Schütze, N., & Eulert, J. (1999). Cytokine response of human macrophage-like cells after contact with polyethylene and pure titanium particles. *Journal of Arthroplasty*, *14*(7), 840–848. http://doi.org/10.1016/S0883-5403(99)90035-9

Randelli, P., Randelli, F., Arrigoni, P., Ragone, V., Masuzzo, P., Cabitza, P., & Banfi, G. (2014). Optimal glenoid component inclination in reverse shoulder arthroplasty . How to improve implant stability. *Musculoskeletal Surgery*, *98*, 15–18. http://doi.org/10.1007/s12306-014-0324-1

Roche, C., Flurin, P. H., Wright, T., Crosby, L. A., Mauldin, M., & Zuckerman, J. D. (2009). An evaluation of the relationships between reverse shoulder design parameters and range of motion, impingement, and stability. *Journal of Shoulder and Elbow Surgery*, *18*(5), 734–741. http://doi.org/10.1016/j.jse.2008.12.008

Sirveaux, F., Favard, L., Oudet, D., Huquet, D., Walch, G., & Molé, D. (2004). Grammont inverted total shoulder arthroplasty in the treatment of glenohumeral osteoarthritis with massive rupture of the cuff. *The Journal of Bone and Joint Surgery*, *86*(3), 388–395. http://doi.org/10.1302/0301-620X.86B3.14024

Terrier, A., Merlini, F., Farron, A., & Pioletti, D. P. (2009). Reverse shoulder arthroplasty: polyethylene wear. *Computer Methods in Biomechanics and Biomedical Engineering*, *12*(sup1), 247–248. http://doi.org/10.1080/10255840903097855

Weber-Spickschen, T. S., Alfke, D., & Agneskirchner, J. D. (2015). The use of a modular system to convert an anatomical total shoulder arthroplasty to a reverse shoulder arthroplasty: Clinical and radiological results. *Bone and Joint Journal*, *97B*(12), 1662–1667. http://doi.org/10.1302/0301-620X.97B12.35176

Wiater, B. P., Baker, E. A., Salisbury, M. R., Koueiter, D. M., Baker, K. C., Nolan, B. M., & Wiater, J. M. (2015). Elucidating trends in revision reverse total shoulder arthroplasty procedures: a retrieval study evaluating clinical, radiographic, and functional outcomes data. *Journal of Shoulder and Elbow Surgery*, *24*(12), 1915–1925. http://doi.org/10.1016/j.jse.2015.06.004

Willing, R., & Kim, I. Y. (2009). A holistic numerical model to predict strain hardening and damage of UHMWPE under multiple total knee replacement kinematics and experimental validation. *Journal of Biomechanics*, *42*(15), 2520–2527. http://doi.org/10.1016/j.jbiomech.2009.07.008

Young, S. W., Everts, N. M., Ball, C. M., Astley, T. M., & Poon, P. C. (2009). The SMR reverse shoulder prosthesis in the treatment of cuff-deficient shoulder conditions. *Journal of Shoulder and Elbow Surgery*, *18*(4), 622–626. http://doi.org/10.1016/j.jse.2009.01.017

Chapter 5

Conclusions and Future Directions

OVERVIEW: This chapter serves to summarize the results encompassed within the present work, concentrating on their relation to the objectives set forth in the introductory chapter. Additional insights as to the strengths and limitations of the work and possible future directions will also be presented.

5.1   Summary and Conclusions

Overall, the main purpose of the present work was to further the understanding of reverse total shoulder arthroplasty (RTSA) performance characteristics, with respect to contact mechanics and tribology, when affected by scapular notching impingement defects of the humeral component. With the prevalence of this complication, this mechanism of damage poses an uncertainty in the growing application of this implant system. The implications of this change in implant geometry was assessed using finite element modeling and wear simulation to gain a better understanding of the changes in the contact mechanics and tribological properties of the humeral cup component. Additionally, the effects of inferior glenosphere tilt, an intraoperative parameter which can reduce the risk of scapular notching without altering the RTSA implant configuration, was also assessed.

The first objective (Objectives 1A and B) of this work was accomplished through the assessment of RTSA contact mechanics, in terms of articular contact area and maximum contact stress, through finite element modeling (Chapter 2). Through the simulations of multiple loading parameters, obtained through previous *in-vitro* studies and for a wide range of abduction angles, it was found that the introduction of simulated humeral cup defects from scapular notching significantly affected both contact area and maximum contact stress, leading to less favourable contact mechanics (Objective 1A). With respect to the propagation of the humeral cup defect (Objective 1B), this was found to only further decrease articular contact area, but did not have a significant observable effect on the maximum contact stress parameter. Both of these effects were largely observed at abduction above 25° humeroscapular abduction, wherein inferior overhang of the humeral cup behind the medial edge of the glenosphere was no longer present. These findings suggest that the effects of humeral cup scapular notching defects encompass a wide range of motion that is commonly employed in daily living. It serves to reason that the more arduous contact stress values could ultimately decrease the longevity of the implant.

With respect to the second objective (Objective 2) of this work, early wear simulation of high-mobility RTSA implants was conducted in the intact state, as well as with two stages of simulated notching defects (Chapter 3). The introduction of simulated humeral cup defects significantly affected the wear rates of the humeral cups, and contrary to the

hypothesis actually resulted in a decrease of the wear rates as the defect was enlarged. Despite these results, a companion finite element model of the simulator parameters indicated an increase in the contact stresses experienced around the margin of simulated notching damage on the inferior aspect for this more damaged component. While the volumetric wear rates were not increased, scapular notching damage of the humeral cup resulted in an observable secondary wear region, localized to the inferior portion of the cup. This would suggest that while scapular notching damage of the humeral cup may not increase the overall volumetric wear rate, it is possible that what wear which occurs is more localized. However further testing, including observations over a longer period of assessment with the addition a more accurate means of evaluating topographical changes of the implant surface from articular wear.

In terms of the third objective (Objective 3), finite element modeling was used to assess articular contact mechanics of intact RTSA implants wherein the angle of glenosphere tilt was altered (Chapter 4). It was found that inferior glenosphere tilt increased articular contact area, however no significant effect was observed for maximum contact stress values. This was mainly observed at low angles of abduction, wherein the inferior tilting of the glenosphere served to reduce the inferior overhang of the humeral cup behind the glenosphere's medial edge. This suggests that this intraoperative parameter provides improved implant performance at the articular surface within a range of motion that encompasses a majority of recorded daily motion. Therefore achieving this component orientation may be beneficial beyond the reduction in adduction deficit, and risk of scapular notching by association. However, this awaits further biomechanical and clinical evaluation, particularly focusing on the bone-baseplate interface where there is currently a lot of conflicting evidence.

5.2 Strengths and Limitations

The incorporation of multiple physiologically relevant load profiles for the finite element modeling exhibits a major strength of the presented work. Subsequently, statistical analysis was able to be performed to provide further merit to the trends observed. While the profiles applied would be limited to the individual anatomy and the muscle load ratios applied in the shoulder simulator, they are representative of the loads experienced by an RTSA system in that individual.

One limitation with respect to the simulation of scapular notching defect on the humeral cups is the use of limited profiles. While various extents of damage were modelled, only a few types of contours were applied that represented a more conservative extent of damage than that reported. With the root cause being highly variable due to individualistic factors, such as anatomy, activity level, and implant configuration, the appearance and progression of damage would vary on a case to case basis. As there is no catch-all in describing the damage from this process, the preceding conclusions of the finite element models and wear simulation may not be applicable in all cases.

In a similar fashion, the simulated use applied in the wear study is only indicative of a single circumduction motion generated through biaxial rotation. While previous studies have included both isolated abduction-adduction and flexion-extension motions, the shoulder utilizes various combinations of motions to accomplish tasks. Therefore it is believed that the current motion profile for wear simulation is advantageous as it is representative of a range of motions in combination that the shoulder would perform. Additionally, the use of finite element modeling to better discern what is occurring at the articular surface aids in further comprehending the conditions of the test and the interpretation of the results.

5.3 Future Directions

As the effects of scapular notching were largely viewed once the overhang of the humeral cup inferior aspect behind the medial face of the glenosphere, it would be of interest to discern the effect of altering parameters which change the angle of abduction in which this occurs. In terms of the present work, inferior glenosphere tilt, which was found to positively affect RTSA contact mechanics but also reduce the humeral cup overhang, thereby increasing the range of abduction that scapular notching could effect. This would also include the alteration of other implant parameters which influence this relationship, such as the neck-shaft angle.

Further assessment of scapular notching damage through *in-vitro* testing would serve to better understand the effects this damage has on overall implant performance. While multiple physiologically relevant joint load profiles were included in the *in-silico* testing, the use of cadaveric testing would be able to better illustrate a complete picture of the effects, through the inclusion of factors that were not modelled in the present work. Specifically, the introduction of osseous notching damage could be included to observe the effects of component loosening and micromotion on RTSA performance, to ascertain if these factors serve to further magnify the trends viewed in the current work.

5.4 Significance

With the growing prevalence of the use of RTSA implants, the reported frequency of scapular notching is of great concern when considering the subsequent complications resulting, such as component loosening. Additionally, with the growing prevalence of RTSA and the increasing expected lifespan of orthopaedic implants, there will likely greater demands placed on implant systems. While previous work has focused on assigning the effect on osseous anatomy, the implications on the implant performance had yet to be fully assessed. The present work sought to evaluate the effects this damage has on the tribological performance and articular contact mechanics. Through these assessments, a better understanding as to the anticipated *in-vivo* performance effects of RTSA once this damage mechanism is apparent, as well as the expected life of the implant, in the absence of other complications such as component loosening.

5.5   Conclusions

Scapular notching is a complex, multifaceted problem wherein the performance and integrity of the RTSA system is effected on multiple fronts. As demonstrated through the current work, scapular notching defects of the humeral cup can result in both degraded articular contact mechanics as well as influencing the location of the development of articular wear. While there may be intraoperative options or component parameters which could reduce the risk of scapular notching, once this process is initiated it is possible that its consequences will affect the longevity of the implant. Therefore, with the growing prevalence of this procedure, further understanding of scapular notching and its associated complications is required to understand at what point it has progressed to where intervention is required.

Appendices

Appendix A: Glossary of Terms

Abduction: To move structure away from body midline.

Adduction: To move structure towards body midline.

Analysis of Variance (ANOVA): A statistical method which compares the differences amongst a group of means to determine the significance between the respective variables.

Anterior: Located or directed towards the front; opposite of posterior.

Arthroplasty: Surgical procedure to replace a joint's articular surfaces with artificial components.

Articular: Relating to a joint.

Contact Mechanics: The study of the deformation of solids in contact at one or more point.

Distal: Located further away from the body center or attachment point; opposite of proximal.

Finite Element Analysis (FEA): A method of determining loads and displacements of an object, by discretizing it into numerous small pieces and analyzing individually using mechanics equations.

Glenohumeral: Relating to the glenoid and humerus (shoulder joint).

Glenosphere: A metallic hemisphere implanted on the glenoid of the scapula in reverse total shoulder arthroplasty.

Humeral Cup (Liner): The polymer (polyethylene) dish which replaces the proximal humeral head in reverse total shoulder arthroplasty.

Humeroscapular: Relating to the humerus and scapula.

Humerothoracic: Relating to the humerus and thorax (torso)

Inferior: Located below or directed downward; opposite of superior.

In-Silico: Performed on a computer or using computer simulation.

In-Vitro: Performed outside a living body in an artificial environment.

In-Vivo: Performed within a living body or organism.

Lateral: Located further from the body midline; opposite of medial.

Medial: Located towards the body midline; opposite of lateral.

Posterior: Located or directed towards the back; opposite of anterior.

Proximal: Located nearer to the body center or attachment point; opposite of distal.

Range of Motion: The arc of motion that can be achieved by a joint.

Rotator Cuff: A group of stabilizing muscles which surround the glenohumeral joint, comprised of the supraspinatus, infraspinatus, teres minor, and subscapularis muscles.

Scapular Notching: Impingement of the scapula and humeral cup in reverse total shoulder arthroplasty resulting in damage to both components.

Scapulothoracic: Relating to the scapula and thorax (torso).

Tribology: The study of interacting surfaces in relative motion, including lubrication and wear.

Wear: The damage or erosion caused through the interaction of two surfaces.

Appendix B: Lubricant Formulation

Lubricant was formulated to have a final protein concentration of 30 g/L. However, each lot had a slightly different initial protein concentration. Below are the formulations for the dilution of the lubricating serum to the desired protein concentration, with the following considerations:

- Alpha calf fraction (ACF) in 500 mL bottle
- Antimycotic antibiotic (AA) solution final concentration of 5 mL/500 mL
- Both phosphate buffer solution (PBS) and AA solution volumes contribute in the dilution of the ACF
- Sodium hyaluronate (HA) concentration of 1.5 g/L (final volume)

Alpha Calf Fraction (Lot AB10200570; [protein] = 3.7 g/dL)
- 500 mL – ACF without iron
- 110.5 mL – PBS
- 6.167 mL – AA
- 0.925 g – HA

Alpha Calf Fraction (Lot AAG205193; [protein] = 4.0 g/dL)
- 500 mL – ACF without iron
- 160 mL – PBS
- 6.667 mL – AA
- 1.000 g – HA

Appendix C: Laser Surface Scanning of Wear Test Specimens

C-1 Surface Scanning Protocols

In an attempt to visualize the location of wear, laser scanning of the humeral cups was conducted before each round of testing, and during each subsequent stoppage for the first two stages of the wear simulation (intact and first notch level). Therefore, a total six sets of scans were collected for each cup in total (0 Mc, 0.1 Mc, 0.25 Mc before and after notching, 0.35 Mc, and 0.5 Mc). A NextEngine Desktop 3D Scanner Model 2020i (NextEngine Inc., Santa Monica, CA, USA) was utilized in high definition macro mode (±0.13 mm accuracy, 7.6x12.7 cm field of view) with the humeral cup located approximately 16.5 cm away from scanner. It should be noted that a similar scanner has been previously used in the assessment of wear on retrieved knee replacements (Stoner, Jerabek, Tow, Wright, & Padgett, 2013; Stoner, Nassif, Wright, & Padgett, 2013). Talcum powder was first applied to the surface of the humeral cups in preparation for scanning, to aid in capturing surface data. The humeral cups were then placed in a custom mount, with four markers surrounding the implant for the purpose of scan alignment, as well as a fifth marker used in aligning the inferior aspect of the humeral cup when positioning in the mount. Six views were taken of each humeral cup, the first three of which were with the inferior-superior axis vertically orientated and scans taken from a straight on perspective as well as rotated approximately 10° both anteriorly and posteriorly. This process was then repeated with the anterior-posterior axis being vertically orientated and scanning straight on, in addition to rotated approximately 10° superiorly and inferiorly. This was done to ensure the detail of the articular surface edges were preserved, predominately the inferior aspect which was of particular interest.

These six views were then aligned using the markers on the mounting surface and fused to a single mesh using the manufacturer's software (NextEngine ScanStudio Version 2.0.2). Next the mount was removed from the generated mesh to isolate the humeral cup surfaces (approximately 275000 to 300000 elements). For each humeral cup, the beginning and end scans for each testing stage (0 Mc and 0.25 Mc before notching; 0.25 Mc after notching

and 0.5 Mc), were aligned using the best fit alignment tool in Geomagic Control X (Version 2017.0.3; 3D Systems Inc., Rock Hill, SC, USA) and mesh deviation maps for the surface were generated. Additionally, this process was also conducted for the scans before and after notching was introduced to assess and verify the depth of material removed.

C-2 Results

It should also be noted that the apparent changes in surface morphology of the humeral cups did not directly correlate to that viewed in the surface deviation analysis of the scans, which can also be in Figure C-1 and Figure C-2. However, the surface deviation maps were well suited in assessing the depth of the simulated notching, as depicted in Figure C-3, where it can be seen that the maximum depth varied from 1.17 to 1.58 mm. It should be noted that these maximum depth values, which are greater than the 1 mm target depth, favoured the outer surface and not the articular margin.
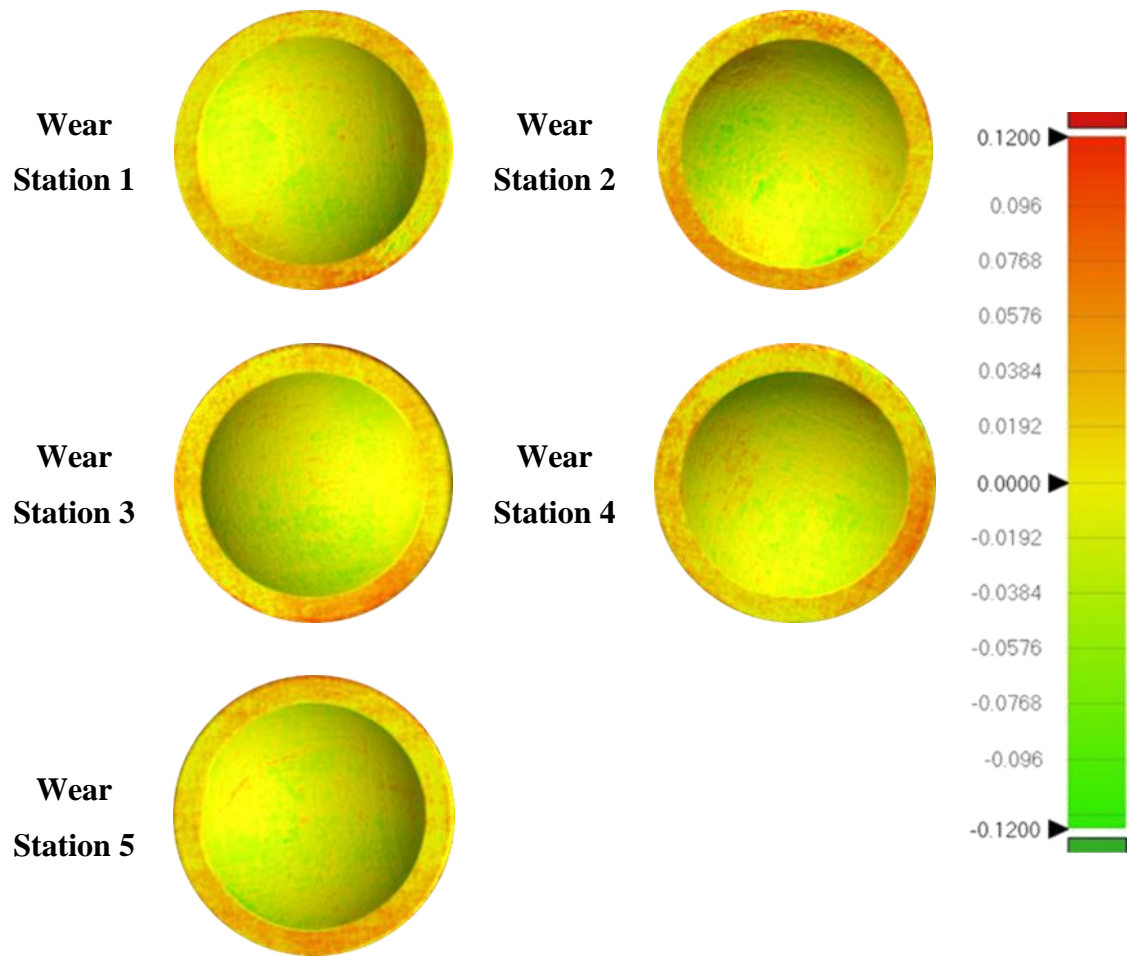
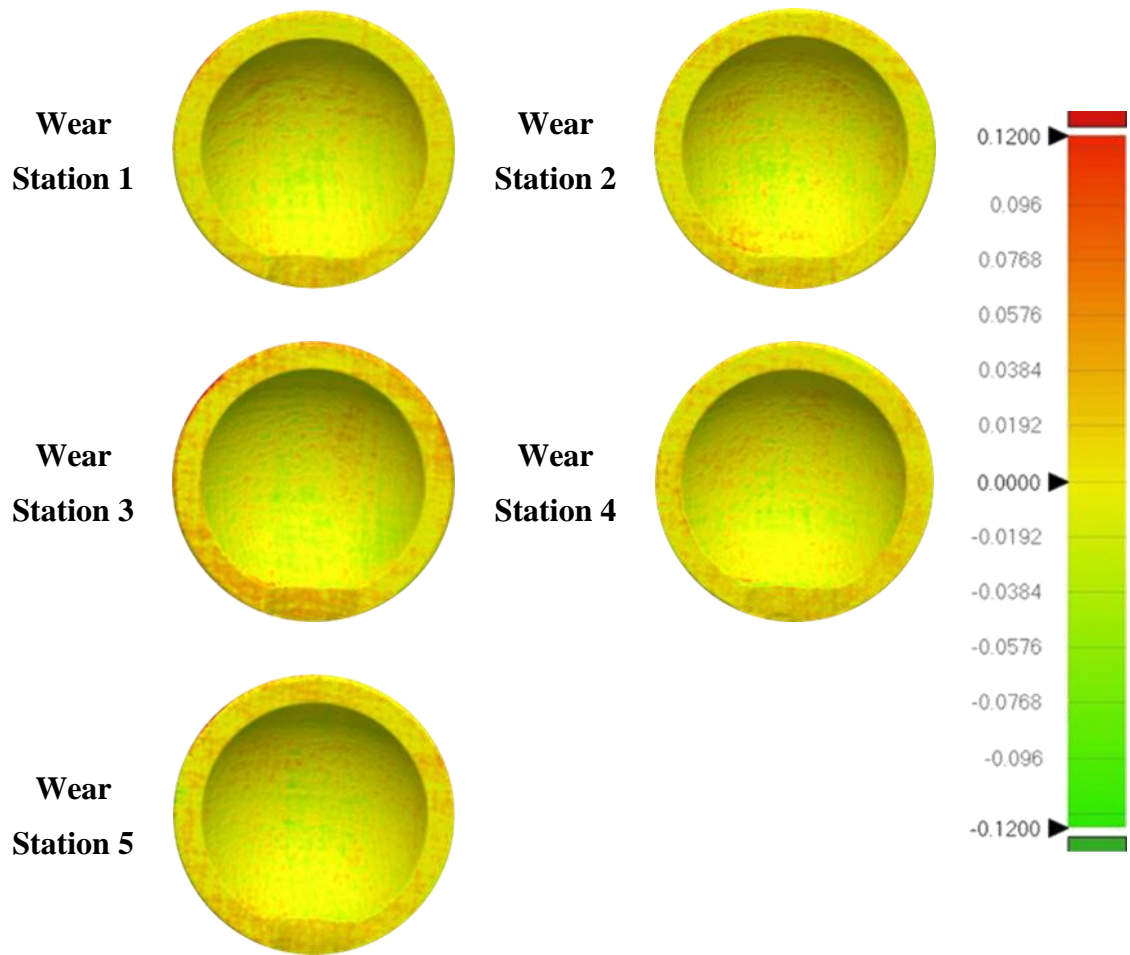**Figure C-1: Surface deviation maps from laser surface scanning (0-0.25 Mc)**

Figure C-2: Surface deviation maps from laser surface scanning (0.25-0.5 Mc)
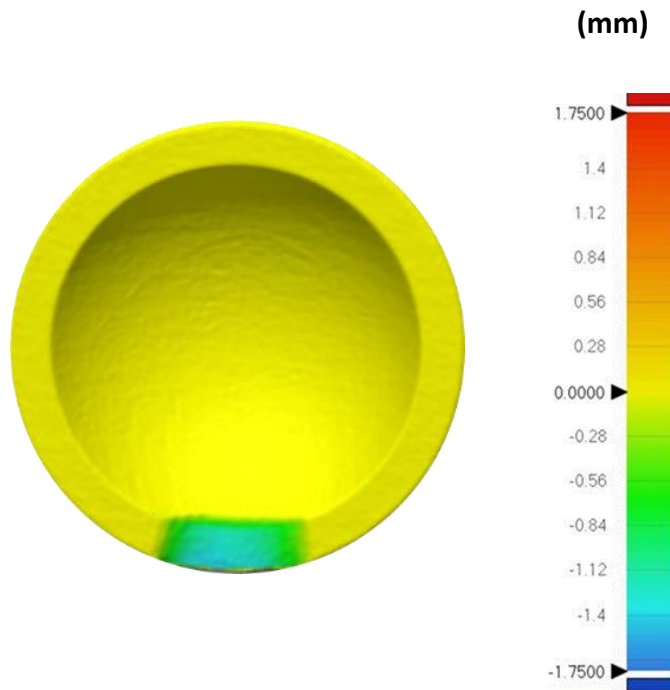
Figure C-3: Sample surface deviation map of a humeral cup from the simulated notching process

C-3 Discussion

A complication stemming from the short duration of testing for each stage was that it was difficult for the laser scanner to clearly discern the resulting wear, as depicted in Figure C-1 and Figure C-2. While the manufacturer states an accuracy of ±0.13, validation studies report less accuracy with an uncertainty of ±0.84 mm (Polo & Felicísimo, 2012), both of which encompass the magnitude of observed articular surface changes in the present work. Even with further testing the wear would be difficult to visualize using this apparatus. Furthermore, the work by Langohr et al (2016) for a single standard depth humeral cup identified a maximum surface deviation of 0.25 mm after 1.0 Mc using micro-CT, for both the intact and notched state. This would indicate that more than 0.25 Mc are required to ensure the laser scanner can adequately identify the regions of material wear.

To verify that this was not due to potential rotation from the best fit algorithm used in mesh alignment, a test was conducted with a single specimen scan from testing, comparing it against an ideal computer model (Figure C-4). Here the magnitude of change was found

to be similar for the articular face but was greater around the outer aspect. It should be noted that the values for the articular face were still found to be within the reported ranges of the scanner's accuracy. Nevertheless, a similar model of scanner has been previously used in assessing the wear of retrieved knee arthroplasty components, however the observed magnitude of change was approximately 1.5 mm (Stoner, Jerabek, et al., 2013; Stoner, Nassif, et al., 2013). Therefore when attempting to visualize surface changes within the smaller scale observed in wear simulation studies, especially in the short term, more reliable and accurate techniques such as micro-CT (Carpenter et al., 2015; Langohr, Athwal, et al., 2016; Teeter, Langohr, Medley, & Holdsworth, 2014) or coordinate measurement machines (Lewicki, Bell, & Van Citters, 2017) would be better suited. It was for these reasons that scanning was not included for the 0.5-0.75 Mc stage of testing in the presented work.
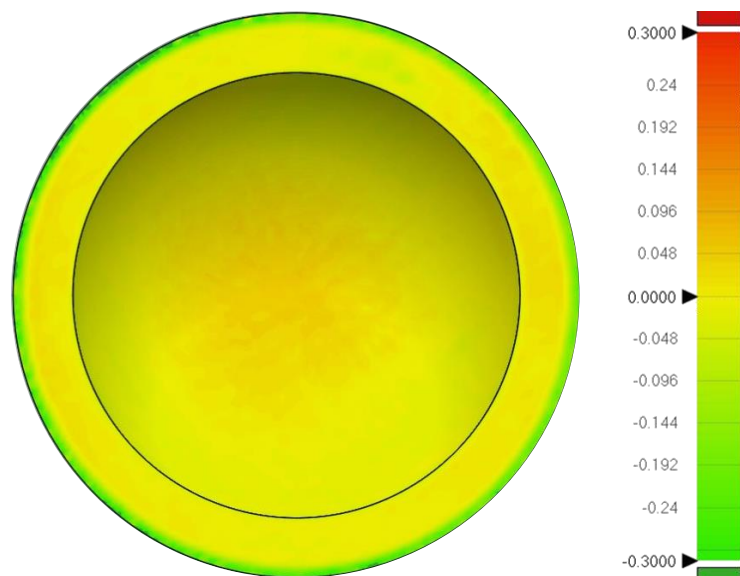

Figure C-4: Surface deviation map of a wear test humeral cup (0.25 Mc) relative to an ideal computer model

C-4   References

Carpenter, S., Pinkas, D., Newton, M. D., Kurdziel, M. D., Baker, K. C., & Wiater, J. M. (2015). Wear rates of retentive versus nonretentive reverse total shoulder arthroplasty liners in an in vitro wear simulation. *Journal of Shoulder and Elbow Surgery*, *24*(9), 1372–1379. http://doi.org/10.1016/j.jse.2015.02.016

Langohr, G. D. G., Athwal, G. S., Johnson, J. A., & Medley, J. B. (2016). Wear simulation strategies for reverse shoulder arthroplasty implants. *Journal of Engineering in Medicine*, *230*(5), 458–469. http://doi.org/10.1177/0954411916642801

Lewicki, K. A., Bell, J. E., & Van Citters, D. W. (2017). Analysis of polyethylene wear of reverse shoulder components: A validated technique and initial clinical results. *Journal of Orthopaedic Research*, *35*(5), 980–987. http://doi.org/10.1002/jor.23353

Polo, M. E., & Felicísimo, A. M. (2012). Analysis of uncertainty and repeatability of a low-cost 3D laser scanner. *Sensors*, *12*(7), 9046–9054. http://doi.org/10.3390/s120709046

Stoner, K. E., Jerabek, S. A., Tow, S., Wright, T. M., & Padgett, D. E. (2013). Rotating-platform has no surface damage advantage over fixed-bearing TKA knee. *Clinical Orthopaedics and Related Research*, *471*(1), 76–85. http://doi.org/10.1007/s11999-012-2530-1

Stoner, K. E., Nassif, N. A., Wright, T. M., & Padgett, D. E. (2013). Laser scanning as a useful tool in implant retrieval analysis: A demonstration using rotating platform and fixed bearing tibial inserts. *Journal of Arthroplasty*, *28*(SUPPL. 1), 152–156. http://doi.org/10.1016/j.arth.2013.07.004

Teeter, M. G., Langohr, G. D. G., Medley, J. B., & Holdsworth, D. W. (2014). Nondestructive microimaging during preclinical pin-on-plate testing of novel materials for arthroplasty. *Proceedings of the Institution of Mechanical Engineers, Part H: Journal of Engineering in Medicine*, *228*(2), 159–164. http://doi.org/10.1177/0954411914522615

Curriculum Vitae

MICHAEL GRIFFITHS

EDUCATION

Master's of Engineering Science (Biomedical Engineering)	**2015 – Present**

Western University, London, Ontario

Supervisor: Dr. James Johnson
Co-Supervisor: Dr. John Medley, The University of Waterloo, Waterloo, Ontario

Thesis Topic: Influence of Scapular Notching on Contact Mechanics and Simulator Wear of Reverse Total Shoulder Arthroplasty Implants

Bachelor of Engineering (Biomedical Engineering – Co-op)	**2010 – 2015**

The University of Guelph, Guelph, Ontario

PROFESSIONAL AFFILIATIONS

Roth McFarlane Hand and Upper Limb Centre	**June 2015 – Present**

St. Joseph's Healthcare, London, Ontario

Professional Engineers Ontario	**Sept 2010 – Present**

Student Membership Program

RESEARCH EXPERIENCE

Graduate Research Assistant	**Sept 2015 – Present**

Western University, London, Ontario
Advisor: Dr. James Johnson
Co-Advisor: Dr. John Medley, The University of Waterloo,
Waterloo, Ontario

Research Assistant	**June – Aug 2015**

Roth McFarlane Hand and Upper Limb Centre, St. Joseph's Healthcare, London, Ontario
Advisor: Dr. James Johnson
Supervisor: Dr. Daniel Langohr

Biomedical Engineering Research Assistant	**May – Aug 2012**

The University of Guelph, Guelph, Ontario
Advisors: Dr. Karen Gordon & Dr. Michele Oliver

TEACHING EXPERIENCE

Teaching Assistant – Biomechanics of Musculoskeletal Systems	**Jan 2017 – Apr 2017**

Western University, London, Ontario

Teaching Assistant – Mechanics of Materials   **Sept 2016 – Dec 2016**
Western University, London, Ontario

Teaching Assistant – Introductory Engineering Design &   **Sept 2015 – Apr 2016**
Innovation Studio
Western University, London, Ontario

PROFESSIONAL EXPERIENCE

Canadian Mist Distillers Limited – Quality Assurance Analyst   **Aug – Dec 2014**
Collingwood, Ontario

Maple Leaf Foods – Process Specialist Technician Co-Op   **Jan – Aug 2013**
Mississauga, Ontario

CONFERENCE PRESENTATIONS AND POSTERS

Griffiths, M.W., Langohr, G.D.G., Athwal, G.S., Johnson, J.A. (2017) Inferior Glenosphere Tilt Improves Reverse Shoulder Arthroplasty Contact Mechanics. *Canadian Orthopaedic Research Society Annual Meeting*, June 15-18, Ottawa, Ontario

Griffiths, M.W., Langohr, G.D.G., Athwal, G.S., Johnson, J.A. (2016) The Effect of Glenosphere Size on Adduction and Abduction Range of Motion in Reverse Total Motion Arthroplasty. *Canadian Orthopaedic Research Society Annual Meeting*, June 16-19, Quebec City, Quebec

Langohr, G.D.G., **Griffiths, M.W.**, Athwal, G.S., Medley, J.B. (2016) Wear Simulation Testing of Reverse Total Shoulder Arthroplasty Implants. *10th World Biomaterials Congress*, May 17-22, Montréal, Quebec

Griffiths, M.W., Langohr, G.D.G., Athwal, G.S., Johnson, J.A. (2016) Reverse Total Shoulder Arthroplasty and the Effect of Component Sizing on Range of Motion. *The Canadian Bone and Joint Conference*, April 8-9, London, Ontario

Griffiths, M.W., Langohr, G.D.G., Athwal, G.S., Johnson, J.A. (2016) The Effect of Glenosphere Size on Adduction and Abduction Range of Motion in Reverse Total Shoulder Arthroplasty. *62nd Meeting of the Orthopaedic Research Society*, March 5-8, Orlando Florida

Langohr, G.D.G., Athwal, G.S., Johnson, J.A., **Griffiths, M.W.**, Medley, J.B (2016) *In-Vitro* Simulator Wear of Reversed Total Shoulder Arthroplasty Implants. *International Society for Technology in Arthroplasty 29th Annual Congress*, October 5-8, Boston, Massachusetts

COMMUNITY INVOLVEMENT

Biomedical Engineering Pedagogy Committee –   **Sept 2015 – Apr 2016**
Biomechanics Representative
Western University, London, Ontario

Collingwood General & Marine Hospital – Emergency Room Volunteer   Sept – Dec 2014
Collingwood, Ontario

Sault Area Hospital – Physiotherapy Clinic Volunteer   May – Aug 2014
Sault Ste. Marie, Ontario

The University of Guelph – Central Orientation Volunteer   Sept 2012 & 2013
Guelph, Ontario

The University of Guelph Interhall Council – East Village Operations Manager   Sept 2011 – May 2012
Guelph, Ontario

The University of Guelph – Residence Orientation Leader   Sept 2011
Guelph, Ontario

HONOURS & AWARDS

Guelph Residence Recognition Program Student of the Year   **2012**